DISSERTATION

AIR QUALITY IMPACTS FROM UNCONVENTIONAL OIL AND GAS DEVELOPMENT

Submitted by

I-Ting Ku

Department of Atmospheric Science

In partial fulfillment of the requirements

For the Degree of Doctor of Philosophy

Colorado State University

Fort Collins, Colorado

Spring 2024

Doctoral Committee:

Advisor: Jeffrey L. Collett, Jr.

Emily V. Fischer
Kenneth H. Carlson
Sonia Kreidenweis

ABSTRACT

AIR QUALITY IMPACTS FROM UNCONVENTIONAL OIL AND GAS DEVELOPMENT

Unconventional oil and natural gas development (UOGD) has expanded rapidly across the United States raising concerns about associated air quality impacts. While significant effort has been made to quantify and limit methane emissions, relatively few observations have been made of emitted Volatile Organic Compounds (VOCs). Extensive air monitoring during development of several large, multi-well pads in Broomfield, Colorado, in the Denver-Julesburg Basin, provides a novel opportunity to examine changes in local concentrations of air toxics and other VOCs during drilling and completions of new wells. With simultaneous measurements of methane and 50 VOCs from October 2018 to December 2022 at as many as 19 sites near well pads, in adjacent neighborhoods, and at a more distant reference location, we identify impacts from each phase of well development and production.

In Part 1, we report how emissions from Broomfield pre-production and production operations influence air toxics and other VOC concentrations at nearby locations. Use of weekly, time-integrated canisters, a Proton Transfer Reaction Mass Spectrometer (PTR-MS), continuous photoionization detectors (PID) to trigger canister collection upon detection of VOC-rich plumes, and an instrumented vehicle, provided a powerful suite of measurements to characterize both transient plumes and longer-term changes in air quality. Prior to the start of well development, VOC gradients were small across Broomfield. Once drilling commenced, concentrations of oil and gas (O&G) related VOCs, including alkanes and aromatics, increased around active well pads. Concentration increases were clearly apparent during certain operations, including drilling, coil tubing/millout operations, and production tubing installation. Emissions of C_8-C_{10} n-alkanes

during drilling operations highlighted the importance of VOC emissions from a synthetic drilling mud chosen to reduce odor impacts. More than 90 transient plumes were sampled and connected with specific UOGD operations. The chemical signatures of these plumes differed by operation type. Concentrations of individual, O&G-related VOCs in these plumes were often several orders of magnitude higher than in background air, with maximum ethane and benzene concentrations of 79,600 and 819 ppbv, respectively. Study measurements highlight future emission mitigation opportunities during UOGD operations, including better control of emissions from shakers that separate drill cuttings from drilling mud, production separator maintenance operations, and periodic emptying of sand cans during flowback operations.

In Part 2 OH reactivities (OHR) were calculated to examine the potential of emitted VOCs to contribute to regional ozone formation. NO_2 was the largest contributor to OHR during winter when OHR values peaked, while VOCs dominated OH sinks during summer. Oxygenated VOCs and C_3-C_7 n-alkanes, closely associated with O&G activities, were primary contributors to OHR levels during the summer ozone season. In Part 3 we leverage observations from Broomfield and other Colorado O&G air quality studies to examine relationships between O&G emissions of methane and VOCs. A key goal is to determine whether more commonly measured methane emissions can serve as a surrogate to estimate emissions of less frequently measured compounds such as benzene, a key air toxic. While strong correlations are observed between benzene and methane emissions in some situations, considerable variability is observed in this relationship across locations and operations suggesting caution in assuming that reductions in methane emissions will yield proportionate reductions in releases of air toxics.

ACKNOWLEDGEMENTS

First, I sincerely thank my advisor, Dr. Jeffrey Collett, for his mentorship throughout the past several years. I learned so much with his guidance on my research work and his support in providing me with many great opportunities to participate in several projects, attend conferences, teach and mentor students, and take a committee role in helping to host a conference. I wouldn't be able to complete my Ph.D. journey without his patience and guidance. I am also very thankful to my committee members, Dr. Emily Fischer, Dr. Kenneth Carlson, and Dr. Sonia Kreidenweis, for serving on my committee and taking the time to understand and provide feedback and support on my work.

I am incredibly thankful for the past and present Collett's Research Group members. A special thank you to Dr. Amy Sullivan for all the support in the lab and the fields since I joined the group and to Dr. Yong Zhou for all the help in collecting and analyzing samples. I would also like to thank Evelyn Bangs and Emily Lachenmayer for all the great conversations, good times, and friendship to support me through this journey. I want to thank the faculty, staff, and students in the CSU ATS community. A special thanks to Julieta Juncosa Calahorrano and all the students in ATSISSA. Your company and support through these years have been precious in helping me through the hard times. I would also like to thank all my friends in the U.S.A. and Taiwan for their company, consistent support, and encouragement throughout these years.

I want to thank my family for being my best support to allow me to pursue my dream carefreely. I am also deeply thankful for the continuous support extended by my aunt's family in Denver throughout these years. Finally, I want to thank my partner, Matt Glanzer, for consistently encouraging and believing in me during moments of discouragement. Special thanks also go to our feline companions, Copper and Pico, for their mental support.

This research is supported by the City and County of Broomfield (CCOB). The field work and measurements conducted in this research were a joint effort of the CCOB, Ajax Analytics, C.S.U., and Boulder A.I.R. I genuinely appreciate all assistance these team members provided.

TABLE OF CONTENTS

LIST OF TABLES

LIST OF FIGURES

Chapter 1

Introduction

1.1 Volatile Organic compounds

Volatile organic compounds (VOCs) are emitted by a wide range of natural and anthropogenic sources, including vegetation, wildfires, traffic, volatile chemical products, and oil and gas extraction (Atkinson and Arey, 2003; Gkatzelis et al., 2021; Permar et al., 2021; Russo et al., 2010; Simpson et al., 2010; Yokelson et al., 2003). VOCs play an important role in atmospheric chemistry by influencing atmospheric oxidative capacity, including the abundance of ozone (O_3), hydroxyl radical (OH), and hydroperoxides (Helmig et al., 2014; Hobbs et al., 2003; Yokelson et al., 2009). VOC contributions to ozone production are of particular interest given the challenge many communities face in reducing unhealthy ozone levels (Benedict et al., 2019; Lindaas et al., 2019; Peng et al., 2021). Some VOCs are important precursors to secondary organic aerosol (SOA) production (Akagi et al., 2012; Evanoski-Cole et al., 2017) and some are air toxics that act as carcinogens and/or otherwise impact human health (McKenzie et al., 2018; McMullin et al., 2018; O'Dell et al., 2020).

1.2 Tropospheric Ozone

Tropospheric (ground-level) ozone is one of six criteria air pollutants regulated by the U.S. Environment Protection Agency (U.S. EPA) due to its negative effects on human health (Chang et al., 2012; Kim et al., 2020; Schlink et al., 2006; Sujith and Sehgal, 2017). It also has detrimental effects on ecosystems (Fuhrer et al., 2016; Ghude et al., 2014; Grulke and Heath, 2020; Van Dingenen et al., 2009) and is an important greenhouse gas (Myhre et al. 2013). Tropospheric ozone is a secondary pollutant, not emitted directly to the atmosphere but produced through a series of

chemical reactions of volatile organic compounds (VOC) in the presence of nitrogen oxides (NO_x = NO + NO_2) and sunlight (Crutzen et al., 1999; Sillman, 2003; Wang et al., 2018). OH is typically the most important oxidant in this chemistry. Emissions of VOCs and/or NO_x originate from a wide variety of sources, including motor vehicles, electric power generation, industries, oil and gas development, agriculture, wildfires, vegetation, and personal care products (Chiang et al., 2007; Coggon et al., 2021; Dinh et al., 2015; Peng et al., 2021; Pierce et al., 1998). Ozone production chemistry is complicated; the formation efficiency is determined by various factors including the VOC/NO_x ratio, VOC composition, oxidant availability, and meteorology (Martins and Andrade, 2008; McDuffie et al., 2016; Peng et al., 2021; Sullivan et al., 2016; Wang et al., 2018). Stratospheric intrusion events and long-range transport of ozone and its precursors can contribute, along with local photochemistry, to elevated concentrations of surface ozone (Lin et al., 2012; Lin et al., 2017).

1.3 Unconventional Oil and Natural Gas Development in the U.S.

Improved horizontal drilling and hydraulic fracturing techniques (Figure 1.1) have enabled rapid expansion of unconventional oil and gas development (UOGD) in the United States (U.S.). The production of petroleum and other related liquids increased from 34.6 to 67.1 quadrillion British thermal units (quads) and from 19.7 to 35.2 quads for natural gas from 2000 to 2019. The United States has continuously led global petroleum and natural gas production since 2014 surpassing other energy-producing countries, including Canada, China, Russia, and Saudi Arabia (U.S. Energy Information Administration (U.S. EIA), https://www.eia.gov/todayinenergy/detail.php?id=48756, accessed on 20 February 2023).

UOGD typically involves several steps, including well drilling (often including long horizontal legs to better access layered hydrocarbon deposits), hydraulic fracturing (the creation

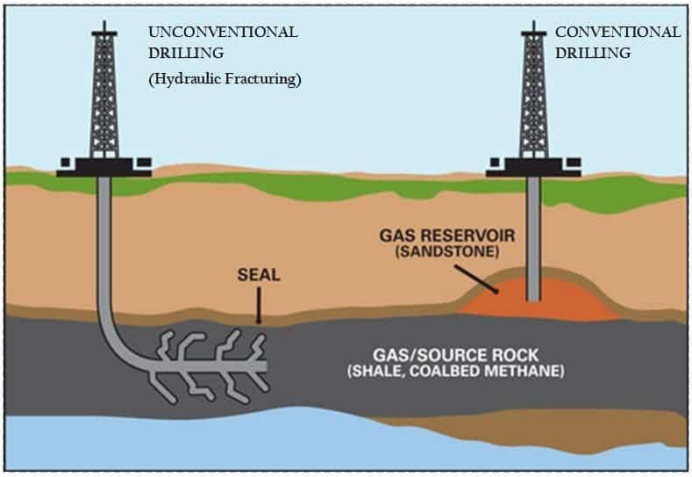

Figure 1.1: Cross-sectional illustration depicting the subsurface geology of natural resources with the portrayal of unconventional versus conventional drilling practices (source: ZME Science, 2014).

of fractures in the hydrocarbon formation to increase permeability and aid in O&G recovery), and flowback (the return of injected fracturing fluids and produced water from the formation to the surface) (U.S. EPA, https://www.epa.gov/uog/process-unconventional-natural-gas-production, accessed on 17 May 2023; Field et al., 2014; Hecobian et al., 2019; Orak et al., 2021). Each of these steps is a complex process and intermediate activities (e.g., coiled tubing operations/millout and installation of production tubing) are also scheduled. For large pads with many wells, these processes typically extend over several months to a year before wells go into production.

1.4 Air Quality Impacts from UOGD

The oil and natural gas (O&G) industry is an important emitter of NO_x, methane (CH_4), and a wide range of VOCs (Ghosh, 2018; Gilman et al., 2013; Goldberg et al., 2021; Hecobian et al., 2019; Miller et al., 2013; Pétron et al., 2012; Prenni et al., 2016; Schade and Roest, 2018; Simpson et al., 2010; Swarthout et al., 2013; Warneke et al., 2014; Wilde et al., 2021). Oxidation of these gas precursors play an important role in atmospheric chemistry by influencing the

oxidation capacity and contributing to tropospheric ozone (Cheadle et al., 2017; Edwards et al., 2014; Evans and Helmig, 2017; Helmig et al., 2014; Lindaas et al., 2019; McDuffie et al., 2016) and secondary aerosol (Evanoski-Cole et al., 2017; Prenni et al., 2022; Naimie et al., 2022) formation. Some VOCs emitted by UOGD are air toxics that are carcinogenic or can cause other health impacts for O&G workers or local residents (McKenzie et al., 2018; McMullin et al., 2018; O'Dell et al., 2020; Weisner et al., 2023; Colborn et al., 2011; Colborn et al., 2014; Esswein et al., 2014).

U.S. UOGD occurs in both rural and populated regions and growing development has raised concerns about impacts on the environment (e.g., noise, water, and air quality) and human health associated with O&G-related emissions (Ku et al., 2024; McKenzie et al., 2016; Thompson et al., 2014). Due to its high global warming potential (28-36 times that of carbon dioxide on an equivalent mass basis over a 100-year average time, Vallero, 2019) and abundance, numerous studies have quantified methane emissions from O&G production through various methodologies (Allen et al., 2013; Brantley et al., 2014; Caulton et al., 2014; Harriss et al., 2015; Katzenstein et al., 2003; Lyon et al., 2015; Marrero et al., 2016; Mead et al., 2023; Peischl et al., 2015; Peischl et al., 2013; Pétron et al., 2014; Townsend-Small et al., 2015). The complexity of VOC measurement and sources, however, means that emissions of individual VOCs are generally much less studied and understood than are methane emissions. Many VOC-focused studies have quantified combined emissions from a large number of sources in an O&G production basin (Hecobian et al., (2019); Helmig et al., (2014); Pétron et al., (2014); *Prenni et al.*, (2016); Simpson et al., (2010); Warneke et al., (2014)). Current understanding of O&G well pad emissions comes, in part, from shorter-term snapshots of process level emissions (e.g., Hecobian et al. (2019)). An analysis utilizing measured emissions distributions (Hecobian et al., 2019), regional meteorological

conditions, and dispersion modeling simulations assessed human health risks from exposure to VOCs emitted from O&G operations in Colorado (Holder et al., 2019) and informed statewide implementation of a 2000 foot (610 m) setback distance to better protect residential populations.

Long-term study of O&G emissions from development of individual O&G well pads remains uncommon. Such air toxics observations around O&G operations, however, are needed to assess the accuracy of modeled concentration fields and exposures. Bari et al. (2016) conducted a long-term study of the impact of emissions from Alberta oil sands development on the surrounding community, examining concentrations of VOCs and their trends in time and comparing them to chronic and acute health risk screening criteria. Jarosławski et al. (2022) reported air pollutant concentration changes during the development of shale gas wells in Poland. Both studies highlight the value of continuous ambient monitoring to inform the public and other stakeholders about air quality impacts of UOGD. Such information is critical to evaluate potential health risks from UOGD in populated regions. Detailed and time-resolved observations around O&G operations can also play an important role in identifying strategies to reduce O&G air pollutant emissions and associated impacts through process improvement in the technologically complex and evolving operational practices associated with new well development.

1.5 Unconventional Oil and Natural Gas Development in Colorado

The State of Colorado, home to the Piceance Basin (PB) and Denver-Julesburg Basin (DJB) (Figure 1.2) and approximately 50,000 active O&G wells (Colorado Oil & Gas Conservation Commission (COGCC), https://cogcc.state.co.us/data2.html#/downloads, accessed on 15 December 2023), ranked seventh among U.S. states for overall 2021 energy production (U.S. EIA, https://www.eia.gov/state/print.php?sid=CO, accessed on 20 February 2023). Home to the majority of Colorado's wells, the Denver-Julesburg Basin (DJB) sits NE of the Denver

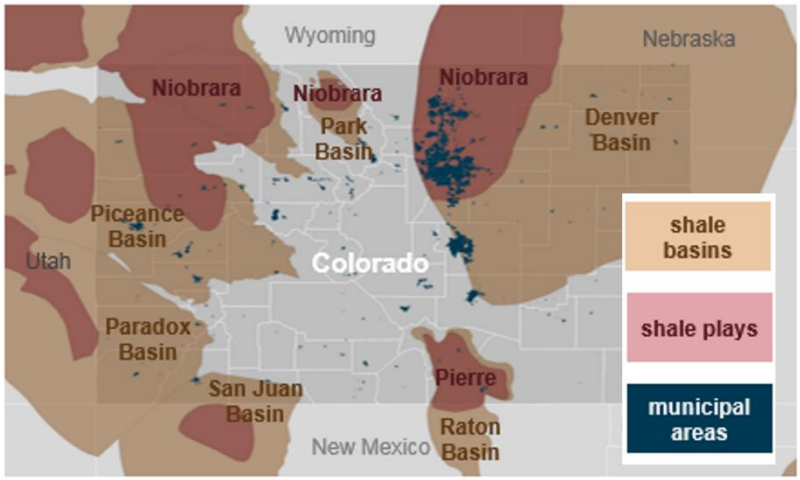

Figure 1.2: Colorado Shale plays and basins (source: U.S. EIA and Colorado Department of Local Affairs, State Demography Office).

metropolitan area and within the Denver Metro/North Front Range ozone non-attainment area. The most extensively drilled region within the DJB is in Weld County. This area hosts the highest number of active wells, accounting for approximately 40% of the total active O&G wells in Colorado. Weld County significantly contributes to Colorado's energy production, comprising 82% of the state's total crude oil and 53% of its natural gas production (COGCC, https://cogcc.state.co.us/data4.html#/production, accessed on 20 February 2023). Considerable UOGD within the basin occurs near residential areas. For example, plans to develop six new large, multi-well O&G pads in areas close to neighborhoods and schools in the City and County of Broomfield, Colorado (CCOB, population 76,000, a small county to the southwest of Weld County) were formulated in 2017. This plan raised local concerns that spurred development of an operator agreement incorporating several management practices to help protect the environment, public health, and safety of residents. These included use of grid-powered electric drill rigs, installation of pipelines and use of closed loop fluid handling systems to reduce truck traffic and reduce air emissions during transport of water and O&G products, and eliminating use of permanent, on-site storage tanks (Broomfield Comprehensive Plan (2016),

https://www.broomfield.org/DocumentCenter/View/25227/11-Oil-and-Gas-Chapter?bidId=, accessed on 14 December 2023). Since the six well pads entered production between 2020 and early 2023, the county has experienced an unprecedented surge in UONG production. Crude oil production has escalated more than 100 times from 2018 to 2023, increasing from 35,799 barrels in 2018 to 3,866,972 barrels in 2023 (updated to October) on an annual basis. Natural gas production has increased approximately 30 times during the same period, rising from 725,638 Mcf in 2018 to 1,671,680 Mcf in 2019, and 20,109,129 Mcf in 2023 (1 Mcf = 1,032 cubic feet, data from COGCC, https://cogcc.state.co.us/data4.html#/production, accessed on 14 December 2023).

Several studies have been conducted in the DJB to characterize VOC emissions and source contributions (Abeleira et al., 2017; Gilman et al., 2013; Pétron et al., 2012; Pétron et al., 2014; Pollack et al., 2021; Swarthout et al., 2013; Thompson et al., 2014). These studies report strong O&G influence on regional air quality. McKenzie et al. (2018) assessed health risks from air pollutants emitted by O&G facilities suggesting higher acute and chronic health risks for residents living close to these facilities. Even back in 2012, prior to recent UOGD and population growth, 19% of the population in the DJ Basin lived within 1.6 km of an active O&G well site (McKenzie et al., 2016).

In addition to air toxics concerns from O&G-related emissions, the Colorado North Front Range (NFR) has consistently failed to meet ozone standards over the past two decades since 2007. Significant decreases in tropospheric ozone levels have been observed across the U.S. in recent decades reflecting regulatory reductions of precursor emissions from vehicles and industries (Simon et al., 2015). Nevertheless, many places in the western U.S. still struggle to comply with ozone National Ambient Air Quality Standards (NAAQS), especially during summertime (Bien and Helmig, 2018; Lin et al., 2017). 8-hour average ozone standards were established and revised

over time from 84 ppb in 1997 to 75 ppb in 2008 and 70 ppb in 2015. Violation of the standard is measured based on three consecutive year averages of the fourth annual maximum from daily 8-hour average ozone levels. Colorado's Northern Front Range (NFR) has been designated an ozone non-attainment area since 2007, with continued exceedances of both the 75 and 70 ppb NAAQS. The region includes the Denver Metro Area and areas to the north (see Figure 1.3). The region was classified as "Marginal" in 2007 for non-attainment of the 1997 ozone NAAQS. Despite continued efforts to reduce ozone precursor emissions from motor vehicles, oil and gas development, and other sources, significant population growth, high ozone background levels, and increasingly hot, dry summers have made ozone standard attainment a challenge (Bien and Helmig, 2018; CDPHE, 2023; Evan and Helmig, 2017; Goetz and Boschmann, 2018; Milford, 2014; Wells, 2017). and the region was recently classified as "Severe" for continued non-attainment of the 2008 ozone NAAQS.

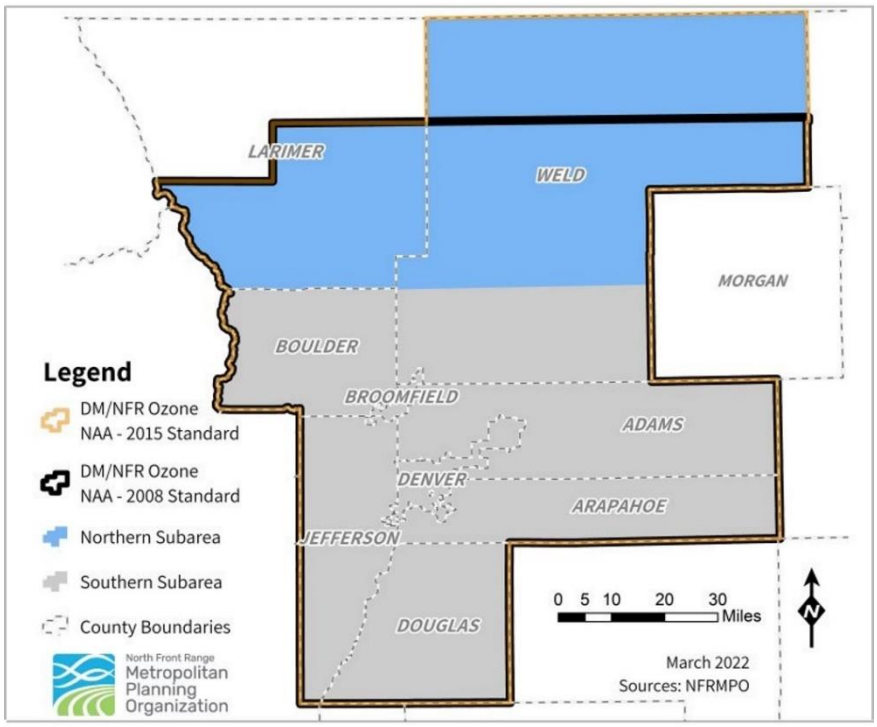

Figure 1.3: Denver Metro – North Front Range ozone non-attainment area. (source: North Front Range Metropolitan Planning Organization).

Several studies have demonstrated that O&G activities are major VOC and NO_x sources that contribute to elevated ozone in the NFR (Abeleira et al., 2017; Benedict et al., 2019; Bien and Helmig, 2018; Cheadle et al., 2017; Evans and Helmig, 2017; Gilman et al., 2013; Halliday et al., 2016; Hecobian et al., 2019; Helmig, 2020; Lindaas et al., 2019; McDuffie et al., 2016; Pétron et al., 2012; Pollack et al., 2021; Swarthout et al., 2013; Thompson et al., 2014). An early report revealing the connection between elevated ozone and O&G emissions in the NFR was published by the Colorado Department of Public Health & Environment (CDPHE, 2008). Integrating back trajectory analysis with daily maximum 8-hour ozone concentrations observed at four NFR sites in summer 2006 showed that elevated ozone events were attributed to air masses transported from the DJB. Evans and Helmig (2017) analyzed 4-year continuous measurements of 1-hr average ozone with wind data at the Boulder Atmospheric Observatory (BAO). This study demonstrated that elevated ozone events were associated with airflow from the O&G production region, accounting for 65% of 1-hr elevated ozone levels, with minor contributions from the direction of the Denver metropolitan area (9%). To better understand sources of high ozone, multiple studies speciated ambient VOCs and apportioned their sources (Abeleira et al., 2017; Gilman et al., 2013; Halliday et al., 2016; Pétron et al., 2012; Swarthout et al., 2013; Thompson et al., 2014). These studies reported significantly enhanced methane, light alkanes, and benzene associated with O&G operations. These source apportionment analyses showed that O&G activities contributed more than 70% of light alkanes (Abeleira et al., 2017; Gilman et al., 2013; Pollack et al., 2021). Air masses containing O&G emissions have also been observed at Rocky Mountain National Park in the mountains west of the NFR, with resulting contributions of up to 20 ppb of ozone (Benedict et al., 2019). Photochemical box model simulations characterizing the influence of VOC emissions on ozone production (Lindaas et al., 2019; McDuffie et al., 2016) indicated that O&G VOCs

contributed 20-30% of photochemical ozone production during summer. Cheadle et al. (2017) reported significantly varied local ozone levels during mobile measurements and concluded that O&G emissions can be a primary contributor to NFR elevated ozone (up to 20-30 ppb).

Research to date has documented a significant influence of O&G-related emissions on elevated ozone in the NFR while indicating a need for additional studies to investigate contributions of other emission sources (e.g., landfills, wastewater treatment, animal operations, and agriculture) to ozone production in the region. Many studies have focused on short observation periods, making it challenging to adequately represent longer term conditions and their variability in time and space. Ozone production efficiency is sensitive to ratios of VOC/NO_x that vary with both season and location (Bien and Helmig, 2018). NO_x levels are strongly influenced by both O&G and vehicle emissions, while VOC levels tend to be determined by spatial patterns in emission sources (e.g., urban areas, O&G operations, and vegetation) across the region as well as meteorological conditions. VOC/NO_x ratios are generally expected to be lower near the Denver metropolitan area, reflecting urban traffic emissions, and higher near O&G operations. Bien and Helmig (2018) analyzed 15-years of hourly surface ozone data from 80 monitoring sites in Colorado from 2000 to 2015. They found larger seasonal cycles in diurnal amplitude during summer at locations near O&G operations than in the Denver metropolitan area and attributed the difference to differing VOC/NO_x ratios. With continuous changes in NO_x and VOC levels from urban and O&G development and increasingly strict regulations on O&G and other industry and traffic emissions, contributions of these sources to NFR ozone levels remain a challenging and moving target.

1.6 Study Objectives and Chapter Overview

This study mainly focuses on analyzing observations obtained in Broomfield during the development of six new multi-well O&G pads from Fall 2018 through 2023. We also examine VOC and methane observations across Broomfield and from other extensive field campaigns conducted in the DJB and the PB of Colorado. The primary study objectives are:

- Use an extensive monitoring program to determine air quality impacts during different UOGD operational phases in nearby residential neighborhoods of Broomfield. Major phases of interest included well drilling, hydraulic fracturing (fracking), flowback, production, and shorter-term processes including coiled tubing operations/millout, installation of production tubing, and production site maintenance activities.
- Investigate ozone formation potential in Broomfield by computing OH reactivities based on VOC measurements associated with specific O&G operations, including well drilling and completions and production.
- Examine relationships between levels of individual VOCs and levels of methane, ethane, and propane in emissions from a range of O&G operations to determine the extent to which emissions of methane, ethane, or propane might serve as useful predictors of other VOC emission rates.

Chapter 1 provides an overview of UOGD in the U.S. and in Colorado and air quality impacts arising from these operations. Chapter 2 introduces the Broomfield Study, where an extensive monitoring program was initiated in October 2018 and continued through 2022. Emissions from O&G operations during well development and O&G production in Broomfield affect VOC composition and concentrations in the surrounding region are investigated. Chapter 3 examines OH reactivities in Broomfield and how they are influenced by O&G emissions while

Chapter 4 explores relationships between UOGD emissions of individual VOCs and methane in order to assess whether more common measurements of methane emissions can provide useful information about O&G emissions of benzene, a key air toxic, or other less commonly measured VOCs. Chapter 5 presents study conclusions and outlines recommendations for future work.

Chapter 2

Air Quality Impacts from the Development of Unconventional Oil and Gas Well Pads: Air Toxics and other Volatile Organic Compounds [1]

2.1 Introduction

Volatile organic compounds (VOCs) are emitted by a wide range of natural and anthropogenic sources, including vegetation, wildfires, traffic, volatile chemical products, and oil and gas extraction (Atkinson and Arey, 2003; Gkatzelis et al., 2021; Permar et al., 2021; Russo et al., 2010; Simpson et al., 2010; Yokelson et al., 2003). VOCs play an important role in atmospheric chemistry by influencing atmospheric oxidative capacity, including the abundance of ozone (O_3), hydroxyl radical (OH), and hydroperoxides (Helmig et al., 2014; Hobbs et al., 2003; Yokelson et al., 2009). VOC contributions to ozone production are of particular interest given the challenge many communities face in reducing unhealthy ozone levels (Benedict et al., 2019; Lindaas et al., 2019; Peng et al., 2021). Some VOCs are important precursors to secondary organic aerosol (SOA) production (Akagi et al., 2012; Evanoski-Cole et al., 2017) and some are air toxics that act as carcinogens and/or otherwise impact human health (McKenzie; McMullin et al., 2018; O'Dell et al., 2020).

The oil and natural gas (O&G) industry is an important emitter of NO_x (NO_x = NO + NO_2), methane (CH_4), and a wide range of VOCs (Cheadle et al., 2017). Improved extraction techniques, including horizontal drilling and hydraulic fracturing, have enabled rapid expansion of

[1]The results outlined in Chapter 2 have been published in the Atmospheric Environment: I-Ting Ku, Yong Zhou, Arsineh Hecobian, Katherine Benedict, Brent Buck, Emily Lachenmayer, Bryan Terry, Morgan Frazier, Jie Zhang, Da Pan, Lena Low, Amy Sullivan, Jeffrey L. Collett, 2024: Air quality impacts from the development of unconventional oil and gas well pads: Air toxics and other volatile organic compounds. Atmospheric Environment, 317, doi: https://doi.org/10.1016/j.atmosenv.2023.120187, URL: https://www.sciencedirect.com/science/article/pii/S1352231023006131

unconventional oil and gas development (UOGD) in the United States (U.S.). These advances in technology helped the U.S. become the world's largest producer of both oil and natural gas (U.S. EIA, https://www.eia.gov/todayinenergy/detail.php?id=48756, accessed on 20 February 2023). U.S. UOGD occurs in both rural and populated regions and growing development has raised concerns about impacts on the environment and human health. Numerous studies have examined methane emissions from the O&G industry; fewer studies (e.g., Buzcu and Fraser (2006); Buzcu-Guven and Fraser (2008); Gilman et al. (2009); Hecobian et al. (2019); Leuchner and Rappenglück (2010); Prenni et al. (2016); Roest and Schade (2020); Rutter et al. (2015); Ryerson et al. (2003)) have examined emissions and air quality impacts of O&G VOCs. Many VOC-focused studies have looked at combined emissions from a large number of sources in an O&G production basin. Long-term study of O&G emissions from development of individual O&G well pads remains uncommon. Bari et al. (2016) conducted a long-term study of the impact of emissions from Alberta oil sands development on the surrounding community, examining concentrations of VOCs and their trends in time and comparing them to chronic and acute health risk screening criteria. Jarosławski et al. (2022) reported air pollutant concentration changes during the development of shale gas wells in Poland. Both studies highlight the value of continuous ambient monitoring to inform the public and other stakeholders about air quality impacts of UOGD. Such information is critical to evaluate potential health risks from UOGD in populated regions and to identify strategies to reduce O&G air pollutant emissions and associated impacts through process improvement in the technologically complex and evolving operational practices associated with new well development.

The State of Colorado, home to the Piceance and Denver-Julesburg (DJ) Basins and approximately 50,000 active O&G wells (Colorado Oil & Gas Conservation Commission

(COGCC), https://cogcc.state.co.us/data2.html#/downloads, accessed on 16 May 2023), ranked seventh among U.S. states for overall 2021 energy production (U.S. EIA, https://www.eia.gov/state/print.php?sid=CO, accessed on 20 February 2023). Home to the majority of Colorado's wells, the Denver-Julesburg Basin (DJB) sits NE of the Denver metropolitan area and within the Denver Metro/North Front Range ozone non-attainment area. Considerable UOGD within the basin occurs near residential areas. Several studies have been conducted in the DJB to characterize VOC emissions and source contributions (Abeleira et al., 2017; Gilman et al., 2013; Pétron et al., 2012; Pétron et al., 2014; Pollack et al., 2021; Swarthout et al., 2013; Thompson et al., 2014). These studies report strong O&G influence on regional air quality, including ozone (Abeleira et al., 2017; Benedict et al., 2019; Gilman et al., 2013; Lindaas et al., 2019; McDuffie et al., 2016; Sullivan et al., 2016; Swarthout et al., 2013). McKenzie et al. (2018) assessed health risks from air pollutants emitted by O&G facilities suggesting higher acute and chronic health risks for residents living close to these facilities. Even in 2012, prior to recent UOGD and population growth, 19% of the population in the DJ Basin lived within 1.6 km of an active O&G well site (McKenzie et al., 2016).

UOGD typically involves several steps, including well drilling (often including long horizontal legs to better access layered hydrocarbon deposits), hydraulic fracturing (the creation of fractures in the hydrocarbon formation to aid in O&G recovery), and flowback (the return of injected fracturing fluids and produced water from the formation to the surface) (U.S. EPA, https://www.epa.gov/uog/process-unconventional-natural-gas-production, accessed on 17 May 2023; Field et al., 2014; Hecobian et al., 2019; Orak et al., 2021). Each of these steps is a complex process and intermediate activities (e.g., coiled tubing operations/millout and installation of production tubing) are also scheduled. For large pads with many wells, these processes extend

over several months to a year before wells are in production. Current understanding of O&G well pad emissions comes, in part, from shorter-term snapshots of process level emissions (e.g., Hecobian et al. (2019)). An analysis utilizing measured emissions distributions (Hecobian et al., 2019), regional meteorological conditions, and dispersion modeling simulations assessed human health risks from exposure to VOCs emitted from O&G operations (Holder et al., 2019) and informed statewide implementation of a 2000 foot (610 m) setback distance to better protect residential populations. Long-term air toxics observations around O&G operations, however, are needed to assess the accuracy of modeled concentration fields and exposures. Further, UOGD emissions have changed as operators implement new, emission-reducing practices.

Plans for the development of six new large, multi-well O&G pads in areas close to neighborhoods and schools in the City and County of Broomfield, Colorado (CCOB, population 76,000) raised local concerns that spurred development of an operator agreement incorporating several management practices to help protect the environment, public health, and safety of residents. These included use of grid-powered electric drill rigs, installation of pipelines and use of closed loop fluid handling systems to reduce truck traffic and reduce air emissions during transport of water and O&G products, and eliminating use of permanent, on-site storage tanks. An extensive monitoring program was also designed and periodically updated to determine air quality impacts during different UOGD operational phases. Major phases of interest included well drilling, hydraulic fracturing (fracking), flowback, production, and shorter-term processes including coiled tubing operations/millout, installation of production tubing, and production site maintenance activities. Air monitoring, begun prior to development and continued through pad production, included extensive spatial monitoring across the community to document air quality changes near well pads and in nearby residential neighborhoods. Weekly integrated measurements were

included to examine spatial gradients and air pollutant exposure on longer (chronic) timescales. Fast measurements (seconds to minutes) were incorporated to better reveal plumes associated with transient emissions and short (acute) exposure events. Findings from this program are presented here to provide important and novel insight into the air quality impacts of modern UOGD operations with extensive best management practices (BMPs) and to help identify operations where opportunities remain for future emission reductions.

2.2 Method

2.2.1 Site description and UOGD operations schedule

Broomfield is located 22 km NW of Denver in the SW corner of the DJ Basin (Figure 2.1 (a)). Air monitoring was initiated in October 2018 and continued through 2022. Measurements discussed include sites equipped with canisters for weekly VOC sampling and real-time photoionization detectors equipped to trigger canisters for characterizing transient VOC plumes. Monitoring sites included ten locations near O&G well pads, eight in nearby neighborhoods, and one at a more distant regional background site (Broomfield Commons ~5–7 km SSE of the new well pads). A proton transfer reaction mass spectrometer (PTR-MS) was operated at a neighborhood location for continuous measurement of benzene, toluene, ethylbenzene, and xylenes (BTEX). As many as 19 sites were operational at a time and a core set of near-pad, neighborhood, and background sites operated throughout the study period. Detailed site information and sampling schedules are shown in Figure 2.1 (b), Figure A.1, and Table A.1 and A.2. A hybrid sport utility vehicle was equipped for fast mobile measurement of methane and ethyne (acetylene, C_2H_2) and in-plume collection of canister grab samples for VOC speciation.

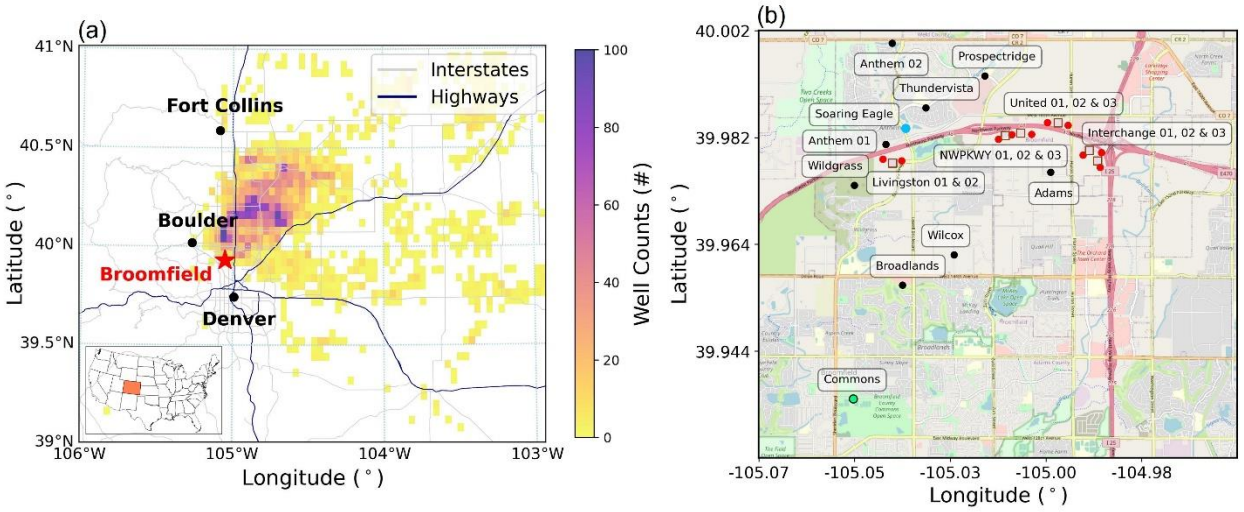

Figure 2.1: (a) Map of the study region. The red star marks the location of Broomfield, approximately 22 km NNW of Denver; well counts are overlaid on the map (COGCC, https://cogcc.state.co.us/data2.html#/downloads, accessed on 10 May. 2023) (b) Map of the Broomfield air quality monitoring program sites. Brown squares indicate the six well pad locations. Red dots indicate air monitoring sites set up around O&G pads; black dots represent neighborhood monitoring sites; the green dot represents the background site (Commons); the blue dot shows the PTR-MS location at Soaring Eagle Park (base map courtesy of OpenStreetMap, https://www.openstreetmap.org/).

Each of the six developed well pads included 8 to 17 wells that underwent drilling, hydraulic fracturing, and flowback before being placed into production. A detailed operations schedule for development of the first two new O&G well pads is shown in Table A.3. The Interchange B pad and the Livingston pad were first to be developed, during 2019 and 2020. With the advent of the COVID pandemic and reorganization and merger of the O&G operator, the remaining pads (Interchange A, NWPKWY A & B, and United) were not developed until 2021-2022.

2.2.2 Sample collection

2.2.2.1 PID continuous air monitoring systems

Beginning in 2020, real-time monitoring systems (APIS, Inc., OR, USA) were deployed to measure a suite of VOCs and meteorological parameters across the Broomfield air monitoring network. Each Apis unit is equipped with wind, humidity, pressure and temperature sensors. VOCs

are detected using a 10.6 eV high sensitivity Photoionization Detector (PID) sensor (MiniPIDs-HS, ION Science Inc., TX, USA). The PID is calibrated using isobutylene; response varies by species and is interpreted here as a semi-quantitative measurement of the integrated mix of total VOC (TVOC) photoionized at 10.6 eV. Response factors for individual VOCs are available from the manufacturer (TA-02, http://www.ionscience.com/usa). The Apis PID sensor features a measurement range from 0.5 ppbv to 3 ppmv (isobutylene equivalent). The sensor has a 15 s sampling rate and reported 1 min integrated data for TVOC and meteorological parameters. Acetone bump tests were conducted in the field to ensure PID functionality. While the PID response is a semiquantitative indicator of the TVOC mixing ratio, it generally works well to detect rapid changes associated with arrival of VOC-rich plumes. During typical background conditions in Broomfield, the PID baseline signal ranged from 80 to 150 mV with ±10 mV drift. Apis PID systems were coupled with automatic canister triggering devices to collect air samples (~15 s fill time) in evacuated 1.4-L Silonite®-coated canisters (*Entech* Instruments, CA, USA). The trigger threshold was initially set at ~300 mV across the network and later increased to 500 mV (neighborhood impact sites, Table A.1) and 800 mV–1500 mV (near-pad O&G sites, Table A.1) in order to better capture peak VOC plume concentration levels. While environmental interference or sensor aging sometimes led to collection of false positive samples (i.e., triggered canister VOC concentrations were not significantly elevated above background), the system overall worked well to detect and characterize plumes with elevated VOC concentrations and VOC compositions indicative of oil and gas emissions. In total 91 PID-triggered canister samples with significantly elevated VOC concentrations (at least 3 standard deviations above the weekly mean total VOC concentration at the Commons reference site) were collected between February 2020 and December 2022.

2.2.2.2 Weekly whole air canister samples

Weekly air samples were collected using evacuated 6.0-L Silonite®-coated stainless steel canisters coupled with CS1200E flow regulation systems (both from *Entech* Instruments). The flow control system enabled each canister to slowly fill over a 7-day sample period. Canisters were cleaned using an *Entech* 3100 Canister cleaning system before field deployment by evacuating the canister to 10^{-2} torr and purging with ultra-high purity nitrogen for 8 cycles at 80 °C. Laboratory blank samples were collected by filling cleaned canisters with ultra-high purity nitrogen.

The weekly canister sampling schedule across the monitoring network is shown in Figure A.1. Briefly, weekly air sample canisters were collected at four sites (Anthem 01, Commons, Interchange 01, and Livingston 02) from October 2018–January 2019. Afterward, once well development was underway, six to eighteen weekly air sample canisters were deployed across the monitoring network according to the varying pre-production activities at the well pads. 1324 weekly integrated samples, collected from 4 October 2018 to 29 July 2021, are included in this study, encompassing the full well development cycle and early stages of production for the first two well pads, Interchange B and Livingston.

2.2.2.3 Proton-transfer-reaction mass spectrometer

A quadrupole proton transfer reaction mass spectrometer (PTR-MS; Ionicon Analytik, Innsbruck, Austria) was operated beginning April 2020 at the Soaring Eagle Park neighborhood site to continuously monitor (measurement cycle ~90 s) BTEX (benzene, toluene, ethylbenzene, and xylene) and select other compound concentrations. The PTR-MS was installed in a climate-controlled shelter operated by Boulder AIR LLC. The sample inlet was ~10 m above the ground; a diaphragm pump drew air at ~9.5 mL min^{-1} through a PFA Teflon tube with a sample sub-stream of ~2 mL min^{-1} drawn into the PTR-MS. The instrument drift tube pressure and temperature were

2.2 mbar and 45 °C, respectively; a potential of 570 V was applied over the 9.3 cm of the drift tube resulting in an E/N of 122 Td (Townsend). Ultrapure water was used to produce the H_3O^+ reagent ion source, and its flow rate was 6 mL min^{-1} with a discharge current of 4 mA. We applied a specific rate constant for each species of interest with H_3O^+ ions as listed in Table A.5. Calibrations of the PTR-MS system were done monthly using two calibration standards containing blends of select VOCs in nitrogen diluted with zero air to ambient levels. Compound accuracies for the calibration standards were < ±5% for all species and measurement precisions ranged from 5 to 9%.

2.2.2.4 Mobile sampling

An instrumented hybrid SUV "plume tracker" (Hecobian et al., 2019) was deployed periodically to survey methane and VOC concentrations across Broomfield and to identify and locate sources of high concentration plumes. The plume tracker was equipped with a Picarro G2203 analyzer (Picarro, Santa Clara, CA), measuring methane and ethyne by cavity ring-down spectroscopy (CRDS) with 2 Hz measurement interval. An AMETEK® Mocon® Baseline 9100 gas chromatograph with PID detector measured BTEX compound concentrations in a 6-min measurement cycle. The inlet for the Piccaro was located in front of the vehicle ~3 m above ground level and was connected with 4.5 m Teflon® tubing; air was sampled at 0.2 L min^{-1}. The inlet for the GC was on the right side of the vehicle, connected with a 1-m Teflon tube sampling at 0.25 L min^{-1}. Picarro and AMETEK® Mocon® manufacturer calibrations were verified using certified calibration gases (methane from SCOTT-MARRIN Inc., CA, USA; BTEX from Airgas, PA, USA). The precisions (2 s, 1 RSD) of methane and ethyne were 3 ppbv and <600 pptv, respectively. Precisions (1 RSD) ranged from 1.6 to 3.7% for BTEX compounds.

An A21 Global Position System (GPS, Hemisphere GNSS Inc., AZ, USA) and Climatronics' SonimometerTM (P/N 102779-A1-C1-D0; Climatronics Co., NY, USA) were

mounted in front of the SUV at a height of ~3 m and featured a 2 Hz measurement rate. Measured data were displayed inside the vehicle to aid plume identification. Manually triggered (~15 s) whole air samples (evacuated 1.4-L Silonite® canisters) were collected outside the vehicle, in background air and in-plume, and analyzed as outlined above.

2.2.3 Chemical analysis of air samples

Methane and VOCs were measured in each canister sample by gas chromatography (GC) at the Colorado State University Atmospheric Science Department. Methane was analyzed using a Shimadzu GC-8A equipped with a digital temperature programmer and flame ionization detector (FID). The analytical column consisted of two 6' x 1/8" O.D. stainless steel columns packed with Porapak Q. Samples were injected at room temperature, and the column oven temperature was held at 40 °C. Ultra-high purity nitrogen (Airgas Inc., NI UHP300) was used as a carrier gas and zero air (Airgas Inc., AI UZ300) plus ultra-high purity hydrogen (Airgas Inc., Hy UHP300) was supplied to the FID. A methane standard (SCOTT-MARRIN Inc., CA, USA), 20.41 ± 1% ppmv in ultrapure nitrogen, was used to calibrate the working standard. At least five working standard injections were analyzed in each analysis batch to assess system drift or malfunction. The methane measurement precision (1 relative standard deviation, RSD) was 4%. The methane method detection limit (MDL) was 0.21 ppmv.

50 VOCs were measured in each canister sample using a custom, multi-channel GC system described in previous studies (Benedict et al., 2019; Sive et al., 2005; Zhou et al., 2005). Briefly, the system includes three GCs and five detectors (three FIDs, one electron capture detector (ECD), and one mass spectrometer (MS)). Analyzed gases included C_2–C_{10} non-methane hydrocarbons (NMHCs, including linear, branched, and cyclic alkanes, alkenes, alkynes, and aromatics) and C_2 halocarbons. A complete list of analyzed compounds and their detection limits is included

in Table A.4. The system was calibrated using a certified mixed hydrocarbon standard (HC Mix56, Airgas, PA, USA). Multiple working standards were analyzed during each analysis batch to check system drift and to derive VOC response factors. The measurement precision (1 RSD) of C_2–C_{10} NMHCs varied from 2% to 18% and from 14% to 20% for C_2 halocarbons. The accuracy for the calibration standard is ±5%.

2.2.4 Data analysis

To compare emission profiles during different pre-production activities, 49 non-methane VOCs (excluding ethane) were grouped into nine categories including C_3–C_7 n-alkanes, C_8–C_{10} n-alkanes, cyclic alkanes, branched alkanes, alkenes, BTEX, aromatic hydrocarbons other than BTEX, halogen-containing hydrocarbons, ethyne and isoprene (see Table A.6 for compound list). To examine impacts of O&G activities near Broomfield well pads, data are categorized into nine groups based on three sampling location types (background, neighborhood impact, and O&G near-pad sites, Table A.1) and three sampling periods (prior to new well pad construction (None), during pre-production activities (well drilling and completions up to the start of production) and after moving to production, Table A.2).

We analyze here weekly data collected from the start of the monitoring program through July 2021. During this period wells were drilled, completed, and went into production at the Interchange B and Livingston pads. These two pads are separated by approximately 4 km, facilitating interpretation of local VOC concentration increases during well development operations at either pad. Weekly observations become more difficult to interpret later in the study when multiple well pads were under development in close proximity. We examine data from PID-triggered canister samples collected from deployment in February 2020 through December 2022 to provide a good overview of VOC concentrations in transient plumes detected during UOGD

pre-production and production activities. Ascertaining the source(s) influencing a triggered-canister sample is easier than for weekly samples because the 15 s collection period of the triggered-canister sample can be directly compared with wind direction.

2.3 Results and Discussion

2.3.1 VOC concentrations and their spatial and temporal variations

Figure 2.2 compares mixing ratios of six VOC species (ethane, propane, n-hexane, n-octane, benzene and ethyne) collected at three groups of sites (background, neighborhood impact, and near-pad O&G sites) in Broomfield with VOC measurements from previous studies in and near-pad O&G sites) in Broomfield with VOC measurements from previous studies in Colorado. These six species are selected to represent light to heavy alkanes that can be associated with O&G development, key air toxic benzene (U.S. EPA, https://www.epa.gov/haps/initial-list-hazardous-air-pollutants-modifications, accessed on 17 May 2023) that often is found at the highest level relative to established health guideline values (McKenzie et al., 2018), and ethyne, a compound often associated with combustion/traffic emissions (Choi and Ehrman, 2004; Gilman et al., 2013; Pollack et al., 2021; Russo et al., 2010; Thompson et al., 2014). Overall statistics for methane and the full suite of VOCs measured in Broomfield are provided in Table A.6. The Broomfield O&G near-pad sites had higher mixing ratios of O&G-related species than observed at Broomfield background and neighborhood impact sites, suggesting impacts from local O&G emissions. We will examine this hypothesis in greater detail below by investigating spatial patterns in conjunction with detailed timelines of well development at individual well pads.

The mean mixing ratios of the six highlighted VOCs measured in Broomfield are significantly higher than mean values reported for Rocky Mountain National Park (ROMO)

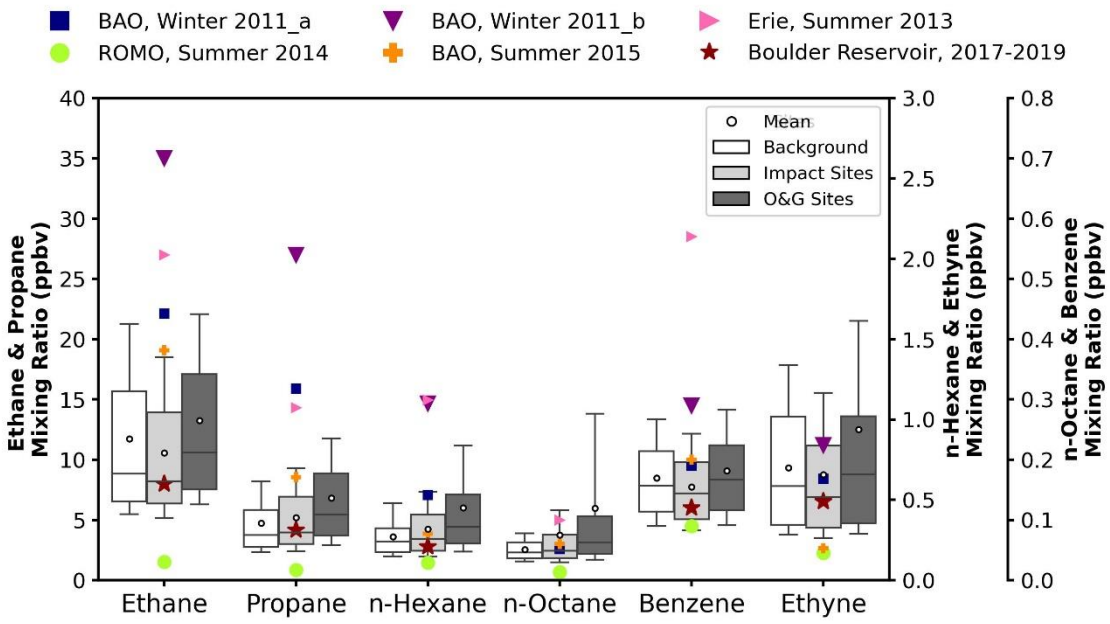

Figure 2.2: Statistics of weekly average mixing ratios for six VOCs measured October 2018 to July 2021 across three categories of Broomfield sampling sites (Background, Neighborhood Impact Sites, and near-pad O&G sites). The boxes show the 25th to 75th percentiles of the data, the line represents the 50th percentile, the white dot indicates the mean, and the 10th and 90th percentiles are represented as whiskers. Mean mixing ratios of these VOCs measured in other studies at the Boulder Atmospheric Observatory (BAO) in Erie, Colorado during winter 2011 (dark blue ■ and purple ▼) and summer 2015 (orange ✚) (Abeleira et al., 2017; Gilman et al., 2013; Swarthout et al., 2013); in Erie, Colorado during spring and summer 2013 (pink ►) (Thompson et al., 2014); at eight rural locations close to Rocky Mountain National Park during summer 2014 (lime ●) (Benedict et al., 2019); and at the Boulder Reservoir in Boulder, Colorado from April 2017 to December 2019 (red ★) (Pollack et al., 2021) are shown for comparison.

(Benedict et al., 2019) and slightly higher than values reported at Boulder Reservoir (Pollack et al., 2021). Although ROMO is impacted by urban and O&G-related emission sources from the Colorado North Front Range (Benedict et al., 2019), dilution during transport to this remote mountain location produces much lower mixing ratios than observed at sites located on the plains. The lower mixing ratios of VOCs at Boulder Reservoir are consistent with its rural location ~20 km NW of Broomfield. Mean Broomfield mixing ratios of ethane, propane, n-hexane and benzene are much lower than those from previous studies at Boulder Atmospheric Observatory (BAO) (Abeleira et al., 2017; Gilman et al., 2013; Swarthout et al., 2013) and other neighborhood

locations in Erie (Thompson et al., 2014), located just north of Broomfield. The BAO tower and other Erie sites are close to active O&G operations and the measurements there were made several years prior to our Broomfield observations. Differences in concentrations of these VOCs, which can all be emitted by O&G operations, likely reflect differences in the seasons samples were collected (e.g., winter vs. summer vs. year-round), proximity to regions of major O&G development, and/or emissions reductions due to implementation of new UOGD practices over time in the DJ Basin and during Broomfield UOGD in particular.

Smaller variations are seen across studies in mean mixing ratios of n-octane and ethyne. Ethyne is often considered as a tracer for urban/traffic combustion emissions and observed levels can be much higher than seen here in metropolitan areas such as downtown Denver or in highly industrialized regions (Leuchner and Rappenglück, 2010; Thompson et al., 2014). As outlined below, however, there is strong evidence of a previously unreported O&G source of ethyne in Broomfield. Even though Wilde et al. (2021) and Swarthout et al. (2013) suggested that O&G production is not a key source of heavy alkanes, we found C_8–C_{10} n-alkanes very strongly enriched locally during Broomfield drilling activities (see discussion below). Roest and Schade (2020) have also observed elevated long-chain hydrocarbons associated with O&G sources in Texas.

Several previous studies show that ethane is a dominant compound among non-methane VOCs both in urban areas and in regions impacted by O&G emissions (Abeleira et al., 2017; Baker et al., 2008; Buzcu and Fraser, 2006; Orak et al., 2021; Pollack et al., 2021; Swarthout et al., 2013). Overall, ethane accounted for 17%–59% of reported non-methane volatile organic compound concentrations in weekly Broomfield samples. To characterize O&G-related hydrocarbon mixing ratio variations without undue influence by the most abundant compounds, O&G-related VOC mixing ratios were calculated by summing all measured alkanes (excluding methane and ethane).

Figure 2.3 shows timelines of the minimum, mean, and maximum O&G-related VOC and benzene mixing ratios across all Broomfield sites with O&G development phases highlighted. Drilling began in April 2019 at the Interchange B pad followed by well completion (hydraulic fracturing and flowback) activities, together comprising the pre-production phase. All wells on this pad were in production by March 2020. Livingston pad drilling began in July 2019 and all

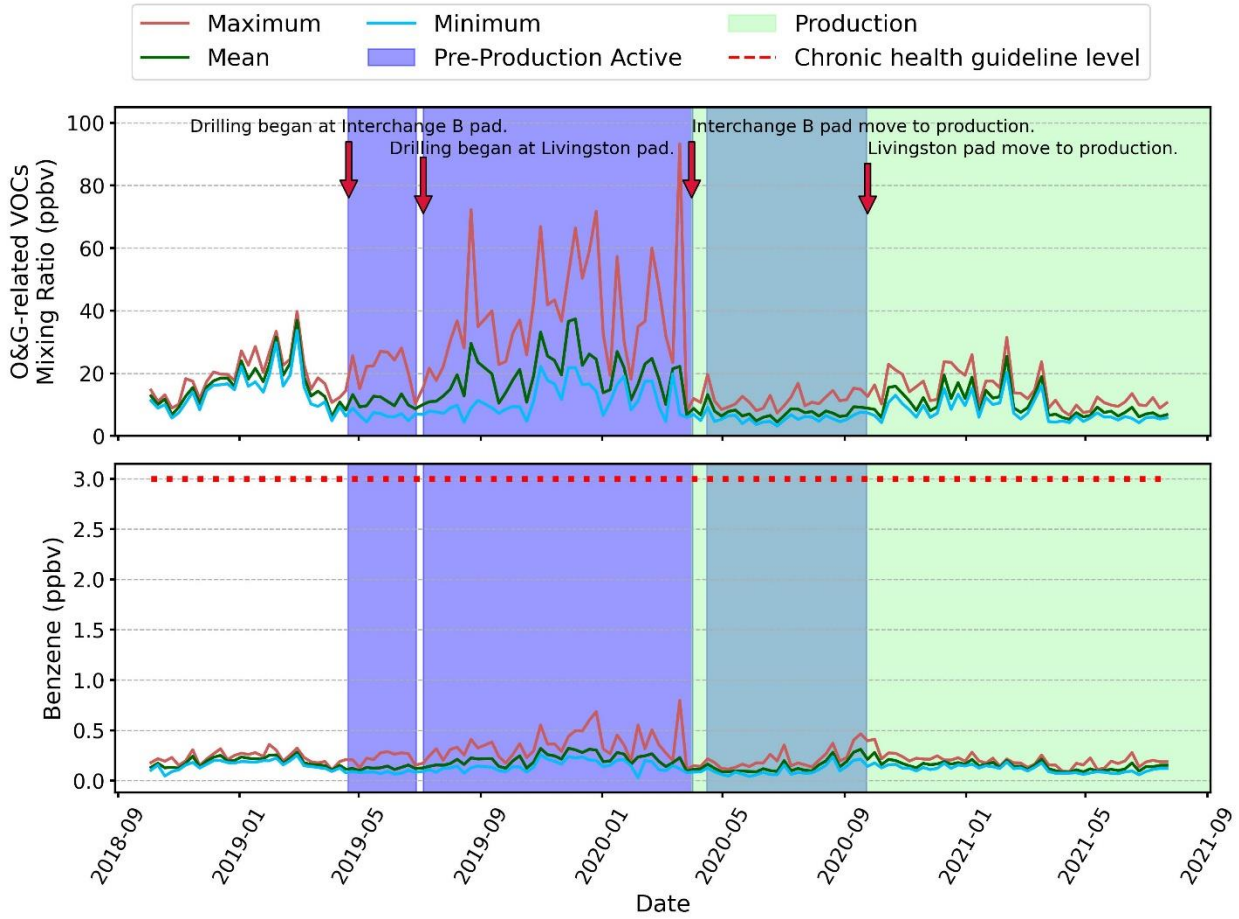

Figure 2.3: Time series of the maximum, mean, and minimum mixing ratios of O&G-related volatile organic compounds excluding ethane (top) and of benzene (bottom) observed across the monitoring network in Broomfield from October 2018 to July 2021. Observations started before O&G development and continued during pre-production activities (purple shading) and production (green shading). The blue shading represents the period when the Interchange B pad had moved to production but the Livingston pad was still in pre-production. The red dashed line indicates the 3.0 ppbv chronic health guideline value for benzene exposure (Agency for Toxic Substances and Disease Registry, ATSDR (Wilbur et al., 2007)).

wells were in production by September 2020. Differences between minimum and maximum O&G-related VOC and benzene mixing ratios measured across Broomfield sites were generally small prior to the start of drilling, increased during well drilling and completion (pre-production) activities, and decreased again as wells went into long term production. Maximum O&G-related VOC values during pre-production activities were measured at near-pad sites 96% of the time, indicating that the increased spread between minimum and maximum O&G-related VOC values was primarily caused by local O&G emissions. The sum of O&G-related VOC compounds ranged from 3.2 ppbv to 93.3 ppbv with an average value of 13.4 ppbv; the maximum value was observed during the week of 19 March 2020 at the Livingston 02 site during Livingston Pad coil tubing/millout operations (the removal of plugs previously used to isolate hydraulic fracturing zones). Weekly average benzene mixing ratios ranged from 0.03 ppbv to 0.80 ppbv with a mean value of 0.16 ppbv. The maximum weekly benzene mixing ratio was seen in the same Livingston 02 sample collected during coil tubing/millout operations; this sample also contained the maximum weekly ethane (61.6 ppbv) and propane (34.1 ppbv) mixing ratios.

The wide range of O&G-related VOC mixing ratios observed during the study reveals significant variability in local air quality and is influenced by several factors. Across the network seasonal changes are driven by changes in emissions, atmospheric stability, and oxidation rates. Spatial concentration differences are influenced by the distance from local emission sources, such as O&G pre-production activities. Monthly variations of weekly O&G-related VOCs across the study's three site categories are shown in Figure 2.4 (a) Consistent with previous studies (Helmig et al., 2014; Pollack et al., 2021; Thompson et al., 2014; Zheng et al., 2018), elevated levels of O&G-related VOCs were observed across all site types during wintertime, when cold temperatures, clear skies, and snow-cover frequently enhance atmospheric stability and enhance accumulation

of local pollutant emissions. Figure 2.4 (b) compares O&G-related VOC mixing ratios observed, by site type, through various O&G operational phases. Mixing ratios of O&G-related VOCs were significantly (t-test, 95% confidence level) higher at near-pad O&G and neighborhood impact sites than at the background site during pre-production operations.

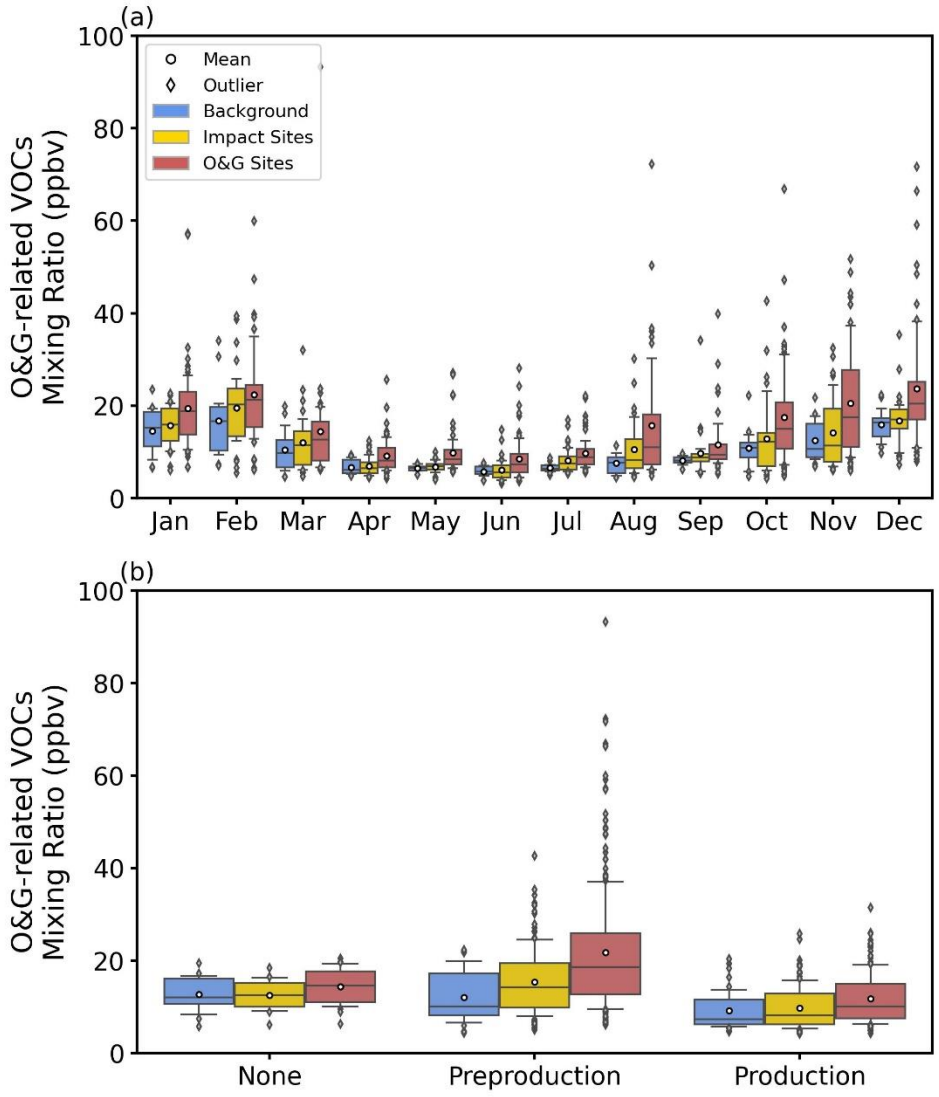

Figure 2.4: Box and whisker plots (90th, 75th, 50th, 25th, 10th percentiles) including mean and outlier values of O&G-related VOC mixing ratio for the Broomfield background, neighborhood impact, and near-pad O&G site types. Panel (a) shows observations by month of the year; panel (b) compares mixing ratios before the start of pad construction (none), during drilling and completion (pre-production) activities, and after the well pads went into production.

Variations of chemical composition in 10 VOC groups for the three site types during different phases of well development are shown in Figure A.2. C_3–C_7 n-alkanes are the dominant VOC species in the region, accounting for ~76% on average of all measured VOC mixing ratios (TVOC-49, excluding methane and ethane). The Commons background site tended to have slightly lower C_3–C_7 n-alkane and slightly higher alkene, BTEX and ethyne abundance compared to neighborhood impact and near-pad O&G sites even before the start of well pad development. This reflects the location of this site closer to the Denver metro area and further from the large number of O&G wells NE of Broomfield as well as greater traffic density on nearby roads. Previous studies found vehicular emissions were a significant source of alkenes and aromatics in the region (Gilman et al., 2013; Pollack et al., 2021). During pre-production operations, we observed increased contributions of C_8–C_{10} n-alkanes, cyclic, and branched alkanes at neighborhood impact and O&G sites. Simpson et al. (2010) reported that > C_5 alkanes and cyclic alkanes are important components of crude oil and several field studies showed that cyclic alkanes were associated with O&G emissions (Gilman et al., 2013; Swarthout et al., 2013). As discussed below, a close association was also seen between Broomfield drilling operations and local concentrations of C_8–C_{10} n-alkanes.

2.3.2 Alkane ratios

Different emission sources often feature distinct VOC signatures; therefore, ratios of various VOCs are sometimes used to characterize changing source contributions (Karl et al., 2009; Leuchner and Rappenglück, 2010). For example, the ratio of i-pentane to n-pentane has been established as a robust indicator to distinguish influence from urban/traffic versus O&G emissions (Abeleira et al., 2017; Gilman et al., 2013; Pollack et al., 2021; Swarthout et al., 2013; Thompson et al., 2014; Wilde et al., 2021). Combustion emissions and evaporation of processed petroleum

products tend to yield higher abundances of i-pentane (Baker et al., 2008; Leuchner and Rappenglück, 2010; Na et al., 2004; Wilde et al., 2021) while i/n-pentane ratios below 1.0 tend to be indicative of O&G emissions (Ghosh, 2018; Gilman et al., 2013; Halliday et al., 2016; Hecobian et al., 2019; Pollack et al., 2021; Prenni et al., 2016; Swarthout et al., 2013; Thompson et al., 2014; Wilde et al., 2021). The two isomers react at similar rates with OH radicals (Atkinson, 1997), helping to preserve source ratios during atmospheric transport. The i/n-pentane ratio observed in weekly samples in this study was lowest (~0.9) during the pre-production period at the near-pad O&G sites and highest (~1.19) during the production phase at the Commons background site (Figure A.4). These values are all lower than mean values measured at Boulder Reservoir (1.26) (Pollack et al., 2021) and in 2018–2020 morning samples in urban downtown Denver (1.25; CDPHE data, https://www.colorado.gov/airquality/tech_doc_repository.aspx, accessed on 27 February 2023), both of which are more distant from regional O&G emissions. The Broomfield values are similar to 2011 measurements at the BAO tower in Erie (0.94–1.11) (Swarthout et al., 2013), located just north of Broomfield and close to O&G operations, except that the pentane ratios at the near-pad sites in Broomfield are lower during pre-production operations. The low i/n-pentane ratios in Broomfield reveal a strong influence from regional O&G activities throughout the study with increased local O&G influence during pre-production activities. Ratios of i/n-butane in the Broomfield study ranged between 0.37 and 0.41, with the lowest values observed during pre-production activities. These are similar to values (0.40–0.42) previously reported in the Denver urban area and the DJB (Halliday et al., 2016) and to the ratio reported for gas matrix samples collected at the Broomfield Livingston and Interchange well pads (https://cogcc.state.co.us/data.html#/cogis, accessed on 27 February 2023). Additional discussion regarding other VOC ratios are presented in Appendix A.1.

2.3.3 VOC increases during well pad operations

Although several studies have been conducted around O&G fields and related facilities (Brantley et al., 2014; Esswein et al., 2014; Ghosh, 2018; Helmig et al., 2014; Hildenbrand et al., 2016; Jobson et al., 2004; Macey et al., 2014; Prenni et al., 2016; Warneke et al., 2014; Wilde et al., 2021; Zheng et al., 2018), only a few have included activity-specific monitoring (Colborn et al., 2014; Hecobian et al., 2019; Orak et al., 2021) and often only for limited time periods. Using the Broomfield observations, we are able to examine how VOC concentrations change over time and spatial scales as O&G wells are drilled, completed, and move into production. Because changes in season, prevailing meteorology, and regional emissions all influence VOC concentrations, we consider VOC excess mixing ratios: the mixing ratio at near-pad O&G sites minus the mixing ratio at the Commons background site. Figure 2.5 depicts time series of the excess mixing ratios of TVOC-49, ethane, benzene, C_8–C_{10} n-alkanes, ethyne, and isoprene at the near-pad O&G sites around the Interchange B and Livingston well pads along with each pad's operations schedule. Similar time series are included in Figure A.3 for alkenes, toluene, BTEX and i/n-pentane ratios. Periods of on-site operations, including drilling, hydraulic fracturing, coiled tubing operations, production tubing installation, and flowback, are illustrated; detailed operations dates are provided in Table A.3. The durations of such operations on a pad can range from days (e.g., coil tubing/millout or production tubing installation) to weeks/months (drilling, hydraulic fracturing, flowback) to years (production).

Excess mixing ratio values for individual VOCs during the period prior to the start of drilling are generally near zero, indicating that gradients in weekly average concentrations of these species across Broomfield were small prior to pad development. Significant local increases in TVOC-49, ethane, benzene, C_8–C_{10} n-alkane, and ethyne concentrations occur at various points

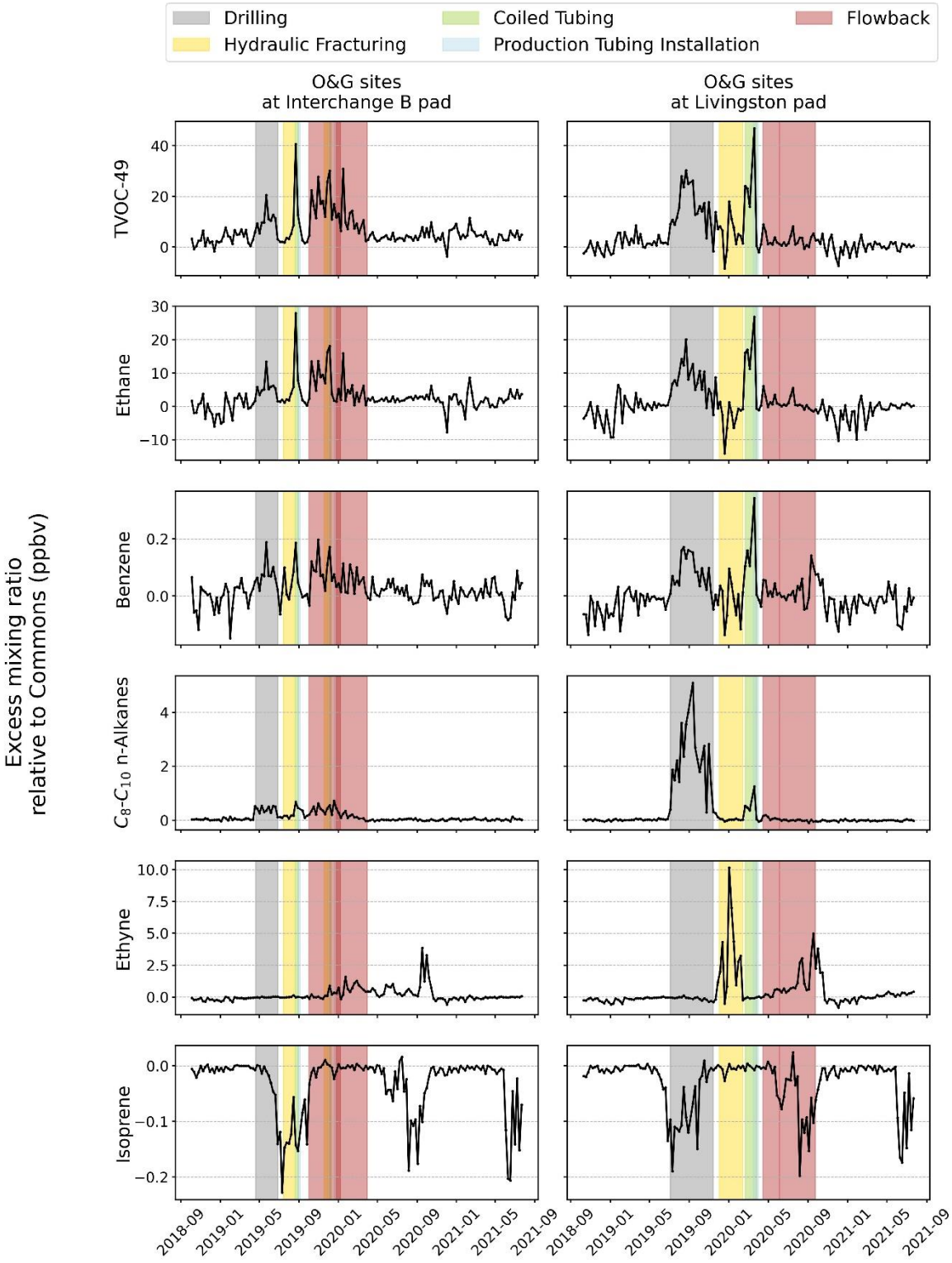

Figure 2.5: Time series of various averaged VOC excess mixing ratios (ppbv) at the Interchange B and Livingston near-pad sites relative to the Commons background site. The overlaid colors are different O&G pre-production activities.

during well pad development. Note that excess mixing ratios of some species rise and fall together during particular operational activities, while peak timing differs between other sets of species. The observed patterns also exhibit some similarities and some differences between the Interchange B and Livingston pads. Timelines of TVOC-49 and ethane excess mixing ratios exhibit similar temporal patterns for each pad. While TVOC-49 does not include ethane concentrations, it does include large contributions from other light alkanes (e.g., C_3–C_7 n-alkanes) that are strongly correlated with ethane in our ambient VOC dataset and in typical O&G emissions. The local increases in TVOC-49 and ethane are readily apparent at the Interchange B pad during drilling, coil tubing/millout, and flowback operations. Emissions of light alkanes occur when material from the subsurface hydrocarbon deposit is released to the atmosphere, especially during drilling through hydrocarbon deposits and during flowback operations when hydraulic fracturing fluids and produced water come to the surface at high temperatures. A lack of significant ethane increases during fracking operations is not surprising since material is being pushed downhole during this period, limiting opportunity for subsurface hydrocarbon venting to the atmosphere. Consistent with our findings here, Hecobian et al. (2019) also found greater emissions of light alkanes during drilling and flowback than during fracking operations in western Colorado. In that study, median ethane emissions during flowback were nearly ten times higher than during drilling. The fact that peak ethane excess mixing ratios during flowback operations at the Broomfield Interchange B pad were only slightly higher than those during drilling suggests that best management practices (e.g., closed loop fluid handling systems) employed to limit on-pad flowback emissions in Broomfield were successful relative to the green completion practices in place in Colorado several years earlier when flowback fluids were typically stored in tanks for some time on the pad. The Broomfield O&G operator made further (undisclosed) changes to control flowback emissions before well

completions at the Livingston pad and the lack of any clear increase in the TVOC-49 and ethane excess mixing ratios around the Livingston pad during flowback again suggests a positive outcome of those actions. As noted below, however, short periods of significant VOC emissions during flowback persist and warrant further attention.

Large increases in local concentrations of C_8–C_{10} n-alkanes were observed during drilling operations at the Livingston pad, with smaller increases apparent during coiled and production tubing operations. A similar pattern was observed during the same set of operations at the Interchange B pad; however, the C_8–C_{10} n-alkane concentration increases during drilling were less significant than at Livingston. This difference likely reflects a change in the drilling mud used at each pad. Drilling mud helps lubricate the drill bit and aids the return of drill cuttings to the surface. Various hydrocarbon-based drilling mud formulations are used depending on the nature of the reservoir, the location of drilling, and other factors. Gibson D822 petroleum hydrocarbon distillate-based drilling mud, used in drilling operations at the Interchange B pad and during drilling of the first well at the Livingston pad, generated significant odor complaints from nearby residents and prompted a change to the use of a synthetic paraffin Neoflo 4633-based drilling mud beginning with the second well at Livingston. Laboratory headspace analyses of Gibson and Neoflo drilling muds completed in our lab (see Figure A.6) revealed greater abundance of C_8–C_{10} n-alkanes volatilized from the Neoflo mud, consistent with the increased C_8–C_{10} n-alkane concentrations seen during drilling operations at Livingston.

Clear enhancements of ethyne were seen near the Livingston pad during hydraulic fracturing and again during the latter part of flowback and early production. Increased mixing ratios of benzene and of ethene, a common combustion emission, were also observed near the Livingston pad during the second ethyne enhancement period. The ethyne enhancements during

fracking are not surprising as this is a period with significant onsite power generation and truck traffic; increases during flowback are unexpected as combustion sources are typically limited on-pad during this phase. Figure 2.6 (a) shows timelines of benzene, toluene, and benzene/toluene ratio measured by the PTR-MS at the Soaring Eagle Park site northeast of the Livingston pad. A substantial increase in periods with benzene concentrations above 1 ppb was observed from mid-September to mid-October 2020, the period when high ethyne, benzene, and ethene levels were seen near the Livingston pad. A conditional probability function (CPF) analysis of high (>1 ppbv) benzene concentrations between 12 September and 12 October 2020 shows strong association with transport (at low wind speeds) from the direction of the Livingston pad to the SW (Figure 2.6 (b)). Similar transport patterns from July through early September did not generally produce elevated

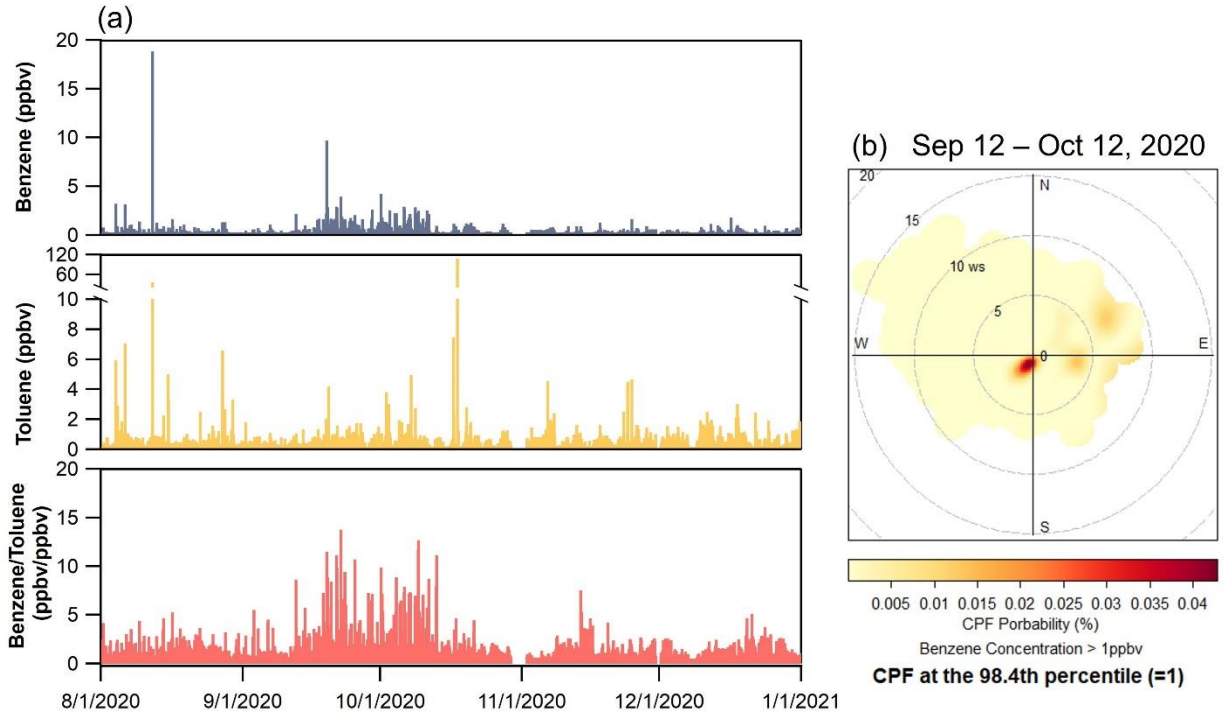

Figure 2.6: (a) Timelines of benzene (top), toluene (center) and benzene to toluene ratio (bottom) from August to December 2020 measured with the PTR-MS at Soaring Eagle Park in Broomfield, CO. (b) Conditional probability function (CPF) plot for elevated benzene mixing ratios at Soaring Eagle Park from September 12 to October 12, 2020.

benzene concentrations at Soaring Eagle Park, suggesting the elevated concentration period in September/October represented a new source of emissions rather than a change in transport that brought existing source emissions to the site (Figure A.7). Previous studies have linked elevated ethyne, alkene and benzene abundances to combustion sources such as flaring (Schade and Roest, 2016, 2018) although the benzene:toluene ratios they reported were much lower than the typical values (~5-10) seen here. No flares were operational at the Livingston pad during this period and infrared camera inspections by CCOB inspectors on the Livingston pad also did not reveal evidence of improperly operating emission control devices.

To further inspect these unusual emission plumes and define their origin, the mobile plume tracker was deployed the night of 17 September 2020 to measure spatial patterns in concentrations of methane, ethyne, and BTEX. Figure 2.7 (a) shows time series of ethyne, methane, benzene, and toluene mixing ratios from the on-board instruments aligned with species concentrations measured in nine grab canisters collected during the drive. Sharp spikes in ethyne and methane indicate transits through the plume by the moving vehicle, while the two broader periods of high ethyne and methane concentrations represent periods when the vehicle sat stationary inside the plume. This high-ethyne plume features a substantial increase in benzene, but little increase in toluene mixing ratios, consistent with the PTR-MS observations at Soaring Eagle Park. Figure 2.7 (b) shows ethyne mixing ratios along the plume tracker path. The observed ethyne concentrations ranged between 0.2 ppbv (a typical background level during the summer-fall season) to 90.9 ppbv with the highest concentrations observed near the SE corner of the Livingston pad. The wind direction during the mobile measurement period was generally from the NW. Low ethyne concentrations upwind (NW) of the pad and the peak concentrations downwind (SE) of the pad indicate the ethyne-rich plume originated on the Livingston pad.

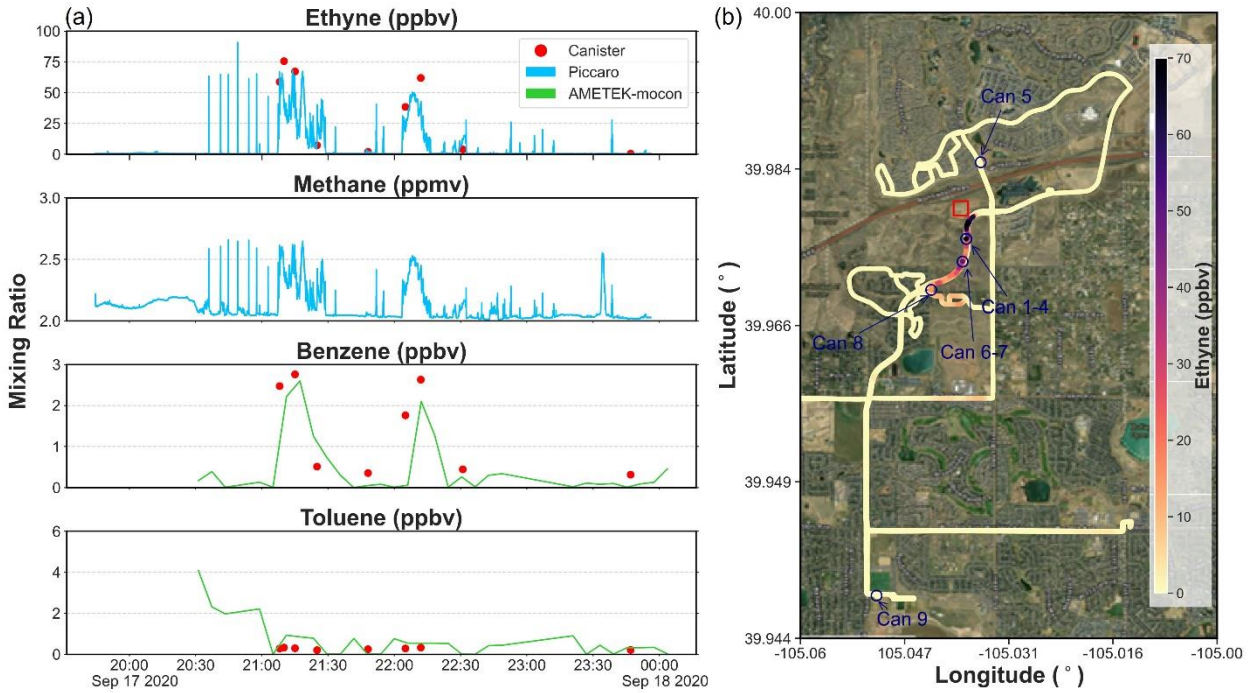

Figure 2.7: (a) Time series of ethyne (ppbv), methane (ppmv), benzene (ppbv) and toluene (ppbv) measured during a plume tracker deployment on the evening of 17 September 2020. Mixing ratios measured in 9 grab canisters collected during the drive are shown as red dots. (b) Broomfield area map showing ethyne mixing ratios measured along the plume tracker driving route (base map is from ESRI: https://www.arcgis.com/apps/View/index.html?appid=df7cee38677f479c8697026ebf920431). Grab canister collection locations are labeled. The red square indicates the location of the Livingston pad.

The compositions of the canister samples collected inside the ethyne-rich plumes on the plume-tracker drive were compared with weekly canister samples collected at the Livingston near-pad sites during the June–September period of elevated ethyne. Both showed substantially increased benzene:toluene, benzene:ethyne, and ethyne:methane ratios compared to values typically measured in other periods near Broomfield O&G well pads (see Figure A.8). The strong inter-species correlations in the canister data, the similarities in species ratios between the canister data and the June to September 2020 near-pad Livingston weekly canister data, and the departures of both from typical near-pad signatures in Broomfield all suggest the influence of a consistent source throughout this period. Although benzene:toluene ratios were unusually high again in these mobile plume measurements, both propene and ethene levels were elevated in plume canister

samples, consistent with a combustion signature. While the exact nature of the source of these emissions from the pad remains unknown, the presence of compounds commonly found in natural gas flaring or combustion emissions, point to some sort of on-pad combustion source as a likely origin. Notably, this plume was no longer detected beginning in mid-October 2020 after its ongoing detection was reported to the well pad operator, an example of the value of the Broomfield air monitoring program in helping to mitigate O&G emissions and their impacts on the surrounding community.

2.3.4 VOC plume observations

2.3.4.1 VOC levels and compositions in triggered canister samples

The network of PID sensors with triggered canister collection allows us to examine short-term (minutes to hours) periods of elevated VOC concentrations in Broomfield, both near well pads and in adjacent neighborhoods. We focus on VOC compositions in triggered canisters collected during specific O&G operations, including drilling, hydraulic fracturing, coil and production tubing operations, flowback, and production. Because some Broomfield well pads are close to each other, and different operations simultaneously occur on adjacent pads, we use well development records and local wind observations to identify emission sources influencing collection of each triggered canister. Only triggered canister samples attributed to emissions from a single operational activity on a nearby well pad are included in this analysis.

Figure 2.8 presents frequency distributions of TVOC-49 and benzene mixing ratios from 91 triggered canister samples grouped by well development activity. Concentrations measured in weekly samples collected at the Commons background site are shown for comparison. A detailed data set of selected compounds measured in triggered canisters is shown in Table A.7. TVOC and benzene mixing ratios measured in event-triggered canister samples were typically 1 to 3 orders

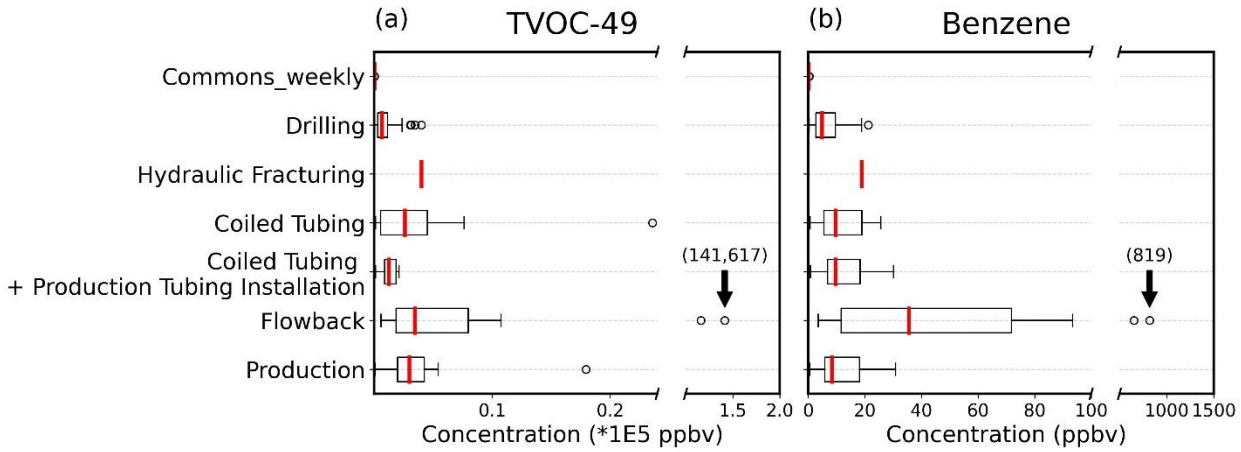

Figure 2.8: Box and whisker plots (90th, 75th, 50th, 25th, 10th percentiles) of (a) TVOC-49 and (b) benzene mixing ratios measured in 91 15-s triggered canister samples during different O&G development operations from February 2020 to December 2022. The black arrows

of magnitude greater than mixing ratios measured in the Commons background samples, confirming successful capture of high concentration plumes during O&G operations. Triggered canister sample concentrations of TVOC-49 ranged from 36.6 ppbv to more than 140,000 ppbv; benzene ranged from 0.4 ppbv to 819 ppbv. The highest levels of each were seen in a sample collected near the United pad during flowback operations. The i/n-pentane ratios in the triggered canister data set were low, with an average value of 0.77, indicating strong influence from O&G emissions (see Figure A.9).

High concentration plumes of TVOC-49 and benzene were observed during all well development activities. Average TVOC-49 and benzene concentrations in captured plumes were highest during flowback and lowest during drilling operations. Because measured concentrations depend on factors beyond emission source strength, including distance from the pad, dispersion conditions, wind direction, and the level at which the PID sensor was set to trigger, we cannot readily relate emission strength to measured plume concentration. Given sensor location choice and varying transport conditions, one likewise should not immediately conclude that the activity with the largest number of triggered canisters would be the most frequent emitter of concentrated

plumes. Nevertheless, the data set collected here, covering nearly three years of measurements, represents a significant step forward in characterizing short-term elevated VOC concentrations that occur under real-world conditions near O&G drilling, completion, and production operations on large, multi-well pads. The VOC compositions measured in these concentrated, often transient, plumes also provide useful information concerning the chemical signatures of emissions from specific O&G operations.

Figure 2.9 compares averaged VOC compositions measured in plumes emitted during various well development operations. Unsurprisingly, C_3–C_7 n-alkanes were the most abundant VOC group in the plumes across all operation types, with an average contribution of 84% (range 67–92%), followed by cyclic alkanes (mean: 5%, range 3–6%). High contents of light and cyclic alkanes have also been observed in other regions impacted by O&G-related emission sources (Gilman et al., 2013; Leuchner and Rappenglück, 2010; Pollack et al., 2021; Simpson et al., 2010; Swarthout et al., 2013; Thompson et al., 2014; Wilde et al., 2021). The contribution of C_8–C_{10} n-alkanes in plumes associated with drilling activity is significantly enhanced, comprising an average of 11% of the measured VOCs vs. just 0.7–2% in plumes associated with other well pad operations. This is consistent with increases in C_8–C_{10} n-alkane concentrations in weekly samples collected near the Livingston pad during drilling operations discussed above, highlighting the importance of drilling mud emissions as a VOC source. Since heavier n-alkanes associated with volatilization from synthetic drilling muds like Neoflo are more reactive with OH radicals than the lighter alkanes more prevalent in emissions from conventional petroleum-derived drilling fluids like Gibson D822, further study should evaluate possible tradeoffs between reduced odor (and aromatics content) and possible enhancements to ozone production when choosing a drilling fluid.

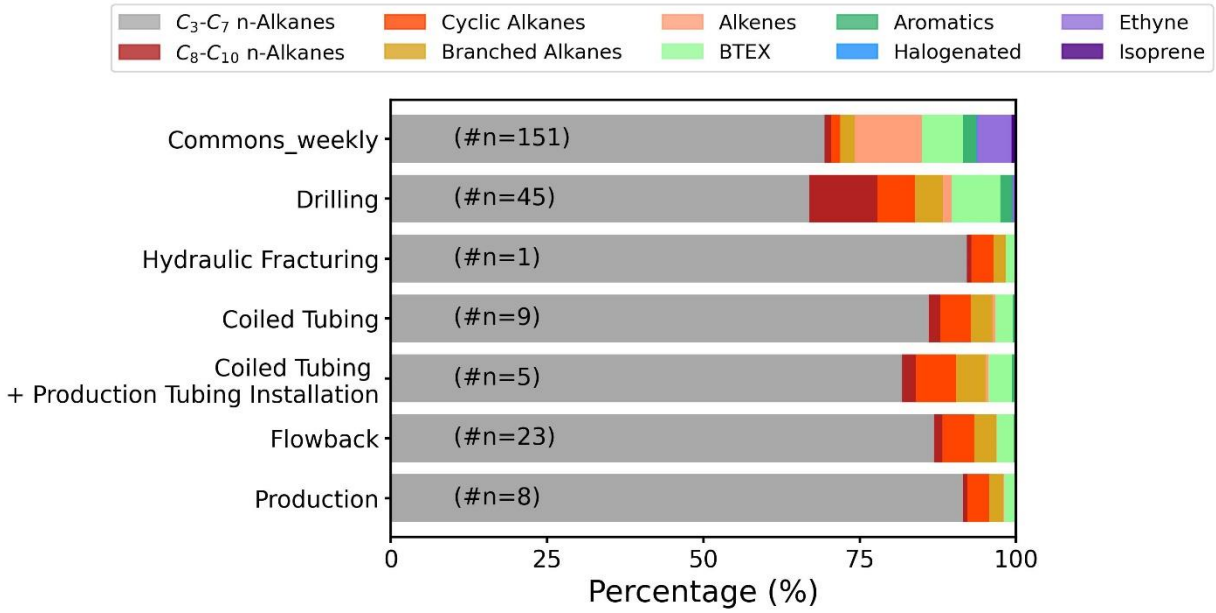

Figure 2.9: Comparison of average VOC compositions in triggered canister samples that captured plumes emanating from different well pad operations. Weekly canister data collected at the Commons (background) site from February 2020 to December 2022 are shown here for comparison.

Only one clear plume sample was captured during hydraulic fracturing operations. Because hydraulic fracturing operations push material downhole, emission of subsurface hydrocarbons is considered less likely during this operation (Field et al., 2014; Hecobian et al., 2019). Significant on-site power generation is, however, typically required to pressurize and fracture wells, meaning that engine emissions of NO_x are important to consider where regional ozone levels are problematic.

2.3.4.2 Case studies of VOC-rich plumes

Here we highlight examples of VOC-rich plumes detected in the study. A concentrated VOC plume was observed at 01:16 LT on 29 July 2022. Two co-located sensors, United 02 and 03, simultaneously detected elevated VOC concentrations and triggered canister collection (see Figure 2.10). This VOC-rich plume saturated both PID sensors and the triggered canister samples contained the highest TVOC-49 concentrations (142,000 and 116,000 ppbv) measured during Broomfield air quality monitoring. The plume persisted at the site for ~30 min. Winds were

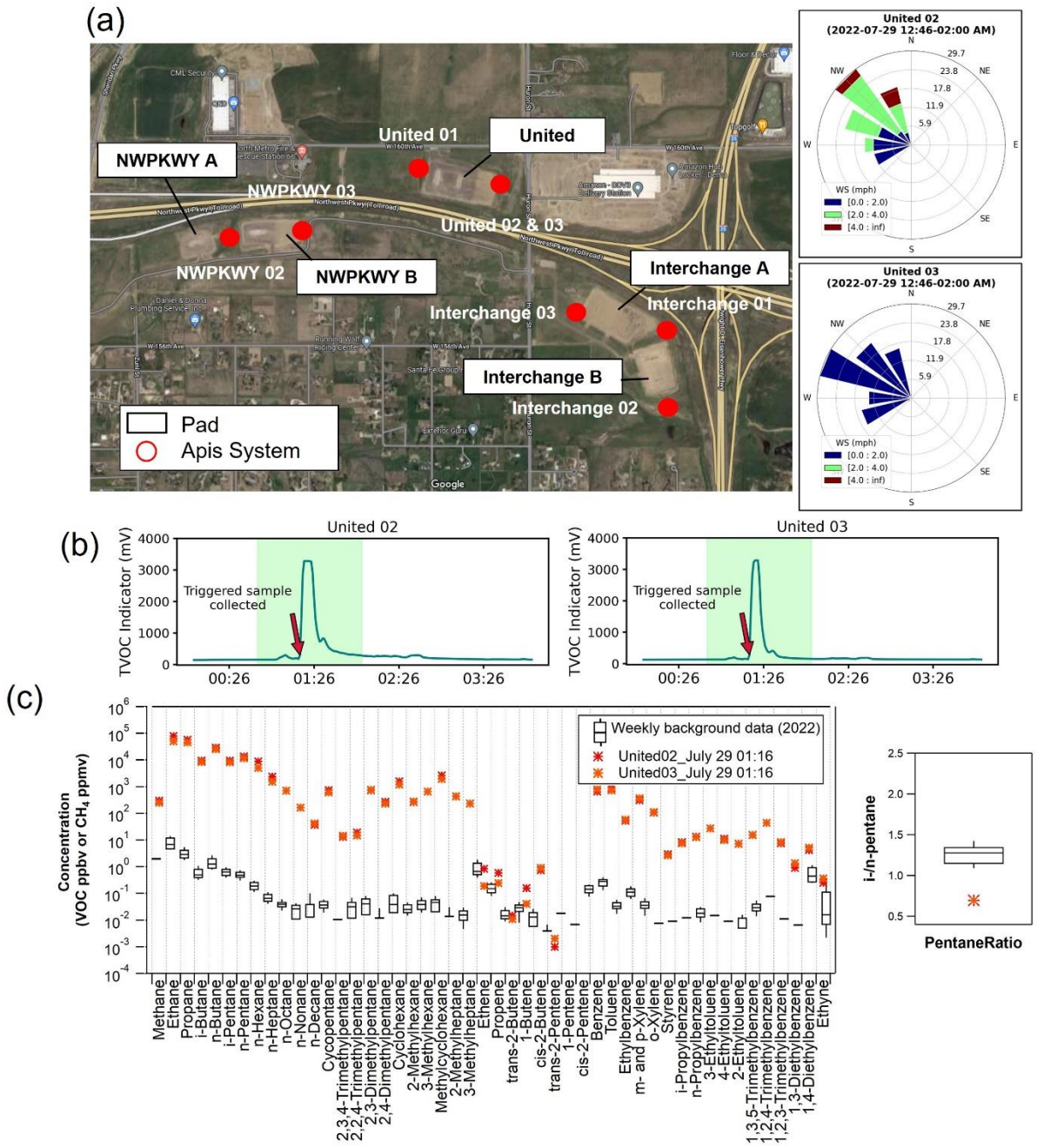

Figure 2.10: (a) Wind information from 29 July 2022 at 00:46 to 02:00 LT (base map from Google map), and (b) Apis-PID response time series from the morning at the United sites. The green-shaded areas in (b) represent the time intervals of the wind data and the red arrows indicate the time triggered canister samples were collected. (c) Comparisons of VOC and i/n-pentane ratios for the triggered canister samples along with the distributions of weekly values measured at the Commons background site in 2022. The box and whisker plots show the 25th and 75th percentiles as the box, the 50th percentile as the line in the box, and the 10th and 90th percentiles as whiskers.

approximately 5 mph and shifted from N to NW prior to the trigger event, indicating the origin of the emission from the direction of the United pad. The two triggered canisters contained very high levels of methane (301 and 254 ppmv), ethane (79,600 and 50,400 ppbv), benzene (819 and 653 ppbv), and other typical O&G emission compounds. Low i/n-pentane ratios of 0.7 further indicate an O&G source of the plume. The United pad was in flowback during this event. While flowback operations have been reported as some of the biggest O&G VOC sources (Hecobian et al., 2019; Orak et al., 2021), flowback operations in Broomfield employed management practices to limit flowback emissions that appear to have successfully limited average increases in VOC concentrations around the pads, as discussed above. Sand cans, however, are required during early stages of flowback to capture sand particles and sediments coming up the well with flowback fluids. These canisters are opened and emptied, up to several times per day, to remove accumulated sand, allowing significant VOC venting to the atmosphere for short periods.

A second example VOC plume was observed ~04:00 to 05:00 LT on 4 December 2021. Four independent PID sensors at NWPKWY 02 and 03 and United 01 and 02 detected this plume and triggered canister collections (Figure A.10), including a sample containing 23,600 ppbv of TVOC-49. Enhanced VOC levels were captured by the PID sensors at 04:06 LT at NWPKWY02, at 04:11 LT at NWPKWY 03, and at 04:34 LT at United 01 and 02. Wind speeds were modest (2-3 mph) with wind direction consistent from the NW to SW, suggesting the plume originated from a source to the west. As shown in Figure A.10 (c), the 4 triggered canister samples contained highly elevated levels of compounds typical of O&G emissions including methane, C_3–C_7 n-alkanes, benzene and aromatics, with an average i/n-pentane ratio of 0.78, indicative of O&G emissions. Coil tubing/millout operations started at the NWPKWY pad A, to the west of the four monitoring sites, on 3 December 2021; emissions from this operation would be consistent with the timing and

composition of the VOC plumes measured at the NWPKWY and United monitoring sites. The plume captured at United 02 had increased heavy alkane content compared to the plumes sampled at the other three sites. Drilling operations were underway at the United B well pad at this time, upwind of the United 02 monitor and downwind of the other three sites.

These two case studied represent emissions during pre-production operations; a few substantial VOC plumes were also observed during maintenance activities after well pads went into production. For example, a triggered canister was collected on 26 April 2021, at Livingston 01 during a period of separator maintenance on the Livingston pad. The TVOC-49 level in the triggered canister was 5,440 ppbv, benzene was 30.9 ppbv, and the i/n-pentane ratio was 0.93. On 23 June 2021, the PID sensor at the Anthem 01 neighborhood site detected a VOC-rich plume transported from the direction of the Livingston pad where separator maintenance was underway. A triggered canister contained 3,870 ppbv TVOC-49, 14.8 ppbv benzene, and an i/n-pentane ratio of 0.75. This event is particularly noteworthy given the lengthy distance (~330 m) between the Livingston pad and the Anthem 01 neighborhood site. Production separators are used to separate mixed production fluids into constituent components (oil, gas, and water) before sending them to pipelines. Operated under pressure and exposed to the elements, regular maintenance is necessary to maintain proper separator performance. Separator maintenance in Broomfield involved isolating the separator from the well, with residual gas in the closed-loop system combusted through an enclosed combustion device (ECD) to purge the flowline. Afterward, a hydrovac (equipped with high-pressure hot water and high-volume vacuum) was used to clean out residual liquids inside the separator. An abundance of light alkanes and the low i/n-pentane ratio on the 23 June 2021 plume suggest the emissions probably derived from direct emission of petroleum hydrocarbons rather than emissions from the combustor.

2.4 Conclusions

This study provides a unique overview of concentrations of air toxics and other VOCs during more than two years of development of large, multi-well pads in suburban Broomfield, Colorado, USA. Measurements at short (seconds to minutes) and longer (weekly) timescales at locations close to and further from O&G well pads offer important insight into how VOC concentrations and both acute and chronic exposure potential vary in time and in space during well drilling and completions on into early stages of production. Key findings from this study include the following:

- Analysis of weekly samples collected near well pads, in adjacent neighborhoods and at a more distant background reference site reveal increased concentrations of many VOCs, including alkanes and aromatics, near well pads during drilling, coiled tubing/millout and production tubing operations, and flowback.
- The use of grid-powered, electrified drill rigs in Broomfield eliminated a significant source of on-pad combustion emissions seen in previous studies (Hecobian et al., 2019), so that VOC increases near the pad bore a signature indicative of direct (uncombusted) hydrocarbon emissions, with low i/n-pentane ratios and an abundance of alkanes. Use of a synthetic, Neoflo-based drilling mud resulted in substantial increases in near-pad concentrations of C_8–C_{10} n-alkanes during drilling operations, highlighting the importance of drilling mud handling and recycling operations to VOC emissions during drilling. While use of the Neoflo-based drilling mud reduced odor complaints compared to a more traditional petroleum hydrocarbon-based drilling mud, emission of more reactive, long-chain alkanes should be further evaluated as precursors to photochemical ozone formation in this ozone non-attainment region.

- Previous O&G pre-production emission measurements in Colorado (Hecobian et al., 2019) found that emissions were typically largest during flowback operations. Comparison of findings from this study with those earlier measurements suggests that management practices utilized by the Broomfield O&G operator to reduce flowback emissions (e.g., use of closed-loop fluid handling systems and elimination of permanent, on-site storage tanks from the pad) helped reduce average emissions during flowback.
- High time-resolution measurements included in the study revealed that even O&G operations that include many best management practices still emit concentrated VOC plumes, at least for short periods. The use of lower cost PID sensors that continuously monitor changes in ambient VOC levels, coupled with triggered collection of rapid-fill canister samples for offline VOC speciation, provided a powerful and cost-effective tool to permit detection and chemical characterization of short-duration VOC plumes emanating from well pads during O&G operations. Concentrated plumes were captured across a wide range of operations. The VOC compositions in these plumes provide important insight into the mix of VOCs emitted by different operations, while the timing of plume detection can help identify targets for future emission reduction strategies (e.g., concentrated plumes detected in conjunction with separator maintenance or the emptying of sand cans during closed-loop flowback operations). The short duration of detected plumes (79% were <30 min) means that fast measurement approaches are needed to adequately characterize these episodic emissions.
- Weisner et al. (2023) analyzed over 400 health surveys completed by Broomfield residents and found more frequent reports of upper respiratory and acute symptoms

from adult residents living within 1.6 km (1 mile) of a well pad than those living further away (>3.2 km). We plan a future analysis to consider potential health risks associated with exposure to VOC levels observed in Broomfield. While all weekly average benzene mixing ratios, even at near-pad monitoring sites, remained well below the 3 ppbv chronic-duration inhalation minimal risk level (MRL), as defined by ATSDR (Wilbur et al., 2007), plumes captured using PID-triggered canisters contained benzene levels reaching as high as several hundred ppbv, compared to the ATSDR-defined acute-duration (14 days or less) inhalation MRL of 9 ppbv. While the acute exposure MRL has been considered by the State of Colorado as a benchmark for exposures as short as 1 h, direct comparison to air toxics concentrations in triggered canisters collected over a period less than 1 min is not appropriate. In a future study we will combine PID response timelines with measured plume VOC concentrations to extrapolate triggered canister concentrations to estimate 1-h average concentrations.

While the characterization of air quality changes associated with specific UOGD pre-production activities in this study is among the most comprehensive to date, a number of challenges remain to fully capture and describe such impacts. For example, one would ideally have even more complete measurements of emissions impacts in both space and time. As implemented, there are likely emission plumes that went undetected due to the limited number of monitoring systems around each well pad. For the many plumes that were captured, the characterization of those plumes was typically limited to a single canister sample. More continuous measurements would better characterize ranges of air toxics exposure over longer time periods, although resource and infrastructure limitations often make deployment of continuous VOC speciation monitors at numerous locations impractical. Some potentially important compounds such as formaldehyde, an

air toxic and an important ozone precursor, were not measured in this study and should be a focus of future measurements. Finally, while available information about well pad operations during air monitoring was reasonably good in this study, even more detailed activity records and opportunities for on-pad monitoring could further inform interpretation of off-pad air quality measurements in future studies.

Chapter 3

Contributions to atmospheric OH reactivity during oil and gas well development

3.1 Introduction

Tropospheric (ground-level) ozone (O_3) is one of six criteria air pollutants regulated by the U.S. Environment Protection Agency (U.S. EPA) due to its negative effects on human health (Chang et al., 2012; Kim et al., 2020; Schlink et al., 2006; Sujith and Sehgal, 2017). It also has detrimental effects on ecosystems (Fuhrer et al., 2016; Ghude et al., 2014; Grulke and Heath, 2020; Van Dingenen et al., 2009) and is an important greenhouse gas (Myhre et al. 2013). Tropospheric ozone is a secondary pollutant, not emitted directly to the atmosphere but produced through a series of chemical reactions of volatile organic compounds (VOC) in the presence of nitrogen oxides (NO_x = NO + NO_2) and sunlight (Crutzen et al., 1999; Sillman, 2003; Wang et al., 2018). The hydroxyl radical (OH) is typically the most important oxidant in this chemistry. Emissions of VOCs and/or NO_x originate from a wide variety of sources, including motor vehicles, electric power generation, industries, oil and gas development, agriculture, wildfires, vegetation, and personal care products (Chiang et al., 2007; Coggon et al., 2021; Dinh et al., 2015; Peng et al., 2021; Pierce et al., 1998). Ozone production chemistry is complicated; the formation efficiency is determined by various factors including the VOC/NO_x ratio, VOC composition, oxidant availability, and meteorology (Martins and Andrade, 2008; McDuffie et al., 2016; Peng et al., 2021; Sullivan et al., 2016; Wang et al., 2018). Stratospheric intrusion events and long-range transport of ozone and its precursors can contribute, along with local photochemistry, to elevated concentrations of surface ozone (Lin et al., 2012; Lin et al., 2017).

Significant decreases in tropospheric ozone levels have been observed across the U.S. in recent decades reflecting regulatory reductions of precursor emissions from vehicles and industries (Simon et al., 2015). Nevertheless, many places in the western U.S. still struggle to comply with ozone National Ambient Air Quality Standards (NAAQS), especially during summertime (Bien and Helmig, 2018; Lin et al., 2017). 8-hour average ozone standards were established and revised over time, most recently to 75 ppb in 2008 and 70 ppb in 2015. Violation of the standard is measured based on three consecutive year averages of the fourth annual maximum from daily 8-hour average ozone levels. Colorado's Northern Front Range (NFR) has been designated an ozone non-attainment area since 2007, with continued exceedances of both the 75 and 70 ppb NAAQS. The region, including the Denver Metro Area and areas to the north (see Figure 3.1), was classified as "Marginal" non-attainment in 2007 for the 1997 NAAQS. Despite continued efforts to reduce ozone precursor emissions from motor vehicles, oil and gas development, and other sources, significant population growth, high ozone background levels, and increasingly hot, dry summers have made ozone standard attainment a serious challenge (Bien and Helmig, 2018; CDPHE, 2023; Evan and Helmig, 2017; Goetz and Boschmann, 2018; Milford, 2014; Wells, 2017) and the region was recently designated as severe nonattainment for the 75 ppbv standard.

Rapid growth of unconventional oil and natural gas development in the NFR, driven by improvements in horizontal drilling and hydraulic fracturing techniques, has raised Colorado's ranking to eighth among U.S. states for combined crude oil and natural gas (O&G) production (U.S. EIA, https://www.eia.gov/state/seds/seds-data-complete.php?sid=US#CompleteDataFile, accessed on 26 June 2023). Several studies have demonstrated that oil and gas (O&G) activities are major VOC and NOx sources (Abeleira et al., 2017; Benedict et al., 2019; Bien and Helmig, 2018; Cheadle et al., 2017; Evans and Helmig, 2017; Gilman et al., 2013; Halliday et al., 2016;

Hecobian et al., 2019; Helmig, 2020; Lindaas et al., 2019; McDuffie et al., 2016; Pétron et al., 2012; Pollack et al., 2021; Swarthout et al., 2013; Thompson et al., 2014) that contribute to elevated ozone in the NFR. An early report revealing the connection between elevated ozone and O&G emissions in the NFR was published by the Colorado Department of Public Health & Environment (CDPHE, 2008). Integrating back trajectory analysis with daily maximum 8-hour ozone concentrations observed at four NFR sites in summer 2006 showed that elevated ozone events were attributed to air masses transported from the Denver-Julesburg Basin (DJB), Colorado's largest O&G basin, northeast of the Denver metro area. Evans and Helmig (2017) analyzed 4-year continuous measurements of 1-hr average ozone with wind data at the Boulder Atmospheric Observatory (BAO). This study demonstrated that elevated ozone events were associated with airflow from the O&G production region, accounting for 65% of 1-hr elevated ozone levels, with minor contributions from the direction of the Denver metropolitan area (9%). To better understand sources of high ozone, multiple studies speciated ambient VOCs and apportioned their sources (Abeleira et al., 2017; Gilman et al., 2013; Halliday et al., 2016; Pétron et al., 2012; Swarthout et al., 2013; Thompson et al., 2014). These studies reported significantly enhanced methane (CH_4), light alkanes, and benzene associated with O&G operations. These source apportionment analyses showed that O&G activities contributed more than 70% of light alkanes (Abeleira et al., 2017; Gilman et al., 2013; Pollack et al., 2021). Air masses containing O&G emissions have also been observed at Rocky Mountain National Park in the mountains west of the NFR, with resulting contributions of up to 20 ppb of ozone (Benedict et al., 2019). Photochemical box model simulations characterizing the influence of VOC emissions on ozone production (Lindaas et al., 2019; McDuffie et al., 2016) indicated that O&G VOCs contributed 20-30% of photochemical ozone production during summer. Cheadle et al. (2017) reported varied

local ozone levels during mobile measurements and concluded that O&G emissions can be a primary contributor to NFR elevated ozone (up to 20-30 ppb).

Research to date has documented a significant influence of O&G-related emissions on elevated ozone in the NFR while indicating a need for additional studies to investigate contributions of other emission sources (e.g., landfills, wastewater treatment, animal operations, and agriculture). Many studies have focused on short observation periods, making it challenging to adequately represent longer term conditions and their variability in time and space. Ozone production efficiency is sensitive to ratios of VOC/NO_x that vary with both season and location (Bien and Helmig, 2018). NO_x levels are strongly influenced by vehicle emissions, while VOC levels tend to be determined by spatial patterns in emission sources (e.g., urban areas, O&G operations, and vegetation) across the region as well as meteorological conditions. VOC/NO_x ratios are generally expected to be lower near the Denver metropolitan area with its large urban traffic emissions and higher near O&G operations. Bien and Helmig (2018) analyzed 15-years of hourly surface ozone data from 80 monitoring sites in Colorado from 2000 to 2015. They found larger seasonal cycles in diurnal amplitude during summer at locations near O&G operations than in the Denver metropolitan area and attributed the difference to differing VOC/NO_x ratios. With continuous changes in NO_x and VOC levels from urban and O&G development and increasingly strict regulations on O&G and other industry and traffic emissions, assessing contributions of these sources to NFR ozone levels remains a challenging and moving target.

Characterizing emission sources and contributions of NO_x and VOCs to ozone formation is a priority to better predict peak ozone and to develop effective emission control strategies to bring the region into compliance with the ozone National Ambient Air Quality Standard (NAAQS). In examining VOC sources, it is important to consider not only mass emission rates, but also the

speciation of emitted VOCs which can greatly influence their atmospheric reactivity and resulting contributions to ozone formation. One particular area of need is to characterize the mix of VOCs emitted by O&G operations, especially during drilling and completion of new wells. Current estimates used in VOC emission inventories often do not reflect recent changes in industry practices. For example, the EPA emissions tool (U.S. EPA, 2016 Nonpoint Oil and Gas Emission Estimation Tool) estimates of VOC emissions from drilling mud volatilization rely on measurements made during offshore drilling operations in the 1970s and do not reflect the increasing use of synthetic drilling muds in the DJ Basin, often used to alleviate odor complaints commonly associated with more traditional, petroleum-based drilling muds.

Development of six large multi-well pads was approved in the city and county of Broomfield in 2017. In response to public concerns about potential health and environmental impacts from O&G development in this suburban zone, several best management practices were included in an operator agreement and an extensive air monitoring program was implemented prior to the start of drilling operations. We have previously reported how emissions from O&G operations during well development and O&G production in Broomfield affect VOC composition and concentrations in the surrounding region (Ku et al., 2024). Here we consider the potential of those VOCs for contributing to ozone formation by computing OH reactivities (OHR) (Gilman et al., 2013; Gilman et al., 2009) for VOC emissions associated with specific O&G operations, including well drilling and completions and O&G production.

3.2 Method

3.2.1 Sampling Location

Speciated VOCs were measured in Broomfield, Colorado, USA from Fall 2018 through 2023 (Figure 3.1). Initial well pad development began in early 2019. A detailed overview of the

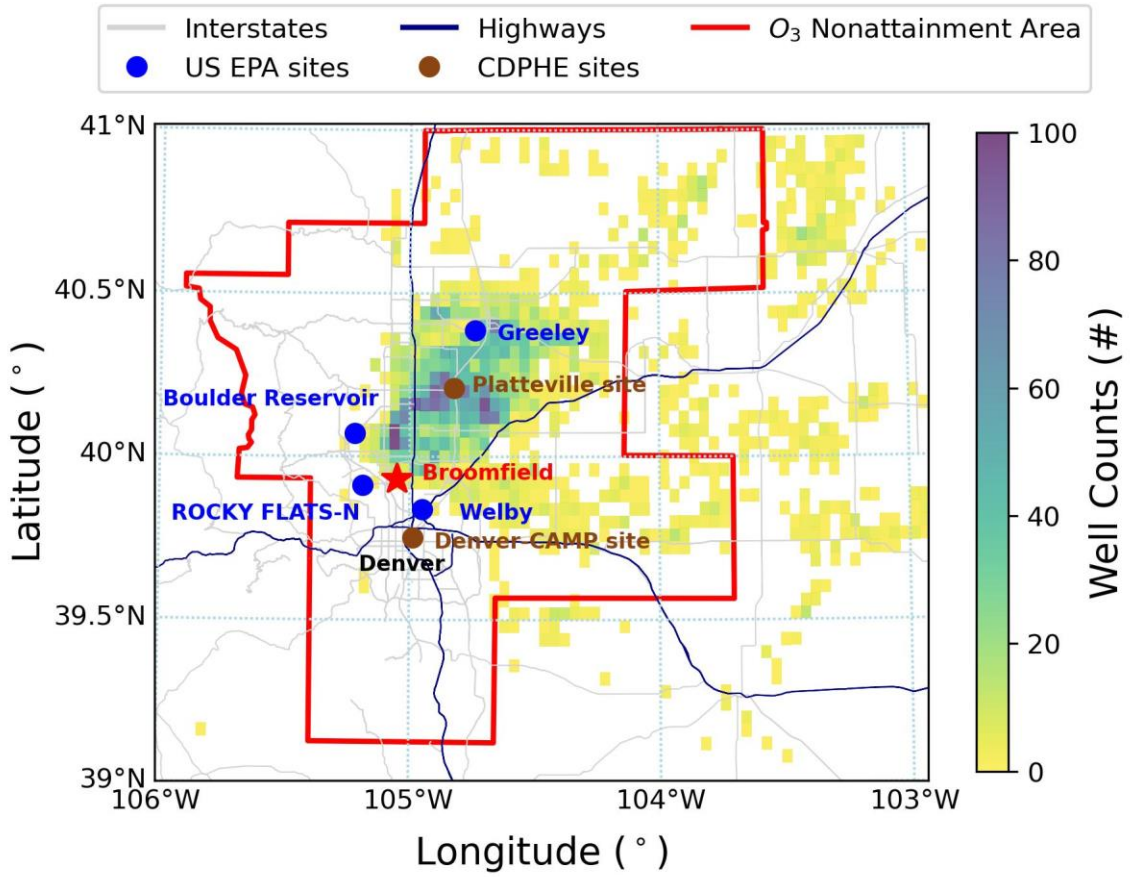

Figure 3.1: Map of the study region with the overlaid well counts (COGCC, https://cogcc.state.co.us/data2.html#/downloads, accessed on 10 May 2023).

well pad development schedule and the VOC sampling strategy and methods is given in Ku et al. (2024). Briefly, nineteen sampling sites were strategically deployed across Broomfield, near well pads, in nearby neighborhoods, and at a regional background location further from O&G operations, to monitor spatially and temporally varying air quality impacts from both new well development and other local and regional sources. At the beginning of the monitoring program, four sites were equipped with weekly air sample canisters. Once well development was underway, six to nineteen weekly canister sampling sites were deployed, based on the timing and location of pre-production (well drilling and completions) operations at the well pads. A total of 2011 weekly integrated samples are included in this study covering the period October 2018 – December 2022.

The sampling period covers the full well development cycle into O&G production for four well pads (Interchange B, Livingston, NWPKWY A & B). Beginning in 2020, real-time monitoring systems, equipped with photo-ionization detectors (PID) and automatically triggered canisters, were added to capture and characterize transient VOC plumes at near-pad and nearby neighborhood sites. These Apis PID-based monitoring systems were calibrated based on their response to isobutylene and triggered collection of a rapid-fill canister sample when PID response exceeded a specified threshold. The PID readings are not directly related to ambient VOC concentrations because the PID (ION Science High Sensitivity 10.6 eV) response varies with VOC speciation. In practice, however, this semi-quantitative PID-based measurement of a suite of ambient VOCs has proven useful for detecting rapid changes in VOC concentrations associated with the passage of a transient plume emanating from O&G operations (Ku et al., 2024).

3.2.2 Measurements and Data

Weekly time-averaged and event-triggered whole air samples were collected utilizing evacuated Silonite®-coated canisters (6.0-liter and 1.4-liter, respectively, *Entech* Instruments, CA, USA). Flow regulation systems were used to slowly fill (7-day sample period) the weekly canisters; fill times for event-triggered canisters were ~ 15 to 30 s to help ensure these samples accurately reflected the composition of transient plumes. Canisters were cleaned and evacuated before deploying to the field using an *Entech* 3100 Canister cleaning system. The canisters were analyzed for methane and a suite of VOCs by gas chromatography (GC) in the laboratory at the Colorado State University Atmospheric Science Department. Details of the analytical system are provided elsewhere (Ku et al., 2024; Sive et al., 2005; Zhou et al., 2005). Briefly, methane was analyzed using a Shimadzu GC-8A equipped with a flame ionization detector (FID). The methane measurement precision (1 relative standard deviation, RSD) was 4% and the method detection

limit (MDL) was 0.21 ppmv. A suite of 52 VOCs, including C_2-C_{10} non-methane hydrocarbons (NMHCs), C_2 halocarbons, and two oxygenated VOCs (OVCOs) were measured using a custom, multi-channel GC system. This system included three GCs and five detectors (three FIDs, one electron capture detector (ECD), and one mass spectrometer (MS)). The complete list of measured compounds and their detection limits is provided in Table B.1. The measurement precision (1 RSD) varied from 2% to 18% for C_2-C_{10} NMHCs, from 14% to 20% for C_2 halocarbons, and 5% to 12% for OVOCs.

3.2.3 OH Reactivities (OHR)

Hydroxyl radical reactivity (OHR) has been used in several previous studies as a surrogate for ozone formation potential from specific compounds (Abeleira et al., 2017; Gilman et al., 2009; Gilman et al., 2013; Ryerson et al., 2003; Swarthout et al., 2013; Wilde et al., 2021). Oxidation of VOCs by OH radical generally is an initial and rate-limiting step in the more complex reaction scheme that leads to tropospheric ozone formation. Thus, potential ozone formation from specific VOC_x can be estimated, in a relative sense, by the product of the rate constant ($k_{OH,VOC}$, Table B.1) for the reaction of VOC_x with OH radical and the VOC_x concentration. While predicting actual ozone production requires a more complex and complete photochemical model incorporating NO_x and speciated VOC levels and reaction mechanisms, comparisons of OHR for individual VOCs provides a simple assessment of those species likely contributing most to ozone formation. Because we did not measure all compounds which can be significant contributors to OHR in Broomfield, NO_2, CO, and formaldehyde measured by the Colorado Department of Public Health and Environment (Figure 3.1) at other Denver metro locations were included in our analysis. 1-h average trace gas concentrations are available from U.S. EPA (https://aqs.epa.gov/aqsweb/airdata/download_files.html, accessed on 07 August 2023). Reported

measurement precisions ranged from 2.2% to 2.6% for CO, and 3.3% to 3.6% for NO_2 for data collected between 2018 and 2022. CO was measured at the Greeley – Weld County Tower and the Welby sites, while NO_2 was measured at the Platteville Atmospheric Observatory and the Welby sites (Figure 3.1). Means of 1-h average values measured at these pairs of monitoring sites were used to calculate OHR for these species. CDPHE collected 3-h (6 to 9 AM) air samples at downtown Denver and at the Platteville site to monitor ozone precursors (methane, NMHCs, and carbonyl compounds) from 2011 to 2020; data are available from their website (https://www.colorado.gov/airquality/air_toxics_repo.aspx, accessed on 07 August 2023). Monthly average formaldehyde mixing ratios measured at the two monitoring sites were used in our OHR calculations. Because data were unavailable for 2021 and 2022, the means of the monthly average formaldehyde mixing ratios measured from 2018 to 2020 were applied to the corresponding months of these two years. The propagated uncertainties in OHR calculation for the measured compounds were from 1 to 40% including contributions from uncertainties in OH rate constants and measured mixing ratios.

3.3 Results and Discussion

3.3.1 Overall OH Reactivities

Figure 3.2 (a) shows October 2018-December 2022 timelines of the weekly average of total OHR calculated for Broomfield aligned with the means of 8-hr ozone observed at three different nearby CDPHE ozone monitoring stations (Boulder Reservoir, Rocky Flats-N, and Welby, Figure 3.1). Periods of O&G pre-production activities (from well drilling through hydraulic fracturing and flowback) are marked with purple shading in panel (a). The mean total OHR was 7.9 ± 2.1 s^{-1} with a weekly maximum of 14.8 s^{-1}. Much higher OHRs have been reported in observations in some megacities and industrial regions. For example, calculated OHRs ranged from < 0.1 – 200

s^{-1} in Houston, TX (Gilman et al. (2009)); from < 10 – 100 s^{-1} in New York City, NA (Ren et al. (2006)); from < 10 – 200 s^{-1} in Mexico City, Mexico (Shirley et al. (2006)), from 3.5 – 130 s^{-1} in Paris, France (Dolgorouky et al. (2012)); from 10 – 80 s^{-1} in Tokyo, Japan (Yoshino et al. (2012));

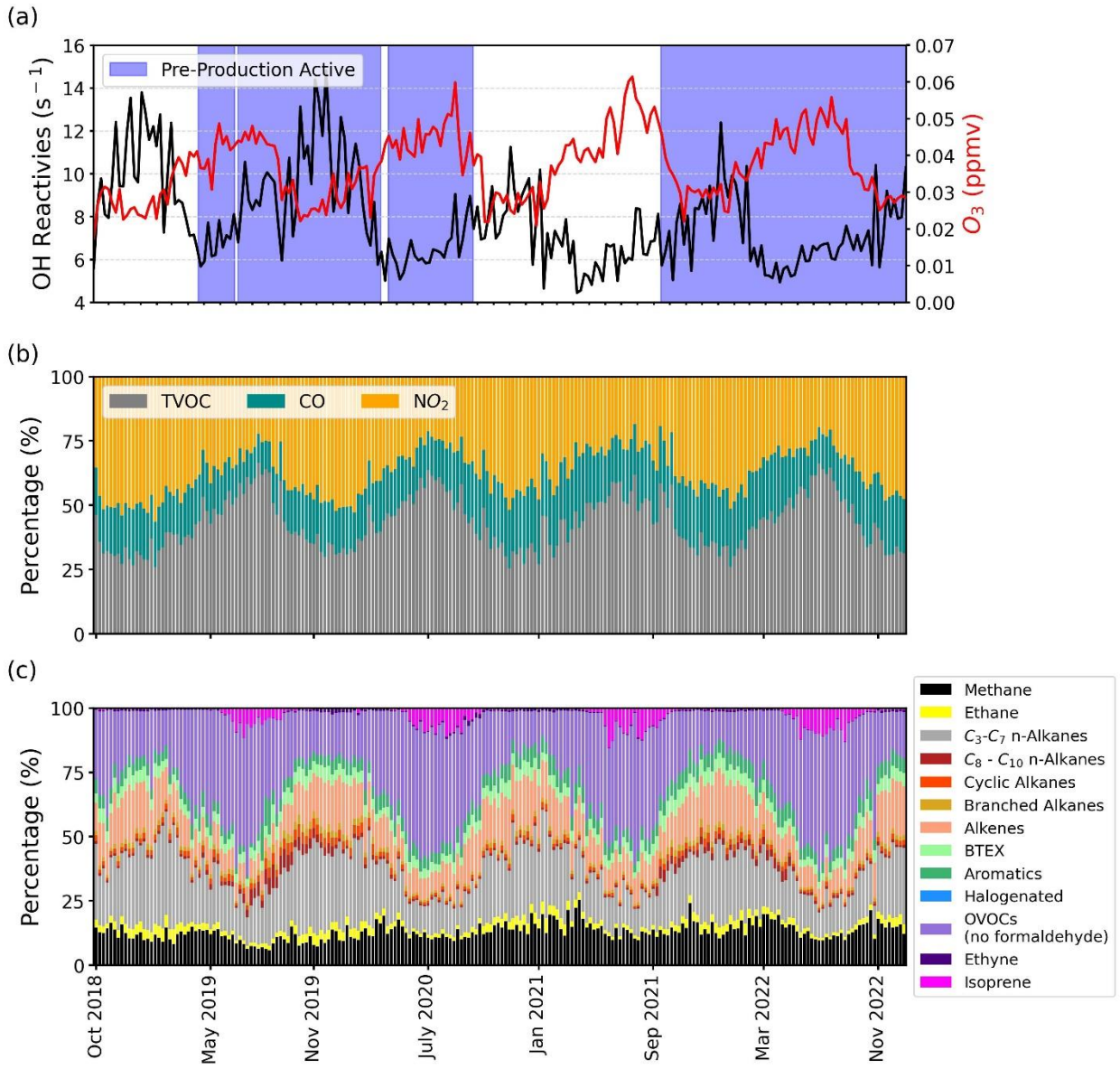

Figure 3.2: Time series of (a) the weekly average of total OH reactivities and the mean of 8-hr running average ozone measured at three U.S. EPA sites near to Broomfield, (b) the comparison of the average TVOC, CO and NO_2 OH reactivities, and (c) the comparison of grouped-VOC OH reactivities calculated from the weekly integrated canister samples from October 2018 to December 2022. Observations started before O&G development and continued during pre-production activities (purple shading) and production.

and from < 10 – 120 s^{-1} in the Pearl River Delta, China (Lou et al. (2010)). Strong seasonal cycles of ozone and OHR were observed. Even though photochemical ozone production has been discovered during winter months in some O&G producing basins in Wyoming and Utah, due to reactions of accumulated pollutants in a shallow boundary layer over highly reflective snow-covered ground (Edwards et al., 2014; Helmig et al., 2014; Rappenglück et al., 2014; Schnell et al., 2009), elevated ozone levels are generally expected during summertime due to increased photochemical activity.

Increased OHRs observed in Broomfield in winter reflect increased surface concentrations of CO, NO_2, and VOCs (Figure B.1 (a), Ku et al., 2024), reflecting increased atmospheric stability, a shallow boundary later, and decreased photochemical loss. Better air dispersion and increased photochemistry both lower total OHR in summer, while the increased photochemistry also produces higher ozone mixing ratios. Previous studies have reported similar OHR seasonal patterns in the NFR region. For example, Swarthout et al. (2013) reported a mean value (7.0 ± 5.0 s^{-1}) of total OHR at the Boulder Atmospheric Observatory (BAO, ~ 8 km away from most of the sampling sites in Broomfield) in winter of 2011, higher than mean values (2.7 to 4.0 s^{-1}) reported at the same location in spring and summer 2015 (Abeleira et al., 2017), despite the warm season increase in biogenic VOC emissions. Despite the large number of VOCs measured in this study, and the inclusion of CO, NO_2, and HCHO data from CDPHE, the estimated OHR remains a lower bound as other, unmeasured compounds also contribute. For example, both Gilman et al. (2013) and Swarthout et al. (2013) reported that ethanol also constituted an important percentage of OVOCs OHRs, comparable to the contribution of acetaldehyde. There are also limitations to directly comparing OHR estimates from previous studies due to some differences in the measured compound sets.

Calculated Broomfield OHRs and relative contributions of CO, NO_2, and VOCs are shown in Figure 3.2 (b) and Figure B.2 (b). The OH sinks were dominated by NO_2 during winter when total OHRs were high, while VOCs were the largest contributor during summers. Relatively consistent contributions from CO were observed across seasons throughout the sampling period. NO_2 (produced by oxidation of emitted NO) and CO both reflect combustion emissions with significant contributions from mobile sources (U.S. EPA NEI, 2020, https://www.epa.gov/air-emissions-inventories, accessed on 07 August 2023). Increased mixing ratios of these two traces gases have also been observed near O&G fields and in wildfire emissions (Orak et al., 2021; Prenni et al., 2016; Simpson et al., 2010; Warneke et al., 2014; Peng et al., 2021). Weekly NO_2 OHRs estimated here for Broomfield ranged from 1.0 to 7.1 s^{-1} with a mean of 3.0 s^{-1}, contributing 27% and 46% to total OHR during summers and winters, respectively. Similar relative contributions of ~ 38% were obtained during spring and fall. For CO, the calculated weekly OHR ranged from 0.8 to 3.2 s^{-1} with a mean of 1.5 s^{-1}. Mean contributions of CO to total OHR ranged from 16% to 21% for different seasons. Like NO_2, lower CO contributions to total OHR tended to be found during summer. Swarthout et al. (2013) reported comparable average winter BAO NO_2 and CO OHR contributions of 40% and 12%, respectively.

Broomfield weekly total VOC OHRs, including methane contributions, ranged from 1.9 to 6.7 s^{-1} with an overall mean of 3.3 s^{-1}. Clear seasonal variation was also observed throughout the sampling period. The maximum seasonal average VOC OHR was 4.0 s^{-1} during summer, decreasing to 3.3 and 2.8 s^{-1} in fall and spring. A similar trend in seasonal percentage contributions of VOC OHR to total OHR, with highest average contributions during summer (57%) followed by spring (45%), fall (40%), and winter (34%). The average VOC OHR measured during winter and spring in this study are comparable to previous observations at BAO (Abeleira et al., 2017; Gilman

et al., 2013; Swarthout et al., 2013). By contrast, much higher average VOCs OHRs were observed in Broomfield during summer, due in part to larger numbers of reactive OVOCs measured in this study.

As discussed above, seasonal changes in boundary layer height (BLH) influence both VOC mixing ratios and related OHRs. Figure B.2 shows three years of weekly average BLH estimated using the Weather Research Forecasting (WRF) model (https://www.weblakes.com/met-data/order-met-data/, accessed on 25 September 2023). The seasonal variations of TVOC mixing ratios noted in Ku et al., (2024) were opposite to the seasonal pattern of the BLH (higher BLH during summer correlated with lower TVOC mixing ratios, and vice versa in winter). This inverse relationship is typical of many VOCs emitted throughout the year or formed locally near the surface; this excepts biogenic VOCs with strong seasonal emission variations peaking in summer. Following the method of Gilman et al. (2009), the approximate average annual mixing height of 300 m was used to normalize the total VOC (TVOC) mixing ratio and total OHRs to examine the influence of BLH (Figure B.3). While BLH normalization removes a fair amount of seasonal variability in TVOC mixing ratios, an increase in OHR remains evident in summertime even after BLH normalization. This pattern reflects the importance of seasonal changes in VOC speciation and the greater summertime abundance of more reactive VOCs including those from biogenic sources. This seasonal change in OHR further reinforces the importance of considering the composition – and not just the amount – of VOCs in designing effective control strategies to mitigate summertime ozone.

The relative contribution of individual hydrocarbons to VOC OHR reactivities is shown in Figure 3.2 (c). This comparison only includes compounds measured in Broomfield (no formaldehyde). As reported in Ku et al., (2024), C_3-C_7 n-alkanes were the most abundant

hydrocarbons measured in this region, accounting for ~ 76% of TVOC (methane, ethane and OVOCs were not included in their calculation) mixing ratios. Here, C_3-C_7 n-alkanes (57%) continue to dominate VOC mixing ratio contributions, even when including the OVOC contribution (25%). The OVOC group (average OHR = 0.8 ± 0.5 s^{-1}, 30%), however, is the largest contributor to VOC OHRs due to their high OH reactivities, followed by C_3-C_7 n-alkanes (average = 0.6 ± 0.3 s^{-1}, 22%). Methane (average = 0.3 ± 0.01 s^{-1}, 13%) and alkenes (average = 0.3 ± 0.1 s^{-1}, 13%) also contributed important percentages of VOC OHRs due to their abundance and reactivity, respectively. The list of the major contributors of VOC OHRs in this study is consistent with previous measurements at BAO (Gilman et al., 2013; Swarthout et al., 2013), although relative contributions differ with alkanes contributing most to VOC OHR in those studies. For a more direct comparison with the winter observations of Swarthout et al. (2013), we analyzed the Broomfield winter data and combined reactivities of all alkane types (C_3-C_{10}, cyclic, and branched) and added formaldehyde to the OVOC group. The outcome reveals alkanes as the largest VOC OHR contributors, accounting for 34%, followed by OVOCs at 31%. Furthermore, close to a 40% reduction in total alkane OHR (1.1 s^{-1}) was estimated for the 2018-2022 Broomfield winter dataset study compared to the winter 2011 values reported by Swarthout et al. (2013) (1.8 s^{-1}). This reduction is consistent with decreases in O&G emissions reported in the region in recent years, despite growing O&G production, although it might also partly reflect spatial differences in O&G emissions (the BAO location to the north of Broomfield sits somewhat closer to the major O&G production regions of the DJ Basin (Lyu et al., 2021).

3.3.2 Source Contributions of VOC OHRs

3.3.2.1 Oxygenated VOCs (OVOCs)

OVOCs can originate from both natural and anthropogenic sources, either through primary emissions or secondary photochemical formation resulting from the oxidation of other hydrocarbons (Anderson et al., 1996; Dutta et al., 2010; Lui et al., 2017; Millet et al., 2010; Parrish et al., 2012; Seco et al., 2007). Acetaldehyde was the major contributor to OVOC OHRs at 99% of the OVOCs measured in Broomfield samples and 51% when CDPHE formaldehyde values are included (Figure 3.3 (a)). Clear seasonal cycles were observed in OVOC OHRs, with higher values in summer than winter. Although average acetone mixing ratios were comparable to those of acetaldehyde and formaldehyde, acetone's reactivity with OH radicals is significantly slower, limiting its OVOC OHR contribution. To explore potential sources of acetaldehyde, we correlated mixing ratios of acetaldehyde with formaldehyde and other VOCs. Strong correlations are observed between acetaldehyde and formaldehyde (despite the different measurement locations), isoprene, and acetone ($r = 0.70$, 0.78 and 0.86, respectively), suggesting they might share similar sources. Formaldehyde and acetaldehyde have been observed to be prevalent carbonyls within urban and industrial environments (Ban-Weiss et al., 2008; Dutta et al., 2010; Lui et al., 2017; Parrish et al., 2012). The main source has been identified as secondary production from oxidation of other VOCs, with a considerably smaller proportion estimated to originate directly from primary sources like vehicle exhaust (Millet et al., 2010; Wert et al., 2003). However, an early study that aimed to investigate acetaldehyde and formaldehyde sources and sinks in the Denver region suggested that motor vehicle emissions are a major source of their presence in this area (Anderson et al., 1996). A positive correlation observed between acetaldehyde and formaldehyde in this study does not discriminate between the possible importance of vehicle emissions or secondary

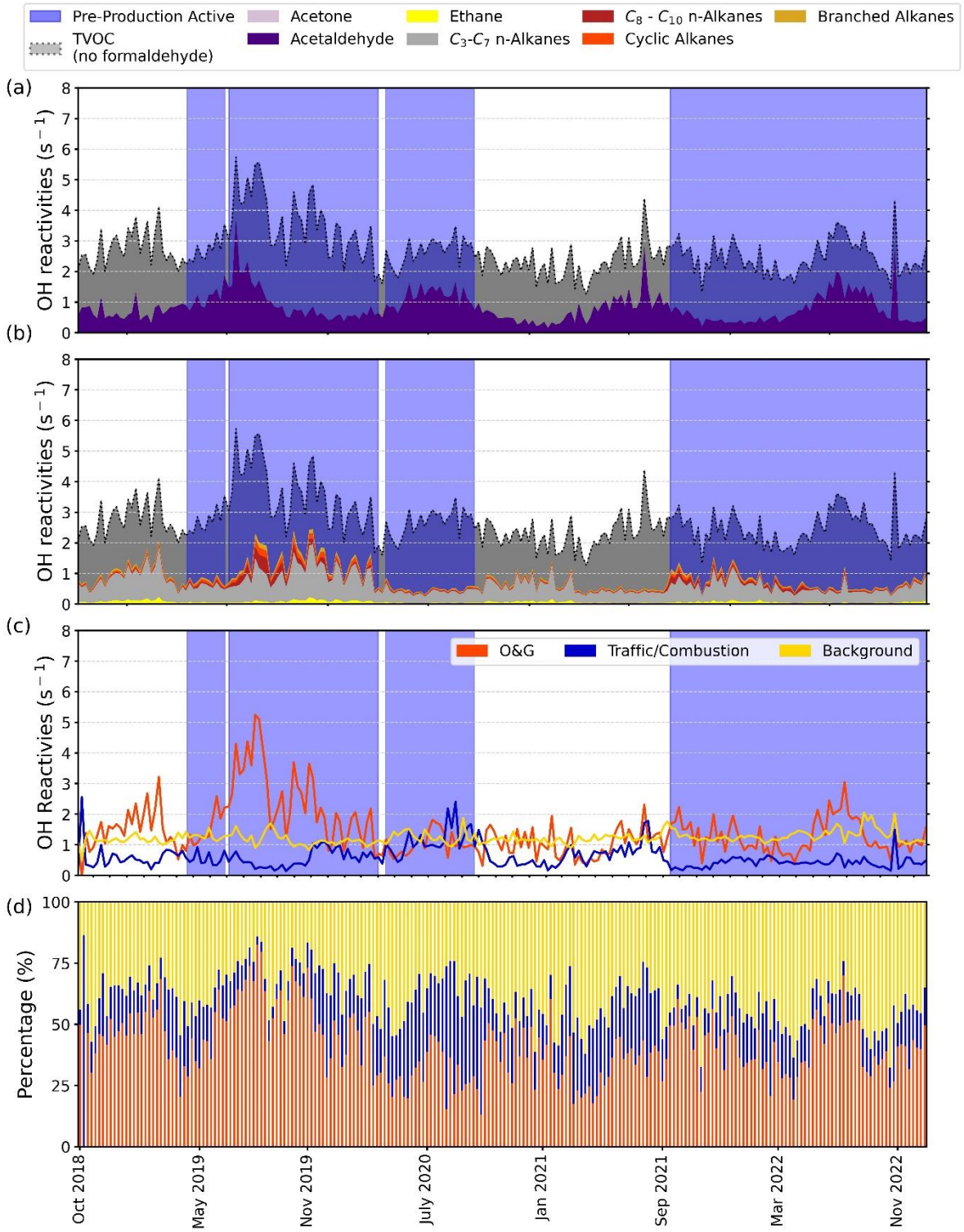

Figure 3.3: Time series of the weekly average of (a) the OVOC OHRs and (b) the overall alkanes OHRs overlapped with total OHRs calculated from the weekly integrated canister samples from October 2018 to December 2022. The purple shading represents the pre-production activities periods.

production; however, the absence of a correlation between acetaldehyde and traffic emission tracers such as CO or ethyne suggests that vehicle emissions may not be the dominant acetaldehyde source. Although similar seasonal trends were observed for acetaldehyde and formaldehyde in the current study, significant variations in acetaldehyde/formaldehyde ratios throughout the sampling period suggest that the sources of these two compounds exhibit seasonal differences. Previous studies have reported similar differences and attributed them to differences in photochemical production and removal rates for acetaldehyde and formaldehyde (Anderson et al., 1996; Lui et al., 2017). Reaction with OH radical is an important removal mechanism for both aldehydes (Atkinson and Arey, 2003), while formaldehyde undergoes more rapid photolysis in the atmosphere. Considering both loss mechanisms, formaldehyde (photolysis rate = 0.3 h^{-1}) tends to degrade more rapidly than acetaldehyde (photolysis rate = 0.018 h^{-1}) during periods of active photochemistry (Anderson et al., 1996), contributing to higher acetaldehyde/formaldehyde ratios observed during summer. In addition to direct emission, acetone is also formed in the atmosphere through the oxidation of other VOCs and undergoes degradation through photolysis and reaction with OH radicals (Fischer et al., 2012). Previous studies revealed the dominant photochemical source of acetone and acetaldehyde were from OH oxidation of ethane and propane, both of which are predominantly emitted from O&G activities (Singh et al., 1994; Sommariva et al., 2011). The strong correlation between acetaldehyde and acetone could suggest indirect influences from O&G emissions on potential ozone formation, as they contribute to the formation of these highly reactive ozone precursors (Lindaas et al., 2019), a topic warranting further study. A strong correlation with isoprene also suggests that biogenic emissions might play an important role in contributing to ambient acetaldehyde levels in this area (Seco et al., 2007), although this correlation might also

reflect the summertime peaks in both isoprene emissions and photochemical production of acetaldehyde.

3.3.2.2 Alkanes and other VOCs

Figure 3.3 (b) shows the contributions of alkanes to total OHR. Propane and n-butane are the largest individual contributors to total alkane OHR, each contributing about 23%. While ethane is more abundant, it is less reactive with OH radicals. Elevated mixing ratios of much more reactive C_8-C_{10} n-alkanes have been connected with emissions from the use of synthetic drilling mud during drilling operations (Ku et al., 2024). The maximum weekly alkane OHR contribution from C_8-C_{10} n-alkanes (shown in dark red) was 24%, observed during drilling operations at the Livingston pad. While synthetic drilling muds can reduce odors and associated complaints, enhanced C_8-C_{10} alkane emissions that result increase the reactivity and ozone formation potential of drilling mud volatiles.

Following the alkanes, methane and alkenes (Figure B.4 (a)) were the next largest contributors to OHR, each accounting for ~13% of the calculated VOC reactivities. The methane contribution is close to values (17-26%) reported in a previous study on ozone production in the region (Lindaas et al., 2019). Although O&G activities have been observed to contribute a significant portion of local methane emissions (Pétron et al., 2014), animal feeding operations are also an important source in the region and both are added onto a large global background. We observed limited variability in methane contributions to overall OHR due to its high background mixing ratio. Ethene and propene were the largest contributors to alkene (excluding isoprene) OHRs. Strong correlations between mixing ratios of these compounds and combustion tracers (CO and ethyne) suggest that urban/traffic emissions were the major sources of these compounds, consistent with findings from a Positive Matrix Factorization (PMF) analysis of this dataset by Lachenmayer (2022). BTEX and other aromatic compounds are typically more reactive with OH

radicals than alkanes; however, their OHR contribution is small in this study due to their relatively low abundances (Figure B.4 (a)).

Although several studies have reported that biogenic contributions to overall OHR and ozone production are relatively low in Colorado's NFR (Gilman et al., 2013; Lindaas et al., 2019; McDuffie et al., 2016; Swarthout et al., 2013), Abeleira et al. (2017) documented a contribution of up to 49% in the afternoon during 2015 summer field observations. This study attributed the discrepancy to varying drought conditions observed during separate study years. In the current study, a notable increase in isoprene contributions was observed during summer months (Figure B.4 (b)), with an average weekly contribution of approximately 7%. The maximum isoprene OHR contribution reached as high as 32% at a neighborhood site in July 2019, while several instances of higher values (higher than 1.0 s^{-1}, >13%) were also calculated throughout the summer sampling periods (Figure B.5). OHR contributions from isoprene and monoterpenes together contributed an average 8% during the summer of 2012 (McDuffie et al., 2016). The absence of monoterpene measurements in the current study mean that we are underestimating the total biogenic VOC contribution, although the work by McDuffie et al. (2016) shows that the average isoprene OHR contribution was about a factor of two higher than from monoterpenes in their observations.

3.3.2.3 Source apportionment of VOC OHRs

To further investigate the relative contributions of UOGD emissions to overall OHR, we applied a Multivariate Regression Analysis (MRA), following Gilman et al. (2013) and Pollack et al. (2021). The method and limitations have been described in detail in these two studies. Briefly, source tracers for O&G production and traffic/combustion emissions, propane and ethyne, were used as independent variables in the MRA. The expression is given in Equation 1 where [VOC] is the observed mixing ratio of a compound, $Bkgd_{VOC}$ is its minimum observed mixing ratio, and

$[propane]_0$ and $[ethyne]_0$ are observed mixing ratios minus the minimum observed values for these two source tracer compounds. The equation is solved for the emissions ratios, $ER'_{propane}$ and ER'_{ethyne}, of an observed VOC relative to propane and ethyne. This analysis does not account for any influences from photochemical production or loss, deposition loss, nor influences from other source emissions. The relative contribution of the O&G source to the observed species mixing ratios was then calculated using Equation 2. Traffic/combustion and background contributions were calculated in the same manner. Given important seasonal variations discussed above and by Ku et al. (2024), a separate MRA was conducted for each seasonal data set.

$$[VOC] = Bkgd_{voc} + \{ER'_{propane} \times [propane_0]\} + \{ER'_{ethyne} \times [ethyne_0]\} \quad (1)$$

$$O\&G\ Fraction = (\{ER'_{propane} \times [propane_0]\}) \,/\, (Bkgd_{voc} + \{ER'_{propane} \times [propane_0]\} + \{ER'_{ethyne} \times [ethyne_0]\}) \quad (2)$$

Results of MRA fit for all VOCs are shown in Table B.2. Figures 3.3 (c) and (d) show time series of absolute VOC OHR values and relative VOC OHR contributions from O&G, traffic/combustion, and background sources. Clear enhancement of the O&G source contribution to VOC OHR (Figure 3.3 (c)) was observed during pre-production periods, especially during development of the first two well pads from March 2019 to July 2020. More consistent contributions from the traffic/combustion source and background were observed throughout the sampling period. On average, O&G sources and background influences each contribute approximately 40% to VOC OHRs, with the remaining 20% from the traffic/combustion source over the entire sampling period. During the pre-production period, the O&G contribution grows to an average 47% of VOC OHR. Outside of the pre-production period the O&G VOC OHR contribution decreases to an average of 36%. It remains an important contributor because air sampled in Broomfield is also impacted by approximately 30,000 producing O&G wells across

the DJ Basin. The value of the average O&G VOC OHR source contribution obtained in this study is somewhat lower than results (55 to 57%) reported from previous studies at the nearby BAO (Gilman et al., 2013; Swarthout et al., 2013). Differences may reflect seasonal differences in other OHR contributions (e.g., stable atmosphere and lower boundary layer which are reduced during the winter periods), the closer proximity of BAO to major O&G producing regions in the DJ Basin, and success in reducing O&G emissions in the region in recent years, as discussed above.

Figure B.6 shows the relative contributions of VOC compound families to each source factor. The VOC source signature for O&G operations clearly differs from the combustion and background factors. The primary contributor to the O&G factor is the group of C_3-C_7 n-alkanes (35%), followed by OVOCs (27%). As shown in Figure 3.4 (a) for OVOCs, the O&G source OHR contributions clearly increase during both pre-production periods. On average, O&G, combustion,

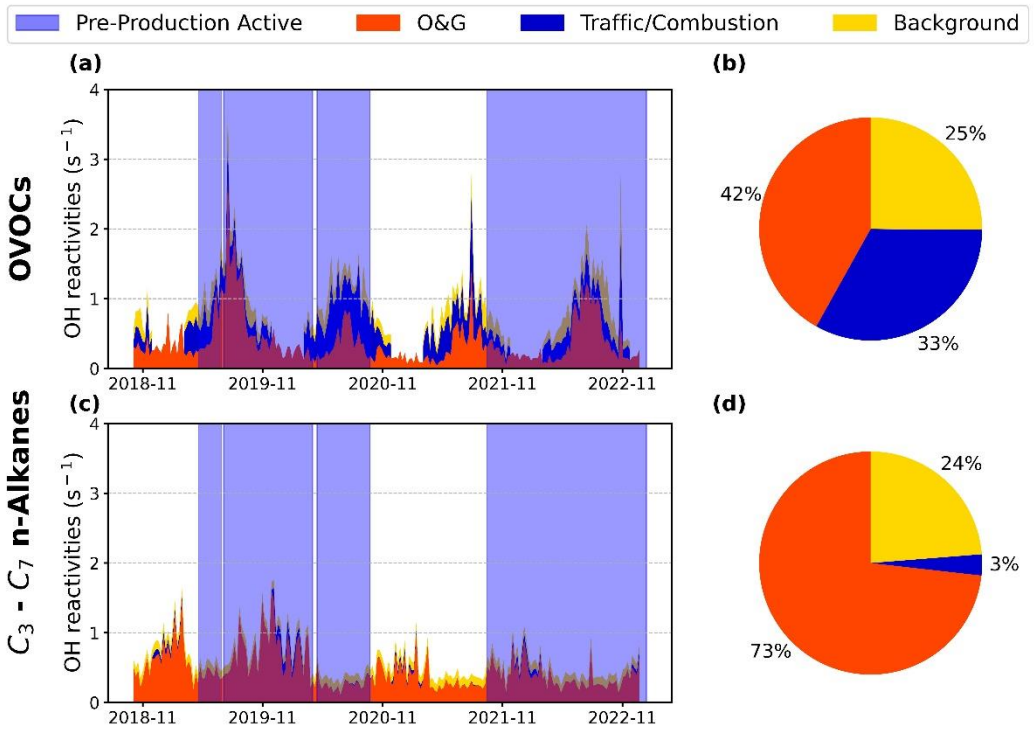

Figure 3.4: The left panel shows the time series of the OHRs derived from the MRA fit for (a) OVOCs, and (b) C_3-C_7 n-alkanes. The right panel shows the pie charts of the mean contribution of each term for (b) OVOCs, and (d) C_3-C_7 n-alkanes.

and background sources are estimated to contribute 42%, 33%, and 25% to OVOC OHRs, respectively. Looking at C_3-C_7 n-alkane OHRs (Figure 3.4 (c)), the O&G source contributes 73% on average, with 24% from background and only 3% from the traffic/combustion source. Overall, results of this analysis suggest that VOCs from O&G emissions are a major sink for OH radicals, suggesting a major contribution to ozone formation potential. Moreover, these contributions increase local OHR and ozone formation potential locally during O&G pre-production activities.

3.3.3 OHR contributions during different stages of O&G development

Figure 3.5 summarizes relative OHR contributions of OHRs from all VOCs measured in (background-corrected) triggered canister samples collected during different well development operations. OHR species contributions for VOCs measured in weekly samples from the Commons background site from February 2020 to December 2022 are included for comparison. The total VOC OHR values calculated for triggered canister samples are, of course, much higher than those

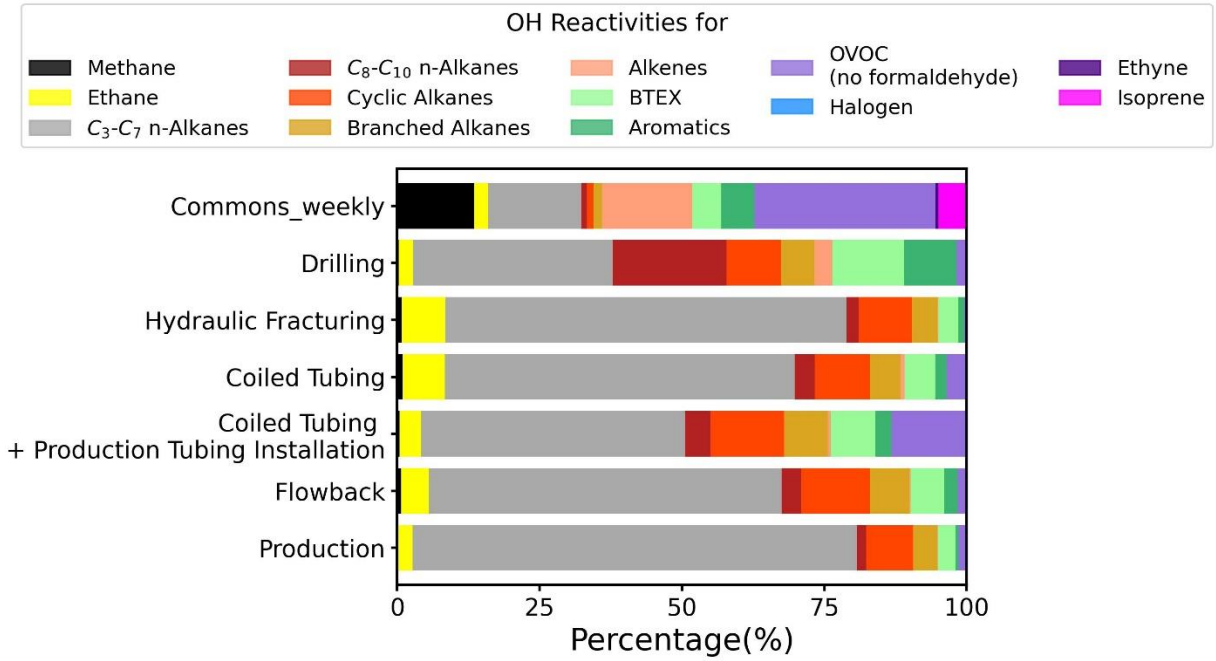

Figure 3.5: Comparison of the contributions of OH reactivities in the different classes of compounds in the Commons site and with the (background-corrected) event-triggered canister samples collected during different O&G development operations.

for weekly VOC samples collected at the Commons background site since triggered canister samples represent collections of transient, VOC-rich plumes. The relative OHR contributions from different VOC classes also differ significantly between the weekly Commons samples and the background-corrected triggered canister samples and even between triggered canister samples associated with capture of plumes from different O&G operations. Although the average OHR for plumes captured from different O&G operation types generally correlated with the average TVOC concentrations in these triggered samples (Figure B.7 (a) & (c)), the varying VOC compositions in plumes across these O&G operation types lead to large differences in relative contributions to VOC OHR (Figure 3.5).

High OHR values associated with triggered canister samples reveal that short-term emissions during O&G pre-production activities can exert a sizeable impact on O_3 formation near O&G operations. We should, however, not over-interpret differences in absolute OHR values between triggered canisters, since these can be strongly influenced by sensor distance from the pad, the PID sensor's threshold for sample collection, and differences in meteorological conditions that affect rates of plume dispersion. These issues are not problematic, however, when considering relative contributions of different VOC compounds to OHR in plumes associated with emissions from different O&G operations.

In weekly VOC samples measured at the Commons background site, OVOCs (32%), C_2-C_7 n-alkanes (19%), alkenes (16%) and methane (13%) are the predominant contributors to the overall VOC OHR, collectively accounting for nearly 80 % on average. The VOC OHR contribution of C_2-C_7 n-alkanes is much larger in background-corrected samples of plumes from O&G operations, accounting for 53% on average. Other important contributors to total VOC OHR varied with O&G operation. During drilling, C_8-C_{10} n-alkanes contributed 20% on average, with

n-octane the largest contributor. C_8-C_{10} alkane OHR contributions were much smaller in plumes from other operations. BTEX, other aromatics, and cyclic alkanes were also important contributors, accounting for 13%, 10% and 9%, respectively, of total VOC OHR in plumes from drilling operations. OVOCs were typically minor contributors to OHR in the plume samples from O&G operations. A notable exception is samples collected during coiled tubing/millout operations and production tubing installation. This result is surprising given that these are fresh plumes collected close to the well pad, some at night, while OVOCs are typically associated with photochemically aged air masses (Gilman et al., 2013; Swarthout et al., 2013; Whalley et al., 2016).

3.4 Conclusion

In this study, we utilized four years of VOCs measurements in Broomfield, CO to estimate OHRs and identify the major sinks of OH radicals. Notably, strong seasonal cycles were observed with higher OHRs during winter. This phenomenon was associated with elevated levels of CO, NO_2, and VOCs, which reflect reduced photochemical activity and increased atmosphere stability during winter months. NO_2 was the primary OH radical sink during winter. During summer VOCs were the largest contributor to total OHR, primarily because of an increase in the abundance of reactive OVOCs. Among VOC OHRs, the OVOCs also stood out as the leading contributor across the full study period, followed by C_3-C_7 n-alkanes. A source apportionment of O&G contributions to measured species mixing ratios and their OHRs, along with an analysis of high OHRs in transient plumes emanating from O&G well pads, demonstrated that emissions from O&G operations significantly contribute to OH radical sinks in the region, especially during pre-production activities. This finding reinforces the importance of considering reductions in O&G emissions as a strategy to help reduce summertime ozone in the region.

Chapter 4

Characterizing potential surrogates for VOC emissions from unconventional oil and gas development

4.1 Introduction

In the past decade advances in extraction techniques, such as horizontal drilling and hydraulic fracturing, have led to a surge in UOGD in the U.S. (U.S. EIA, https://www.eia.gov/todayinenergy/detail.php?id=48756, accessed on 20 February 2023). The explosive growth of UOGD is not confined to rural areas; it extends into populated regions (Ku et al., 2024; McKenzie et al., 2016; Thompson et al., 2014). This widespread growth has prompted numerous studies aimed at understanding potential UOGD impacts on climate, environment, and human health. Field and satellite observations show that O&G-related activities are important sources of NO_x and VOC in the atmosphere (Ghosh, 2018; Gilman et al., 2013; Goldberg et al., 2021; Hecobian et al., 2019; Miller et al., 2013; Pétron et al., 2012; Prenni et al., 2016; Schade and Roest, 2018; Simpson et al., 2010; Swarthout et al., 2013; Warneke et al., 2014; Wilde et al., 2021). Oxidation of these gas precursors plays an important role in atmospheric chemistry by influencing the oxidation capacity and contributing to tropospheric ozone (Cheadle et al., 2017; Edwards et al., 2014; Evans and Helmig, 2017; Helmig et al., 2014; Lindaas et al., 2019; McDuffie et al., 2016) and secondary aerosol (Evanoski-Cole et al., 2017; Prenni et al., 2022; Naimie et al., 2022) formation. Some VOCs are air toxics that are carcinogens or can cause other health impacts for O&G workers or local residents (McKenzie et al., 2018; McMullin et al., 2018; O'Dell et al., 2020; Weisner et al., 2023; Colborn et al., 2011; Colborn et al., 2014; Esswein et al., 2014).

Methane, constituting 45-98% of typical petroleum gases and liquids, along with ethane (1-21%) and propane (trace-15%), stand out as the primary hydrocarbon components of O&G emissions (Lyons et al., 2016). According to the U.S. national emissions inventory, the "natural gas and petroleum system" contributes 30% to anthropogenic methane sources (U.S. EPA, 2023), with additional important contributions from agriculture and waste management sources, including landfills and wastewater treatment. Due to its high global warming potential (28-36 times that of carbon dioxide on an equivalent mass basis over a 100-year average time, Vallero, 2019) and abundance, numerous studies have quantified methane emissions from O&G production through various methodologies (Allen et al., 2013; Brantley et al., 2014; Caulton et al., 2014; Harriss et al., 2015; Katzenstein et al., 2003; Lyon et al., 2015; Marrero et al., 2016; Mead et al., 2023; Peischl et al., 2015; Peischl et al., 2013; Pétron et al., 2014; Townsend-Small et al., 2015). Bottom-up approaches include estimations or direct measurements of methane emission rates from well pads or other O&G facilities through stationary or mobile measurements on the ground. Such results can be combined with activity factors and aggregated to derive total emissions for particular O&G production regions (Brantley et al., 2014; Pétron et al., 2012; Swarthout et al., 2013; Townsend-Small et al., 2015). One novel technique employed by Mead et al. (2023) used near-IR open-path dual-comb spectroscopy to track variations of methane, ethane and propane during drilling and new well completion processes. Bottom-up approaches can provide accurate emission data for specific source types, contributing to the development of effective emission reduction strategies (Allen et al., 2013; Lyon et al., 2015; Mead et al., 2023); however, drawbacks to this approach can include limited coverage of the large number of individual O&G emission sources and geographic areas. This is, in part, because bottom-up emission measurements tend to be time and resource intensive. Obtaining access to well pads or other facilities for measurements can also add

complexity. An alternative top-down approach uses relatively well-mixed air masses measured from satellite or aircraft and offers more comprehensive estimates of total emissions on regional scales but cannot easily distinguish different emission sources within a specific area (Caulton et al., 2014; Chen et al., 2023; Pétron et al., 2012; Schwietzke et al., 2014; Smith et al., 2015). Recent studies used multiple-scale measurements, i.e., integrated top-down and bottom-up approaches, in an attempt to better constrain methane emission inventories (Daniels et al., 2023; Harriss et al., 2015; Miller et al., 2013; Riddick and Mauzerall, 2023).

O&G-related industries are also important VOC sources, contributing 27% of national anthropogenic VOC emissions (U.S. EPA, 2023). The complexity of VOC measurements and sources, however, means that emissions of individual VOCs are generally much less studied and understood than for methane. Significant elevated air toxics and other VOC concentrations and/or emissions have been measured around O&G operations (Edie et al., 2019; Esswein et al., 2014; Ghosh, 2018; Hecobian et al., 2019; Hildenbrand et al., 2016; Ku et al., 2024; Orak et al., 2021). Because methane has several sources beyond O&G operations, some studies have used the simultaneously measured abundance of ethane or other alkanes to help distinguish O&G emissions of methane from other (e.g., agricultural) sources (Ghosh, 2018; Peischl et al., 2013; Smith et al., 2015; Townsend-Small et al., 2015). Some have utilized ratios between alkanes and methane along with methane emission inventories (Marrero et al., 2016) or VOC levels observed in air samples coupled with meteorological information to estimate local and regional VOC emissions (Swarthout et al., 2013). While these efforts have provided important insights, more comprehensive characterization of VOC emissions from particular O&G operations is critical for source identification, assessing the impact of O&G emissions on ozone levels and health, and developing effective emission control strategies. Given the much larger body of work examining methane

emissions, one possibly useful approach would be to examine whether methane emissions can serve as a useful predictor of VOC emissions from O&G. For example, if ratios of the important air toxic benzene to methane are constant across emissions from O&G operations – or even for individual O&G activities such as drilling or production – one could reliably estimate seldom measured emission rates of benzene from the much larger body of work characterizing methane emissions.

Colorado is experiencing a significant boom in energy production. As of 2021 the state ranks as the fifth-largest producer of crude oil and the eighth-largest producer of natural gas in the United State (U.S. EIA, https://www.eia.gov/state/seds/seds-data-complete.php?sid=US#CompleteDataFile, accessed on 12 December 2023). Colorado's primary O&G production areas are situated in the Denver-Julesburg Basin (DJB) in the northeast and in the Piceance Basin (PB) in western Colorado (Figure 4.1). In this study we examined relationships between concentrations of individual VOCs and methane across four extensive field campaigns conducted in the DJB and PB regions of Colorado. These campaigns included measurement of methane and VOC concentrations and/or emission rates during a wide range of O&G activities. In examining species relationships, we focus on correlations between levels of individual VOCs and levels of methane, ethane, and propane in plumes emitted by a range of O&G operations including well drilling and completions and production in two distinct production basins. Our overall goal is to determine the extent to which emissions of methane, ethane, or propane might serve as useful predictors of other VOC emission rates across O&G operations more broadly or for individual activities.

4.2 Methods

4.2.1 Site description and sample information

Data considered in this analysis were from the Piceance and Denver-Julesburg Basins (Figure 4.1). Over 400 source-dominated whole air samples were collected in the vicinity of emission sources on well pads during drilling, completion, and production activities. Measurements came from four different field campaigns (one in the PB and three in the DJB). Two of these campaigns were conducted between 2013 and 2016 to quantify methane and VOC emission rates from well pads in the PB and DJB. Hecobian et al. (2019) provide detailed information on the measurements and emission rates of 48 VOCs for specific O&G activities studied during these campaigns. The complete data sets can be found at https://mountainscholar.org/items/3db2e0a3-6350-4763-b02c-c9ad8e8ede70 (PB) and https://mountainscholar.org/items/3e65c83f-7cdd-424b-978d-ff70eafa7607 (DJB). These studies are referred to as PB and DJB1. Subsequent field campaigns examined well pad operations located

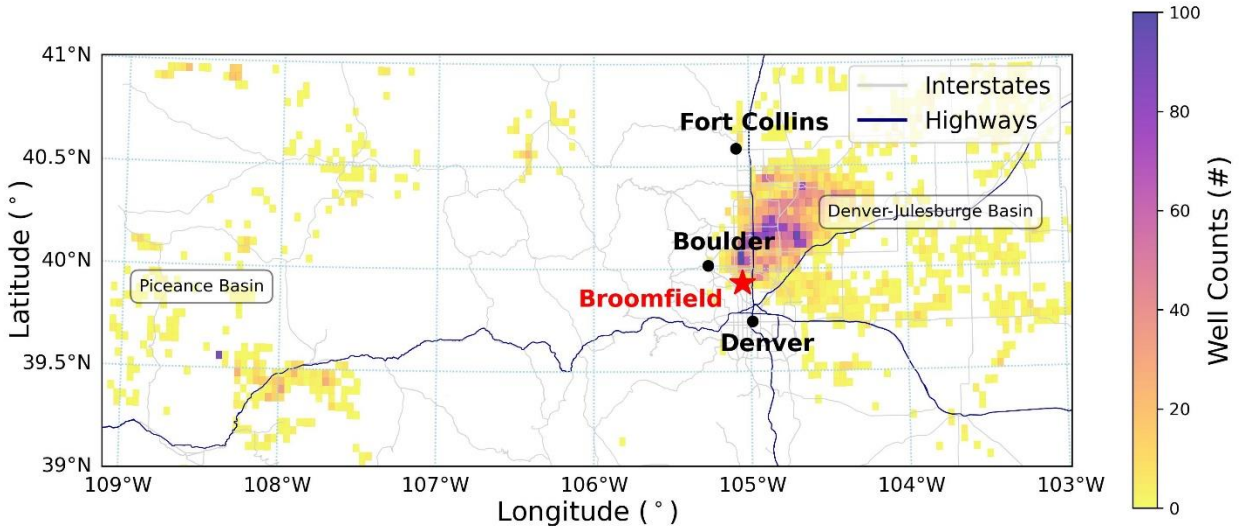

Figure 4.1: Map showing well counts in the Piceance Basin (PB) and the Denver-Julesburg Basin (DJB). Locations of the well sites are obtained from Colorado Energy & Carbon Management Commission (https://cogcc.state.co.us/data2.html#/downloads, accessed on 10 May. 2023). The red star marks the location of Broomfield.

in City and County of Broomfield from 2018 to 2022 (Ku et al., 2024) and at more remote locations in the DJB (study referred to as DJB2) in 2020. Locations of the well pads studied in Broomfield are given by Ku et al. (2024) while, consistent with project agreements with cooperating O&G operators, precise locations of the other study pads are confidential.

To measure emission rates of individual compounds during O&G pre-production or production operations in the first two campaigns, Hecobian et al. (2019) released ethyne from the pad as a tracer. Whole air canister samples were collected upwind of the pad and in the tracer plume downwind, with the plume detected using a Picarro cavity ringdown spectrometer continuously measuring ethyne onboard a hybrid "plume tracker" SUV. In the later campaigns several real-time VOC monitoring systems (APIS, Inc., OR, USA) were deployed around well pads to monitor VOC concentration variations during well drilling, completion, and production activities. Each APIS system was equipped with a 10.6 eV high-sensitivity photoionization detector (PID, IonScience) and an automatic canister triggering device. The PID measured changes in a suite of VOCs that can be photoionized at 10.6 eV (commonly referred to as TVOC). The PID response ranged from 0.5 ppbv to 3 ppmv, based on the PID response to isobutylene. When a VOC-rich plume was detected by the PID at a signal level that exceeded a user defined threshold, an attached canister was automatically triggered to collect an air sample (~ 15 s fill time). During the campaigns, upwind 3-min (Hecobian et al PB and DJB1 studies) or weekly (Broomfield) or 24-hr (remote DJB2 study) samples collected at a designated regional background site were used to background correct the methane and VOC concentrations in the captured plumes. During the four campaigns distances from the well pad or production facility to the point of plume sampling ranged from 14 to 1000 m.

4.2.2 Sample and Data Analyses

All triggered air samples were collected in evacuated 1.4-L Silonite®-coated canisters (*Entech* Instruments, CA, USA) for subsequent VOC analysis at the Colorado State University Atmospheric Science Department. Methane and up to 50 individual VOCs were analyzed in each canister by gas chromatography (GC). The analytical systems are described in detail in previous studies (Ku et al., 2024; Sive et al., 2005; Zhou et al., 2005). Briefly, methane was analyzed using a Shimadzu GC-8A equipped with a flame ionization detector (FID). Individual VOCs (C_2-C_{10} non-methane hydrocarbons (NMHCs) and C_2 halocarbons) were analyzed using three GCs coupled with five detectors including three FIDs, one electron capture detector, and a mass spectrometer. A complete list of measured compounds is shown in Table C.1. Working standards were analyzed with each analysis batch for methane and VOCs to assess any drift in system response and to derive response factors for measured compounds. The measurement precision (1 relative standard deviation, RSD) was 4% for methane and 2%-20% for other VOCs. The calibration standard accuracy is ±5%.

Mixing ratios lower than the detection limits were replaced with half the detection limit prior to further analysis. We subtracted the background mixing ratio of each compound from the mixing ratio measured in the plume source sample to isolate methane and VOC concentrations emitted by the source of interest from other regional source contributions. Mixing ratios of selected compounds were then plotted against methane, ethane, and propane mixing ratios for each field experiment and for each source type. Linear regression slopes are obtained to define ratios of the selected compounds to our three potential O&G tracers (methane, ethane, and propane), and the quality of fit is determined by the regression correlation coefficient.

4.3 Results and Discussion

4.3.1 Comparison of VOC Measurements

Figure 4.2 compares mixing ratios of key compounds of interest (methane, ethane, benzene, C_8-C_{10} n-alkanes, and BTEX – sum up of benzene, toluene, ethylbenzene, and xylenes), separated

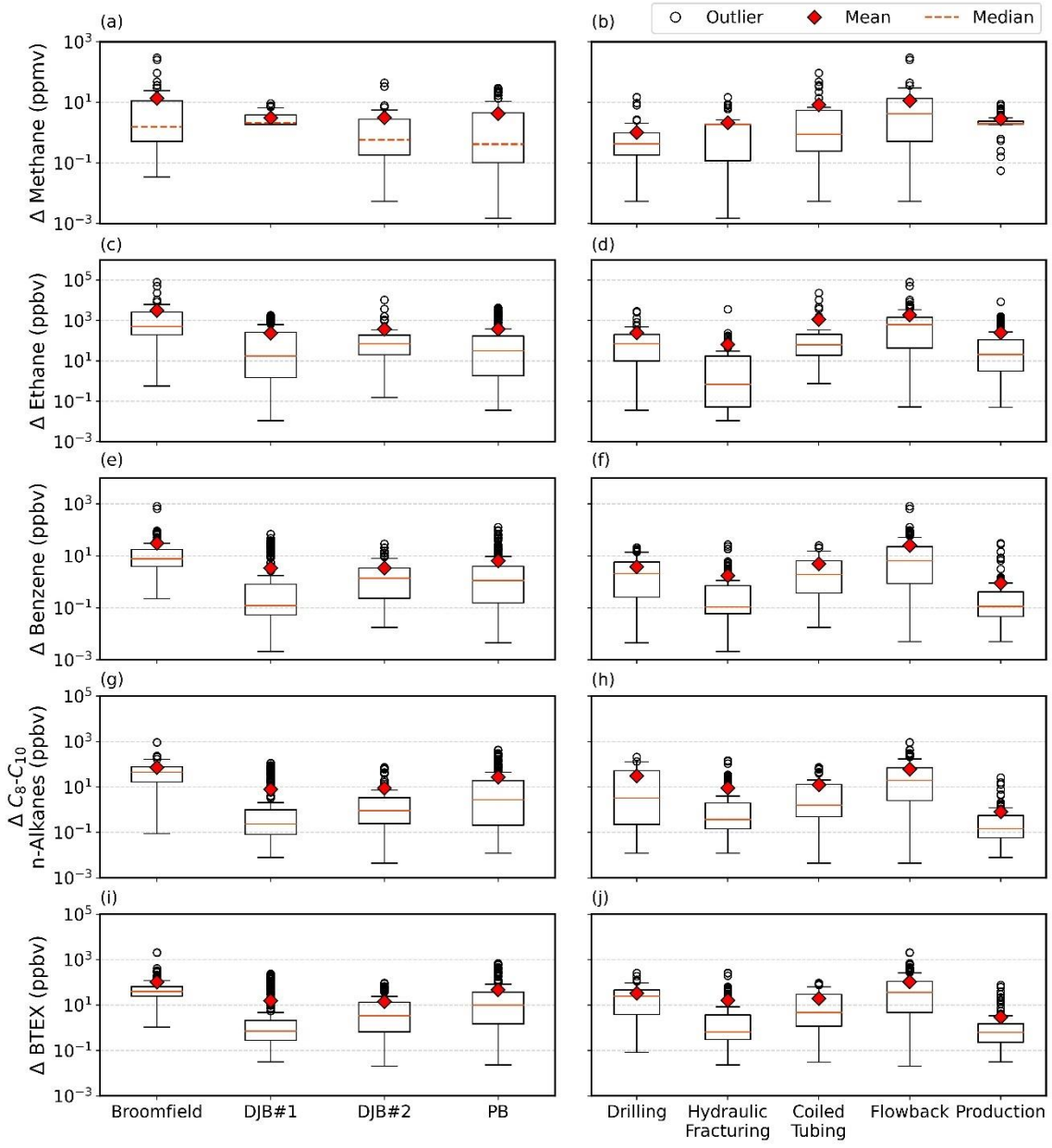

Figure 4.2: Box and whisker plots (90th, 75th, 50th, 25th, 10th percentiles) including mean and outlier values of excess (background-corrected) mixing ratios for methane, ethane, benzene, C_8-C_{10} n-alkanes, and BTEX measured across four studies (left panels) and different O&G pre-production activities (right panels).

across field campaigns (left panels) and by O&G activity (right panels). Similar variations are seen across compounds in their mean mixing ratios, suggesting common origins related to O&G activities. Substantial variations were observed in the mixing ratios of these compounds within each field study and O&G operation. It is not surprising to see variability, given the variability in operations and environmental conditions in each grouping, including measurement distance from the source, time of year, time of day, and meteorological conditions for each measurement, and inclusion of various operation types or locations. Dispersion of emissions increases with distance from the source at a rate that is strongly influenced by environmental conditions, including atmospheric stability, wind speed, and surface roughness. Differences between the nature of individual O&G operations influence the magnitude and composition of VOC emissions (Ku et al., 2024). For example, volatilization of drilling mud along with outgassing of volatile subsurface hydrocarbons brought to the surface with drill cuttings combine with drill rig engine emissions during drilling operations. During hydraulic fracturing, by contrast, when material is being pushed downhole, emissions are dominated by generation of the power needed to frack the wells. In order to remove some of the variability associated with these factors, we instead look at background-corrected ratios of individual compounds or compound families. This is also the approach needed to examine whether emissions of more commonly measured compounds (e.g., methane) can serve as useful predictors of emissions of less commonly measured compounds of interest (e.g., benzene). Figure 4.3 shows example comparisons of the background-corrected mixing ratios of benzene and methane. The data are separated into groups by study location and by O&G activity type as in Figure 4.2.

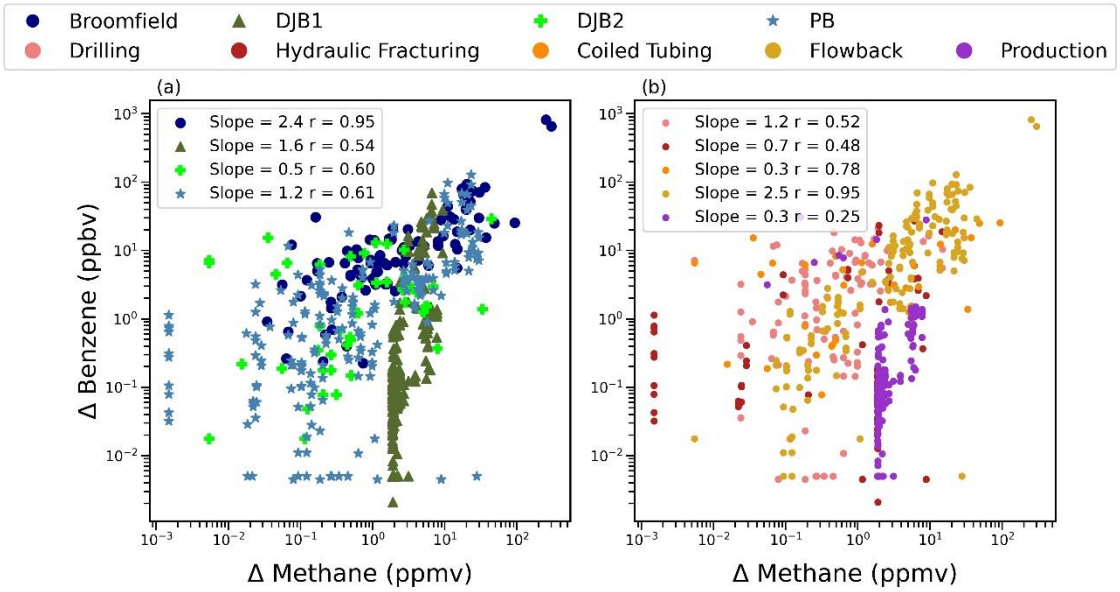

Figure 4.3: Scatter plots of benzene to methane excess mixing ratio (ppb/ppm, background-corrected) in UOGD plume samples. (a) The left panel includes all samples, grouped by studies. (b) The right panel groups samples by UOGD activity.

4.3.2 Correlation with tracer compounds

To help assess whether methane, ethane, or propane are useful surrogates for other less commonly measured O&G-emitted VOCs, we examined the correlation of all measured compounds with each of these compounds for each operation type and field experiment. As a rough indicator of predictive ability, we counted the number of compounds having a correlation coefficient (r) higher than 0.6-0.9 with each of the three candidate surrogate species. The resultsare shown in Figure 4.4 (a) and (b). Although propane sometimes appears to exhibit greater frequency of higher correlation with more compounds than the other two surrogates (e.g., during drilling and production operations), this analysis does not reveal a clear overall "winner" as the best surrogate. To refine our analysis, we focused only on select compounds of particular interest (e.g., air toxics) and/or strongly associated with O&G emissions, specifically alkanes, benzene, and BTEX (the sum of benzene, toluene, ethylbenzene, and xylenes) (see Figures 4.4 (c) and (d)). These figures reveal some interesting patterns. First, variations in the correlation coefficient (r) values with each surrogate candidate species are generally smaller. Consistently strong correlations were observed

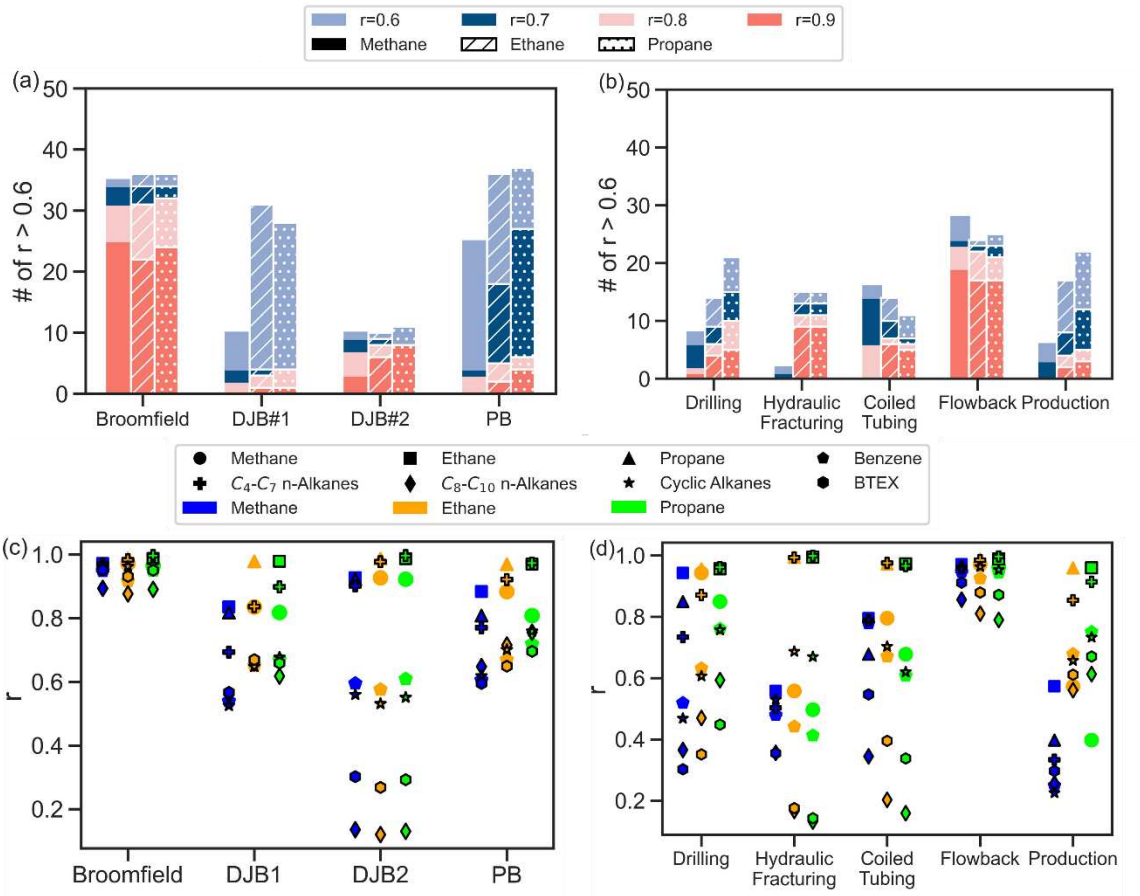

Figure 4.4: The bar charts in the top panel (a) and (b) show the number of species-specific correlation coefficients (r) larger than 0.6, 0.7, 0.8 and 0.9 for samples collected (a) in each study, (b) during different UOGD operations. The different bars represent correlations with methane, ethane, or propane. 50 species were included in the analysis. The plots in the bottom panel depict correlation coefficients (r) between methane, ethane, and propane and selected compounds/compound groups for samples collected (c) in each field campaign and (d) during different UOGD operations.

between the selected compounds and all three surrogates in the Broomfield campaign and during flowback operations at all study locations. Greater variability in the strength of correlations exists for other study locations and other operation types. The three candidate surrogate species are highly correlated with each other ($r > 0.8$) during drilling, in addition to flowback, but the correlation decreases during other operation types, including fracking (when emissions tend to be dominated by diesel or natural gas frack engines), coil tubing/millout operations (when plugs inserted to frack the well in stages are drilled out) and production. Relatively weak correlations

were observed between C_8-C_{10} n-alkanes or BTEX with the three candidate surrogate species during drilling, hydraulic fracturing, and coil tubing operations. While BTEX naturally occurs in crude oil and can be found in O&G emissions (Lyons et al., 2016; Hecobian et al., 2019; Ku et al., 2024), BTEX is also emitted from combustion (e.g., truck traffic or on-pad power generation) and various industrial sources (Hecobian et al., 2019; Na et al., 2004; Pollack et al., 2021; Russo et al., 2010). Edie et al. (2019) documented inconsistent variations in methane and BTEX abundance in O&G plumes during near-source measurements. Regarding C_8-C_{10} n-alkanes, prior studies suggested O&G production is not a primary source of heavier alkanes (Swarthout et al., 2013; Wilde et al., 2021). However, Ku et al. (2024) reported a significant enrichment of this compound group during drilling activity in Broomfield, attributed to the use of a synthetic, low odor drilling mud. C_8-C_{10} alkane emissions in Broomfield were much lower on wells drilled with a petroleum-based drilling mud. Given differences in industry practices, including drilling mud choice, therefore, it is not surprising that emissions of these C_8-C_{10} alkane emissions might vary relative to emissions of methane or other light alkanes.

One pattern seen in several of the comparisons is that correlations of higher molecular weight hydrocarbons with propane and ethane are often somewhat higher than correlations with methane. This is especially noticeable in the comparisons for hydraulic fracturing, coil tubing, and production processes. Propane has been commonly chosen as an O&G tracer for source apportionment purposes in several previous studies (Gilman et al., 2013; Pollack et al., 2021; Swarthout et al., 2013; Wilde et al., 2021). Light alkanes predominantly originate from O&G-related industries, constituting a large fraction of observed non-methane VOCs in various measured environments. The robust correlations between propane and C_4-C_7 n-alkanes, for example, affirm that key O&G activities are a source of all of these compounds.

Our analysis thus far indicates that while there are definitely good correlations between emissions of individual hydrocarbons or hydrocarbon families and methane, ethane, or propane in some situations, none of the three candidate compounds are ideal surrogates across all operation types. Further, while ethane and propane may offer somewhat stronger predictive ability in more situations than methane, it is important to remember that methane emissions are much more commonly measured than ethane or propane emissions. Given these limitations, in the next section, we present more quantitative assessments of the relationships between selected hydrocarbon mixing ratios and mixing ratios of the three candidate surrogate compounds.

4.3.3 Emissions ratios

Table 4.1 summarizes the relationships between mixing ratios of the selected compounds/families and those of the three surrogates. All species mixing ratios were background corrected. Mixing ratios of methane are given in ppmv while mixing ratios for all other species are given in ppbv. Intercepts were forced to zero for all of the regression analyses. For the values presented in Table 4.1, only those with significant correlations ($p > 0.05$) between the targeted compound and surrogate are reported. Figure 4.5 provides an overview of the average of these emission ratios related to each surrogate from different O&G activities with propagation of uncertainties. The emission ratios obtained from the integration of the four studies generally fall within the ranges observed in different O&G operations. However, wide ranges, up to an order of magnitude difference, of emission ratios are revealed for paired compounds across various O&G activities. Higher emission ratios were observed during drilling, and flowback compared to other processes. The relative intensities of emission ratios were inconsistent for different pairs of compounds across O&G operations and surrogates. For example, the highest emission ratios of propane/methane and i-butane/methane were observed during flowback operations, whereas the

Table 4.1: Summary of the slopes (emission ratios) for relationships between mixing ratios of indicated hydrocarbons and mixing ratios of each of the three surrogate compounds derived from linear regression analysis. Intercepts were forced to zero for all of the regression analyses. Units are in ppmv for methane and ppbv for all other species in this analysis. The uncertainty was determined as the average distance between the observed values and the regression line.

		Integrated data from the four field experiments	Drilling	Hydraulic Fracturing	Coil Tubing	Flowback	Production
Methane	Ethane	165.3 ± 30.97	222.2 ± 7.86	64.8 ± 10.45	178.0 ± 22.90	224.5 ± 4.37	136.8 ± 15.64
	Propane	101.0 ± 27.75	106.7 ± 6.65	27.2 ± 5.14	92.0 ± 16.85	170.6 ± 3.80	108.5 ± 20.03
	i-Butane	16.1 ± 3.96	18.5 ± 1.45	5.5 ± 1.02	11.9 ± 1.83	30.2 ± 0.61	14.5 ± 2.96
	n-Butane	43.1 ± 10.04	46.0 ± 3.60	11.6 ± 2.25	31.8 ± 4.68	89.9 ± 2.16	36.3 ± 7.50
	i-Pentane	12.6 ± 2.94	13.9 ± 1.40	4.1 ± 0.78	7.7 ± 0.93	29.2 ± 0.69	8.2 ± 2.18
	n-Pentane	16.8 ± 3.59	18.7 ± 2.06	5.8 ± 1.12	9.7 ± 1.08	41.5 ± 1.04	8.3 ± 2.27
	n-Hexane	8.7 ± 1.96	9.6 ± 1.39	3.2 ± 0.60	4.5 ± 0.41	23.5 ± 0.66	2.4 ± 0.97
	n-Heptane	2.8 ± 0.83	4.0 ± 0.71	1.6 ± 0.27	1.0 ± 0.16	6.9 ± 0.18	0.5 ± 0.19
	n-Octane	1.3 ± 0.62	2.2 ± 0.47	1.4 ± 0.37	0.3 ± 0.11	2.6 ± 0.09	0.2 ± 0.05
	n-Nonane	0.8 ± 0.46	1.5 ± 0.36	0.9 ± 0.27		0.7 ± 0.05	0.04 ± 0.01
	n-Decane	1.1 ± 1.18	3.7 ± 1.16	0.5 ± 0.16		0.2 ± 0.04	0.03 ± 0.01
	Cyclopentane	1.0 ± 0.26	1.3 ± 0.17	0.4 ± 0.08	0.6 ± 0.07	2.3 ± 0.07	0.5 ± 0.15
	Cyclohexane	2.0 ± 0.54	2.7 ± 0.44	1.0 ± 0.16	0.9 ± 0.11	4.9 ± 0.12	0.6 ± 0.21
	Methylcyclohexane	3.1 ± 0.99	3.3 ± 0.79	2.2 ± 0.45	1.0 ± 0.18	8.2 ± 0.24	0.7 ± 0.26
	Benzene	1.0 ± 0.28	1.2 ± 0.21	0.7 ± 0.14	0.3 ± 0.05	2.5 ± 0.07	0.3 ± 0.09
	Toluene	1.5 ± 0.57		2.0 ± 0.54	0.4 ± 0.09	3.0 ± 0.14	0.5 ± 0.11
	Ethylbenzene	0.2 ± 0.10	0.2 ± 0.09	0.2 ± 0.04		0.2 ± 0.01	0.02 ± 0.004
	m- and p-Xylene	1.2 ± 0.72	1.4 ± 0.33	1.9 ± 0.64		1.3 ± 0.06	0.1 ± 0.03
	o-Xylene	0.3 ± 0.17	0.6 ± 0.14	0.3 ± 0.10		0.4 ± 0.02	0.04 ± 0.01

Table 4.1: Summary of the slopes (emission ratios) for relationships between mixing ratios of indicated hydrocarbons and mixing ratios of each of the three surrogate compounds derived from linear regression analysis. Intercepts were forced to zero for all of the regression analyses. Units are in ppmv for methane and ppbv for all other species in this analysis. The uncertainty was determined as the average distance between the observed values and the regression line (continued).

		Integrated data from the four field experiments	Drilling	Hydraulic Fracturing	Coil Tubing	Flowback	Production
Ethane	Methane	0.004 ± 0.0010	0.004 ± 0.0001	0.005 ± 0.0008	0.004 ± 0.0005	0.004 ± 0.0001	0.002 ± 0.0003
	Propane	0.685 ± 0.0375	0.510 ± 0.0154	0.468 ± 0.0053	0.590 ± 0.0201	0.758 ± 0.0090	1.097 ± 0.0256
	i-Butane	0.108 ± 0.0076	0.091 ± 0.0040	0.093 ± 0.0010	0.070 ± 0.0024	0.133 ± 0.0018	0.151 ± 0.0056
	n-Butane	0.277 ± 0.0205	0.226 ± 0.0102	0.203 ± 0.0027	0.184 ± 0.0059	0.399 ± 0.0061	0.375 ± 0.0154
	i-Pentane	0.081 ± 0.0078	0.071 ± 0.0043	0.071 ± 0.0009	0.040 ± 0.0017	0.129 ± 0.0021	0.094 ± 0.0058
	n-Pentane	0.105 ± 0.0101	0.098 ± 0.0065	0.101 ± 0.0013	0.049 ± 0.0023	0.184 ± 0.0032	0.093 ± 0.0066
	n-Hexane	0.053 ± 0.0063	0.052 ± 0.0049	0.055 ± 0.0009	0.020 ± 0.0016	0.107 ± 0.0014	0.033 ± 0.0032
	n-Heptane	0.016 ± 0.0037	0.021 ± 0.0029	0.018 ± 0.0020	0.004 ± 0.0008	0.030 ± 0.0005	0.006 ± 0.0007
	n-Octane	0.008 ± 0.0039	0.012 ± 0.0019	0.007 ± 0.0034		0.011 ± 0.0005	0.002 ± 0.0002
	n-Nonane	0.004 ± 0.0015	0.008 ± 0.0014			0.003 ± 0.0002	0.0003 ± 0.00004
	n-Decane	0.007 ± 0.0048	0.020 ± 0.0048			0.001 ± 0.0002	0.0001 ± 0.00003
	Cyclopentane	0.007 ± 0.0008	0.007 ± 0.0006	0.007 ± 0.0001	0.003 ± 0.0002	0.010 ± 0.0003	0.006 ± 0.0005
	Cyclohexane	0.012 ± 0.0020	0.014 ± 0.0016	0.013 ± 0.0008	0.004 ± 0.0005	0.021 ± 0.0004	0.007 ± 0.0007
	Methylcyclohexane	0.017 ± 0.0051	0.019 ± 0.0031	0.019 ± 0.0038	0.004 ± 0.0009	0.036 ± 0.0010	0.009 ± 0.0009
	Benzene	0.005 ± 0.0016	0.006 ± 0.0008	0.006 ± 0.0013	0.001 ± 0.0002	0.011 ± 0.0003	0.003 ± 0.0003
	Toluene	0.006 ± 0.0009			0.001 ± 0.0005	0.013 ± 0.0007	0.003 ± 0.0004
	Ethylbenzene	0.001 ± 0.0004				0.001 ± 0.00003	0.0001 ± 0.00002
	m- and p-Xylene	0.004 ± 0.0014	0.007 ± 0.0013			0.005 ± 0.0003	0.001 ± 0.0001
	o-Xylene	0.002 ± 0.0006	0.003 ± 0.0006			0.002 ± 0.0001	0.0002 ± 0.00003

Table 4.1: Summary of the slopes (emission ratios) for relationships between mixing ratios of indicated hydrocarbons and mixing ratios of each of the three surrogate compounds derived from linear regression analysis. Intercepts were forced to zero for all of the regression analyses. Units are in ppmv for methane and ppbv for all other species in this analysis. The uncertainty was determined as the average distance between the observed values and the regression line (continued).

		Integrated data from the four field experiments	Drilling	Hydraulic Fracturing	Coil Tubing	Flowback	Production
Propane	Methane	0.006 ± 0.0020	0.007 ± 0.0004	0.009 ± 0.0017	0.005 ± 0.0009	0.005 ± 0.0001	0.001 ± 0.0003
	Ethane	1.529 ± 0.0845	1.796 ± 0.0543	2.113 ± 0.0241	1.606 ± 0.0547	1.290 ± 0.0153	0.840 ± 0.0196
	i-Butane	0.163 ± 0.0062	0.182 ± 0.0044	0.199 ± 0.0006	0.117 ± 0.0028	0.175 ± 0.0010	0.140 ± 0.0032
	n-Butane	0.415 ± 0.0157	0.456 ± 0.0089	0.435 ± 0.0010	0.305 ± 0.0082	0.529 ± 0.0023	0.348 ± 0.0097
	i-Pentane	0.125 ± 0.0076	0.149 ± 0.0048	0.152 ± 0.0005	0.065 ± 0.0036	0.171 ± 0.0017	0.090 ± 0.0042
	n-Pentane	0.167 ± 0.0108	0.207 ± 0.0077	0.216 ± 0.0006	0.078 ± 0.0051	0.244 ± 0.0024	0.088 ± 0.0050
	n-Hexane	0.086 ± 0.0087	0.114 ± 0.0071	0.117 ± 0.0013	0.030 ± 0.0034	0.138 ± 0.0023	0.033 ± 0.0025
	n-Heptane	0.027 ± 0.0063	0.049 ± 0.0043	0.037 ± 0.0043	0.005 ± 0.0015	0.039 ± 0.0009	0.006 ± 0.0005
	n-Octane	0.014 ± 0.0031	0.028 ± 0.0031			0.014 ± 0.0006	0.002 ± 0.0002
	n-Nonane	0.008 ± 0.0024	0.020 ± 0.0024			0.003 ± 0.0003	0.0003 ± 0.00004
	n-Decane	0.016 ± 0.0085	0.047 ± 0.0085			0.001 ± 0.0002	0.0001 ± 0.00002
	Cyclopentane	0.011 ± 0.0010	0.015 ± 0.0008	0.015 ± 0.0001	0.005 ± 0.0004	0.013 ± 0.0003	0.006 ± 0.0004
	Cyclohexane	0.020 ± 0.0032	0.033 ± 0.0025	0.028 ± 0.0017	0.006 ± 0.0009	0.028 ± 0.0006	0.007 ± 0.0006
	Methylcyclohexane	0.029 ± 0.0098	0.047 ± 0.0050	0.039 ± 0.0082	0.005 ± 0.0016	0.046 ± 0.0015	0.009 ± 0.0007
	Benzene	0.009 ± 0.0030	0.015 ± 0.0012	0.011 ± 0.0027	0.002 ± 0.0004	0.014 ± 0.0004	0.003 ± 0.0002
	Toluene	0.013 ± 0.0122	0.032 ± 0.0121		0.002 ± 0.0008	0.016 ± 0.0009	0.003 ± 0.0004
	Ethylbenzene	0.001 ± 0.0007	0.003 ± 0.0007			0.001 ± 0.00004	0.0001 ± 0.00001
	m- and p-Xylene	0.008 ± 0.0023	0.017 ± 0.0023			0.007 ± 0.0004	0.001 ± 0.0001
	o-Xylene	0.003 ± 0.0010	0.007 ± 0.0010			0.002 ± 0.0001	0.0002 ± 0.00003

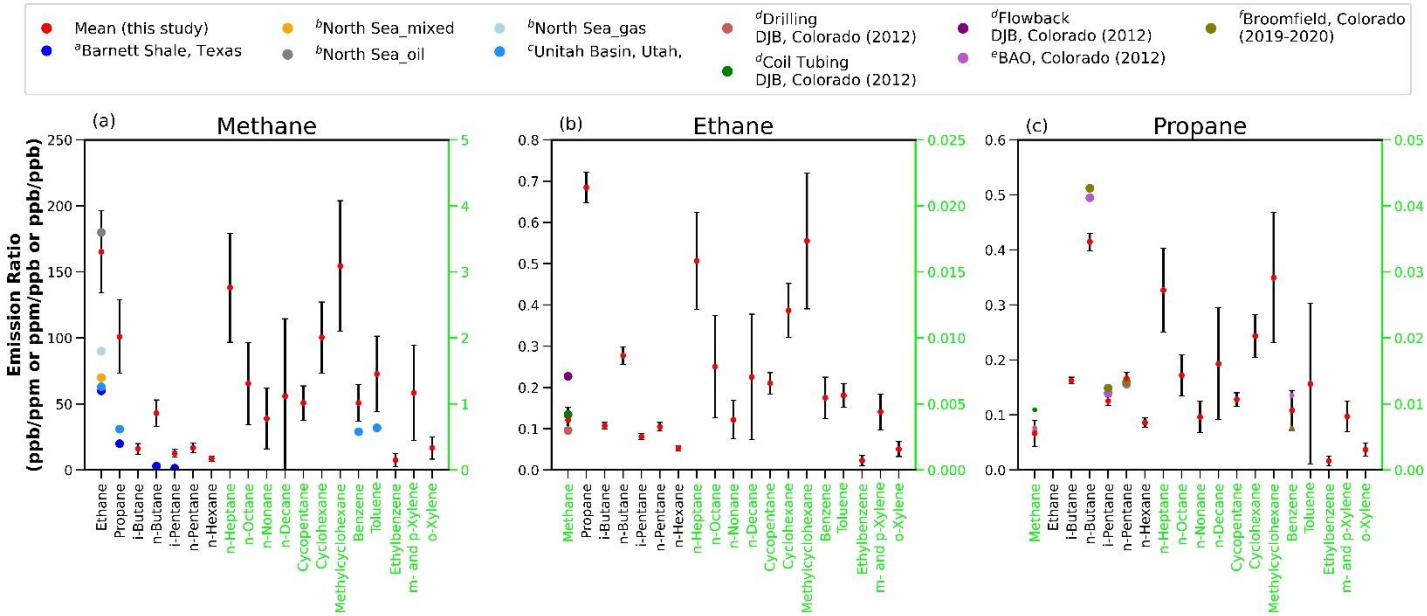

Figure 4.5: The emission ratios for select compounds in relation to each candidate surrogate. The emission ratios reported in previous literature are overlaid for comparison ([a]Townsend-Small et al. 2015, [b]Wilde et al., 2021, [c]Helmig et al., 2014, [d]Pétron et al., 2014, [e]Gilman et al., 2013; Swarthout et al., 2013, [f]Mead et al., 2023).

ratios between these compounds and ethane were highest during production. Various relationships between C_8-C_{10} n-alkanes and BTEX and the surrogates were observed. A lack of correlation was noted between C_8-C_{10} n-alkanes and BTEX with methane during coil tubing processes. Similar conditions were also found between these compounds with ethane and propane during the hydraulic fracturing, and coil tubing processes. These findings suggest that methane, ethane, and propane might not be suitable surrogates for emissions of these hydrocarbon groups during all O&G operations.

Table 4.2 presents a comparison of selected emission ratios reported in this study with those from previous O&G studies. If multiple emission ratios were reported under the same sample type in previous studies, we calculated and reported the average emission ratio with associated uncertainty here. Our study found much higher emission ratios in some cases, some up to ~ 10 times different, relative to methane compared to studies conducted in the North Sea, Barnett Shale in Texas, and Uintah Basin in Utah (Helmig et al., 2014; Townsend-Small et al., 2015; Wilde et al., 2021). Differences in extraction location, formation geology, and operational practices could contribute to differences in observed ratios (Field et al., 2014). Examining emissions ratios relative to ethane and propane, our results are more consistent with values reported in prior studies conducted in Colorado, even those conducted a decade ago. This suggests that the emission ratios related to ethane and propane reported in this study may be representative of O&G emissions across the major O&G production fields in Colorado.

4.4 Conclusion

This study examined a large dataset of emission ratios involving three O&G tracers observed at different stages of operations across two major O&G-producing fields in Colorado. Significant variations, spanning up to an order of magnitude, were observed in emission ratios

Table 4.2: Summary of correlation slopes of the selected paired from current and previous studies. Units are in ppmv for methane and ppbv for other species in this analysis.

Surrogate		Sample Type	[a]DJB + PB, Colorado, 2013-2022	[b]DJB, Colorado, May 2012	[c]BAO, Colorado, Feb 2012	[d]Broomfield, Colorado 2019-2020	[e]Barnett Shale, Texas, October 2013	[f]North Sea 2015-2019	[g]Unitah Basin, Utah, Winters in 2012 & 2013
Methane	Ethane	Mixed	165.3 ± 30.97				60	70	63
	Ethane	Oil						180	
	Ethane	Gas						90	
	Propane	Mixed	101.0 ± 27.75				20		31
	i-Butane	Mixed	16.1 ± 3.96						
	n-Butane	Mixed	43.1 ± 10.04				3		
	n-Pentane	Mixed	16.8 ± 3.59				1.4		
	Benzene	Mixed	1.0 ± 0.28						0.58
	Toluene	Mixed	1.5 ± 0.57						0.64
Ethane	Methane	Drilling	0.004 ± 0.0001			0.003			
	Methane	Coil Tubing	0.004 ± 0.0005			0.0042			
	Methane	Flowback	0.004 ± 0.0001			0.0071			
Propane	Methane	Mixed	0.006 ± 0.0020	0.006 ± 0.0003					
	Methane	Drilling	0.007 ± 0.0004			0.0064			
	Methane	Coil Tubing	0.005 ± 0.0009			0.00915			
	Methane	Flowback	0.005 ± 0.0001			0.0055			
	n-Butane	Mixed	0.415 ± 0.0157	0.495 ± 0.007	0.512 ± 0.0001				
	i-Pentane	Mixed	0.125 ± 0.0076	0.14 ± 0.004	0.149 ± 0.0001				
	n-Pentane	Mixed	0.167 ± 0.0108	0.156 ± 0.003	0.160 ± 0.0001				
	Benzene	Mixed	0.009 ± 0.0030	0.0113 ± 0.0009	0.0063 ± 0.000001				

Reference: [a]Current study, [b]Pétron et al. (2014), [c]Gilman et al. (2013) & Swarthout et al. (2013), [d]Mead et al. (2023), [e]Townsend-Small et al. (2015), [f]Wilde et al. (2021), [g]Helmig et al. (2014).

between alkanes, and air toxics with the three tracers in and across different stages of O&G operations. None of the candidate compounds, methane, propane, or ethane were ideal surrogates for prediction of emissions of other VOCs in all circumstances, although some measurements in some locations and during some operations did sometimes exhibit strong correlations. While ethane and, especially, propane, sometimes showed greater promise as a surrogate for other VOC emissions than methane, it is important to keep in mind that methane emissions are much more commonly measured.

Chapter 5

Conclusions and Future Work

5.1 Summary and Conclusions

Rapid growth of unconventional oil and natural gas development in the United States has raised concerns about impacts on air quality and human health associated with O&G emissions. While significant effort has been made to quantify methane emissions, relatively few observations have been made of VOCs, especially during drilling and completion of new wells. This study presented measurements and analyses from an extensive air monitoring program during development of several large, multi-well pads in suburban Broomfield, Colorado, USA. Measurements began prior to development and continued through well drilling and completions and on into pad production. Several monitoring sites, with short (seconds to minutes) and/or longer (weekly) timescale measurements, were deployed across the community to document air quality changes near well pads and in nearby residential neighborhoods and offer important insight into how VOC concentrations and both acute and chronic exposure potential vary in time and space. We also calculated OH reactivities of VOCs measured in Broomfield to consider their ozone formation potential and apportion those contributions between O&G-associated emissions and other sources. In a third analysis, we investigated the potential use of UOGD methane, ethane, and propane emissions as surrogates to predict emissions of air toxics and other less frequently measured VOCs during various UOGD activities.

Hecobian et al. (2019) previously reported significant VOC emissions during drilling operations, with a strong combustion signature reflecting the substantial on-site power generation needed to power drilling rigs in use at studied well pads. The use of electrified, grid-powered drill

rigs in Broomfield eliminated those large engine emissions helping to reveal the underlying emissions associated with drilling mud volatilization. Hecobian et al. (2019) also reported much higher emissions of many VOCs, including ethane, propane, n-decane, and benzene, during flowback compared to drilling operations. Our measurements in Broomfield; however, reveal a contrasting pattern, with larger near-pad concentration increases of these compounds during drilling operations in comparison to flowback, especially at the Livingston pad. Given the elimination of large engine emissions during drilling operations at Broomfield, this is strong evidence that improvements to flowback operations in Broomfield, including the use of closed-loop fluid handling systems and elimination of permanent fluid storage tanks on the well pad, helped reduce average VOC emissions during flowback.

Despite these and other emission reduction measures, however, elevated concentrations of air toxics and other VOCs near well pads and in adjacent neighborhoods were still observed and linked to O&G development in Broomfield. These impacts were much larger during periods of well drilling and completions than after well pads moved into production. Analysis of weekly samples collected near well pads, in adjacent neighborhoods and at a more distant background reference site reveal increased concentrations of many VOCs near well pads during drilling, coiled tubing/millout and production tubing operations, and flowback. Additionally, specific groups of VOC emissions were observed to be associated with particular processes. For example, the use of synthetic (Neoflo) drilling mud resulted in substantial increases in near-pad concentrations of C_8–C_{10} n-alkanes during drilling operations. The utilization of the Neoflo-based drilling mud effectively reduced odor complaints, but the emission of more reactive long-chain alkanes highlighted the importance of drilling mud handling and recycling operations as a source of ozone precursors, especially in this ozone non-attainment region.

Maximum weekly concentrations of benzene, which typically range between approximately 0.1 and 0.2 ppbv in Broomfield, did not exceed 0.8 ppbv even at near well pad sites during the height of pre-production activities. This level is well below the 3 ppbv health guideline value for chronic exposure used by the State of Colorado for non-cancer health effects. The weekly observations, however, while helping assess long-term exposure potential can mask much more dynamic concentration variations tied to short-term emission events.

High time-resolution measurements (PTR-MS and PID sensor systems) included in the study revealed that concentrated VOC plumes were emitted across a wide range of operations, at least for short periods. Concentrated plumes were tied, for example, to emissions from volatilization of drilling mud during drilling operations, to the emptying of sand canisters during closed-loop flowback operations, and to separator cleaning and maintenance operations during production. The VOC compositions of detected plumes provide important insight into the composition of VOCs emitted by different operations and can help identify targets for future emission reduction strategies, including volatilization during separation of drill cuttings and drilling mud, relocating separator cleaning maintenance operations, and seeking ways to limit VOC loss during emptying of sand canisters during flowback operations. Moreover, the short duration of detected plumes (79% of O&G-attributed plumes lasted <30 min) underscores the need for rapid measurement approaches to effectively characterize these episodic emissions.

The health guideline value (HGV) used by the State of Colorado for acute benzene exposure is 9 ppbv for exposures of at least one hour. Numerous plumes were captured emanating from O&G operations with benzene concentrations exceeding 9 ppbv, with a maximum plume concentration in excess of 800 ppbv. Because these plume samples (~15 s canister fill time) were much shorter than an hour in duration, however, they cannot be directly compared to the acute

HGV. An initial assessment using the continuously measured PID signal to extrapolate measured benzene concentrations to an hour does suggest that exposures exceeding 9 ppbv for an hour are likely at near-pad locations. Our finding that exceedances of acute exposure HGVs are more likely than exceedance of chronic exposure HGVs reinforces the conclusions, based on dispersion model analyses, of a prior health risk analysis during well pad development in Colorado's DJ Basin (Holder et al., 2019).

Using VOCs measured in Broomfield to calculate OH reactivities (OHRs) revealed strong seasonal cycles with higher OHRs during winter. NO_2 was the primary OH radical sink during winter, while VOCs were the largest contributor to total OHR during the summertime ozone season, primarily because of an increase in reactive OVOCs. A source apportionment of O&G contributions to measured species mixing ratios and their OHRs, along with an analysis of high OHRs in transient plumes emanating from O&G well pads, demonstrated that emissions from O&G operations significantly contribute to OH radical sinks in the region, especially during pre-production activities.

Significant variations were observed in emission ratios of individual VOCs to three O&G tracers (methane, ethane, and propane) at different stages of operations across two major O&G-producing fields in Colorado, the Piceance and DJ Basins. None of the candidate compounds, methane, propane, or ethane were ideal surrogates for prediction of emissions of other VOCs in all circumstances. Correlations between concentrations of key air toxics and other O&G-related VOCs were sometimes higher with ethane and, especially, propane concentrations than with methane; however, it is important to keep in mind that methane emissions are much more commonly measured.

5.2 Recommendations for Future Work

Here, we discuss the limitations and potential future extensions to this work.

- While this study conducted comprehensive measurements to characterize air quality changes associated with specific UOGD pre-production activities in the surrounding neighborhood of Broomfield, it would ideally have even more complete measurements of emissions impacts in both space and time. For example, more continuous measurements would better characterize ranges of air toxics exposure over longer periods. Moreover, some potentially important compounds such as formaldehyde, an air toxic and an important ozone precursor, were not measured in this study and should be a focus of future measurements. Of course, continuously measuring speciated VOCs is an expensive and resource intensive endeavor, especially at the dense spatial resolution needed to capture transient emissions near to well pads.
- Broomfield is one of the wealthier communities with active O&G exploration and production in the DJ Basin. Extensive citizen engagement and substantial resource investments by the City and County of Broomfield helped to ensure implementation of important best management practices to reduce air emissions, to fund the hire of city inspectors to help monitor O&G operations, and to fund implementation of an extensive air monitoring program. There is a compelling need to mount similar efforts in other communities, especially disproportionately impacted communities where O&G operations and their air quality impacts tend to receive much less scrutiny.
- Acute and chronic health impacts of new well development in Broomfield were explored by comparing the air toxics concentrations in triggered and in weekly integrated canisters to the suggested health guideline values (HGVs) by the Agency for Toxic Substances and

Disease Registry (ATSDR) also used by the State of Colorado. However, suggested exposure guideline values differ between organizations such as the WHO and various U.S. states or organizations. These reference or guideline values also differ depending on the health endpoint of interest (e.g., cancer vs. a range of non-cancer health effects), the duration of exposure, and whether the reference value is a point above which health impacts are expected (e.g., U.S. EPA – AEGL-1) or a point below which health impacts are not expected such as the ATSDR-HGVs. While the State of Colorado has employed ATSDR HGVs as a benchmark level, it is important to note that the assumed acute exposure duration was set to one hour. This indicates that directly comparing our triggered canister measurements (~15 s) with the acute exposure ATSDR HGV is not appropriate. In future work, we intend to combine PID response timelines with measured plume VOC concentrations to extrapolate triggered canister concentrations to estimate 1-h average concentrations. This approach will provide a better assessment of potential health risks associated with exposure to VOC levels observed in Broomfield.

- Elevated mixing ratios of much more reactive C_8-C_{10} n-alkanes associated with emissions from the use of synthetic (Neoflo) drilling muds, suggested additional work is needed to consider potential tradeoffs in the choice of these muds in drilling operations. While they are increasingly favored for drilling operations in populated areas, due to their lower odor impacts and decreased aromatics content, their potential to contribute to enhanced ozone formation is an important concern in ozone non-attainment regions like the Colorado North Front Range. To gain a better understanding of Neoflo emissions during drilling mud recycling operations, we plan to conduct field and laboratory analyses on drilling mud and drill cutting samples on an operational pad. These experiments will include airborne VOC

measurements above shakers that separate drill cuttings from drilling mud as a first step in drilling mud recycling and near storage bins used to accumulate drill cuttings before they are hauled away for disposal. They also include laboratory headspace analysis of drilling mud samples, conducted at a range of temperatures, to examine how VOC the composition of emitted VOCs changes as a function of changing temperatures with increasing well depth.

- Calculation of OH reactivities provides one simple approach to assess the potential of VOCs to generate ozone by characterizing the initial rate of attack by this important atmospheric oxidant, a step that is often rate-limiting in the overall NO_x-VOC photochemistry that leads to ozone production. This approach, however, neglects important factors that can influence overall influence on ozone formation, including VOC attack by other oxidants (e.g., ozone or nitrate radical) or direct VOC photolysis and variations in the importance of a range of possible radical termination reactions to form, for example, hydroperoxides or nitrates. To gain a deeper understanding of the contribution of O&G-related VOCs to ozone formation, a comprehensive photochemical mechanism assessment is essential. Utilizing an idealized box model is a viable and recommended option for further investigating the formation of ozone in the presence of observed VOCs and available NO_x. Such an approach can consider multiple and multi-step reaction schemes leading to summertime ozone episodes and provide a convenient way to assess how ozone formation during these episodes would be affected by increasing or decreasing emission of O&G-related VOCs and NO_x.
- Despite incorporating a substantial number of trace gases (CO, NO_2, and VOCs measured in this study) into our calculations, our results remain a lower bound on OH reactivity in

the region. Future investigations should more fully examine concentrations of other VOCs, especially monoterpenes and other OVOCs like methanol and ethanol. Previous studies conducted in the vicinity reported differing conclusions regarding the significance of biogenic contributions to overall ozone formation potential and OH reactivity. The observed disparity was attributed to varying drought conditions in the study years. Subsequent investigations into the biogenic contributions to OH reactivity over several years of measurements in Broomfield will offer valuable insights, aiding a better understanding of the importance of their role in ozone production potential.

- Multivariate regression analysis (MRA) is a simple source apportionment method for identifying emission sources of measured hydrocarbons and for estimating emissions contributions from each emission source. Propane and ethyne were used as source tracers for O&G and traffic emissions and were assumed to be independent of each other in the MRA. However, our observation of ethyne-rich plumes originating from the Livingston pad suggest that ethyne emissions can, at least at certain times, also come from O&G operations. Previous studies have also detected elevated ethyne from gas flaring emissions (Schade and Roest, 2016, 2018). In general, combustion of carbon-containing fuels can result in the simultaneous production of small amounts of propane and ethyne (Warneke et al., 2017). Going forward, a more cautious and explicit quantification of influences on atmospheric levels of these species from O&G and traffic sources is needed to ensure their use as source tracers in MRA analyses does not significantly bias the targeted source apportionment.
- The third objective of this research was to investigate if any of three O&G tracers, methane, ethane, and propane, might serve as useful surrogates to predict other VOC emissions

across O&G operations or even for individual O&G activities. While none of the candidate compounds proved to be ideal surrogates for prediction of emissions of other less commonly measured VOCs in all circumstances, further investigation will focus on more detailed analysis of the relationship between benzene as a priority air toxic and the three tracers to better assess when and where emissions especially of methane, the most commonly measured compound, can be used, and with what error, as a surrogate for predicting air toxics emissions. This assessment is important for defining the uncertainty associated, for example, with claims that efforts to reduce methane emissions (often driven by climate concerns) will also produce proportionate reductions in emissions of air toxics.

References

Abeleira, A., Pollack, I. B., Sive, B., Zhou, Y., Fischer, E. V., and Farmer, D. K.: Source characterization of volatile organic compounds in the Colorado Northern Front Range Metropolitan Area during spring and summer 2015, J. Geophys. Res.-Atmos., 122, 3595–3613, https://doi.org/10.1002/2016jd026227, 2017.

Akagi, S. K., Craven, J. S., Taylor, J. W., McMeeking, G. R., Yokelson, R. J., Burling, I. R., Urbanski, S. P., Wold, C. E., Seinfeld, J. H., Coe, H., and Alvarado, M. J.: Evolution of trace gases and particles emitted by a chaparral fire in California, Atmos. Chem. Phys., 12, 1397–1421, https://doi.org/10.5194/acp12-1397-2012, 2012.

Allen, D. T., Torres, V. M., Thomas, J., Sullivan, D. W., Harrison, M., Hendler, A., Herndon, S. C., Kolb, C. E., Fraser, M. P., and Hill, A. D.: Measurements of methane emissions at natural gas production sites in the United States, Proceedings of the National Academy of Sciences, 110, 17768-17773, https://doi.org/10.1073/pnas.1304880110, 2013.

Alvarez, R. A., Zavala-Araiza, D., Lyon, D. R., Allen, D. T., Barkley, Z. R., Brandt, A. R., Davis, K. J., Herndon, S. C., Jacob, D. J., and Karion, A.: Assessment of methane emissions from the US oil and gas supply chain, Science, 361, 186-188, https://www.science.org/doi/10.1126/science.aar7204, 2018.

Anderson, L. G., Lanning, J. A., Barrell, R., Miyagishima, J., Jones, R. H., and Wolfe, P.: Sources and sinks of formaldehyde and acetaldehyde: An analysis of Denver's ambient concentration data, Atmospheric Environment, 30, 2113-2123, https://doi.org/10.1016/1352-2310(95)00175-1, 1996.

Atkinson, R.: Gas-Phase Tropospheric Chemistry of Volatile Organic Compounds: 1. Alkanes and Alkenes, J. Phys. Chem. Ref. Data, 26, 215–290, https://doi.org/10.1063/1.556012, 1997.

Atkinson, R. and Arey, J.: Atmospheric Degradation of Volatile Organic Compounds, Chem. Rev., 103, 4605–4638, https://doi.org/10.1021/cr0206420, 2003.

Baker, A. K., Beyersdorf, A. J., Doezema, L. A., Katzenstein, A., Meinardi, S., Simpson, I. J., Blake, D. R., and Sherwood Rowland, F.: Measurements of nonmethane hydrocarbons in 28 United States cities, Atmos. Environ., 42, 170–182, https://doi.org/10.1016/j.atmosenv.2007.09.007, 2008.

Ban-Weiss, G. A., McLaughlin, J. P., Harley, R. A., Kean, A. J., Grosjean, E., and Grosjean, D.: Carbonyl and nitrogen dioxide emissions from gasoline-and diesel-powered motor vehicles, Environmental Science & Technology, 42, 3944-3950, https://doi.org/10.1021/es8002487, 2008.

Bari, M. A., Kindzierski, W. B., and Spink, D.: Twelve-year trends in ambient concentrations of volatile organic compounds in a community of the Alberta Oil Sands Region, Canada, Environ. Int., 91, 40–50, https://doi.org/10.1016/j.envint.2016.02.015, 2016.

Benedict, K. B., Zhou, Y., Sive, B. C., Prenni, A. J., Gebhart, K. A., Fischer, E. V., Evanoski-Cole, A., Sullivan, A. P., Callahan, S., and Schichtel, B. A.: Volatile organic compounds and ozone in Rocky Mountain National Park during FRAPPE, Atmos. Chem. Phys., 19, 499-521, https://doi.org/10.5194/acp-19-499-2019, 2019.

Bien, T. and Helmig, D.: Changes in summertime ozone in Colorado during 2000–2015, Elementa: Science of the Anthropocene, 6, https://doi.org/10.1525/elementa.300, 2018.

Brantley, H. L., Thoma, E. D., Squier, W. C., Guven, B. B., and Lyon, D.: Assessment of methane emissions from oil and gas production pads using mobile measurements, Environ. Sci. Technol., 48, 14508-14515, https://doi.org/10.1021/es503070q, 2014.

Burkholder, J. B., Sander, S. P., Abbatt, J., Barker, J. R., Cappa, C., Crounse, J. D., Dibble, T. S., Huie, R. E., Kolb, C. E., Kurylo, M. J., Orkin, V. L., Percival, C. J., Wilmouth, D. M., and Wine, P. H.: Chemical Kinetics and Photochemical Data for Use in Atmospheric Studies, Evaluation No. 19, JPL Publication 19-5, Jet Propulsion Laboratory, Pasadena, http://jpldataeval.jpl.nasa.gov, 2019.

Buzcu-Guven, B. and Fraser, M. P.: Comparison of VOC emissions inventory data with source apportionment results for Houston, TX, Atmos. Environ., 42, 5032-5043, https://doi.org/10.1016/j.atmosenv.2008.02.025, 2008.

Buzcu, B. and Fraser, M. P.: Source identification and apportionment of volatile organic compounds in Houston, TX, Atmos. Environ., 40, 2385-2400, https://doi.org/10.1016/j.atmosenv.2005.12.020, 2006.

Caulton, D. R., Shepson, P. B., Santoro, R. L., Sparks, J. P., Howarth, R. W., Ingraffea, A. R., Cambaliza, M. O., Sweeney, C., Karion, A., and Davis, K. J.: Toward a better understanding and quantification of methane emissions from shale gas development, Proceedings of the National Academy of Sciences, 111, 6237-6242, https://doi.org/10.1073/pnas.1316546111, 2014.

Chang, Y.-K., Wu, C.-C., Lee, L.-T., Lin, R. S., Yu, Y.-H., and Chen, Y.-C.: The short-term effects of air pollution on adolescent lung function in Taiwan, Chemosphere, 87, 26-30, https://doi.org/10.1016/j.chemosphere.2011.11.048, 2012.

Cheadle, L. C., Oltmans, S. J., Petron, G., Schnell, R. C., Mattson, E. J., Herndon, S. C., Thompson, A. M., Blake, D. R., and McClure-Begley, A.: Surface ozone in the Colorado northern Front Range and the influence of oil and gas development during FRAPPE/DISCOVER-AQ in summer 2014, Elem. Sci. Anth., 5, 61–83, https://doi.org/10.1525/elementa.254, 2017.

Chen, Z., Jacob, D. J., Gautam, R., Omara, M., Stavins, R. N., Stowe, R. C., Nesser, H., Sulprizio, M. P., Lorente, A., and Varon, D. J.: Satellite quantification of methane emissions and oil–gas methane intensities from individual countries in the Middle East and North Africa: implications for climate action, Atmospheric Chemistry and Physics, 23, 5945-5967, https://doi.org/10.5194/acp-23-5945-2023, 2023.

Chiang, H.-L., Tsai, J.-H., Chen, S.-Y., Lin, K.-H., and Ma, S.-Y.: VOC concentration profiles in an ozone non-attainment area: a case study in an urban and industrial complex metroplex in southern Taiwan, Atmospheric Environment, 41, 1848-1860, https://doi.org/10.1016/j.atmosenv.2006.10.055, 2007.

Chin, J.-Y. and Batterman, S. A.: VOC composition of current motor vehicle fuels and vapors, and collinearity analyses for receptor modeling, Chemosphere, 86, 951-958, https://doi.org/10.1016/j.chemosphere.2011.11.017, 2012.

Choi, Y.-J. and Ehrman, S. H.: Investigation of sources of volatile organic carbon in the Baltimore area using highly time-resolved measurements, Atmos. Environ., 38, 775-791, https://doi.org/10.1016/j.atmosenv.2003.10.004, 2004.

Coggon, M. M., Gkatzelis, G. I., McDonald, B. C., Gilman, J. B., Schwantes, R. H., Abuhassan, N., Aikin, K. C., Arend, M. F., Berkoff, T. A., and Brown, S. S.: Volatile chemical product emissions enhance ozone and modulate urban chemistry, Proceedings of the National Academy of Sciences, 118, e2026653118, https://doi.org/10.1073/pnas.2026653118, 2021.

Colborn, T., Kwiatkowski, C., Schultz, K., and Bachran, M.: Natural gas operations from a public health perspective, Human and ecological risk assessment: An International Journal, 17, 1039-1056, https://doi.org/10.1080/10807039.2011.605662, 2011.

Colborn, T., Schultz, K., Herrick, L., and Kwiatkowski, C.: An exploratory study of air quality near natural gas operations, Hum. Ecol. Risk Assess. Int. J., 20, 86-105, https://doi.org/10.1080/10807039.2012.749447, 2014.

Crutzen, P. J., Lawrence, M. G., and Pöschl, U.: On the background photochemistry of tropospheric ozone, Tellus B: Chemical and Physical Meteorology, 51, 123-146, https://doi.org/10.3402/tellusb.v51i1.16264, 1999.

Daniels, W., Wang, J. L., Ravikumar, A., Harrison, M., Roman-White, S., George, F., and Hammerling, D.: Towards multi-scale measurement-informed methane inventories: reconciling bottom-up site-level inventories with top-down measurements using continuous monitoring systems, ChemRxiv. Cambridge: Cambridge Open Engage, https://doi.org/10.26434/chemrxiv-2023-jp5nt-v2, 2023. This content is a preprint and has not been peer-reviewed.

Dinh, T.-V., Kim, S.-Y., Son, Y.-S., Choi, I.-Y., Park, S.-R., Sunwoo, Y., and Kim, J.-C.: Emission characteristics of VOCs emitted from consumer and commercial products and their ozone formation potential, Environmental Science and Pollution Research, 22, 9345-9355, https://doi.org/10.1007/s11356-015-4092-8, 2015.

Dolgorouky, C., Gros, V., Sarda-Esteve, R., Sinha, V., Williams, J., Marchand, N., Sauvage, S., Poulain, L., Sciare, J., and Bonsang, B.: Total OH reactivity measurements in Paris during the 2010 MEGAPOLI winter campaign, Atmospheric Chemistry and Physics, 12, 9593-9612, https://doi.org/10.5194/acp-12-9593-2012, 2012.

Dutta, C., Chatterjee, A., Jana, T., Mukherjee, A., and Sen, S.: Contribution from the primary and secondary sources to the atmospheric formaldehyde in Kolkata, India, Science of the total environment, 408, 4744-4748, https://doi.org/10.1016/j.scitotenv.2010.01.031, 2010.

Edie, R., Robertson, A. M., Soltis, J., Field, R. A., Snare, D., Burkhart, M. D., and Murphy, S. M.: Off-site flux estimates of volatile organic compounds from oil and gas production facilities using fast-response instrumentation, Environmental Science & Technology, 54, 1385-1394, https://doi.org/10.1021/acs.est.9b05621, 2019.

Edwards, P. M., Brown, S. S., Roberts, J. M., Ahmadov, R., Banta, R. M., DeGouw, J. A., Dubé, W. P., Field, R. A., Flynn, J. H., and Gilman, J. B.: High winter ozone pollution from carbonyl photolysis in an oil and gas basin, Nature, 514, 351-354, https://doi.org/10.1038/nature13767, 2014.

Esswein, E. J., Snawder, J., King, B., Breitenstein, M., Alexander-Scott, M., and Kiefer, M.: Evaluation of some potential chemical exposure risks during flowback operations in unconventional oil and gas extraction: preliminary results, J. Occup. Environ. Hyg, 11, D174–D184, https://doi.org/10.1080/15459624.2014.933960, 2014.

Evanoski-Cole, A., Gebhart, K., Sive, B., Zhou, Y., Capps, S., Day, D., Prenni, A., Schurman, M., Sullivan, A., and Li, Y.: Composition and sources of winter haze in the Bakken oil and gas extraction region, Atmos. Environ., 156, 77-87, https://doi.org/10.1016/j.atmosenv.2017.02.019, 2017.

Evans, J. M. and Helmig, D.: Investigation of the influence of transport from oil and natural gas regions on elevated ozone levels in the northern Colorado front range, Journal of the Air & Waste Management Association, 67, 196-211, https://doi.org/10.1080/10962247.2016.1226989, 2017.

Field, R. A., Soltis, J., and Murphy, S.: Air quality concerns of unconventional oil and natural gas production, Environ. Sci.-Proc Imp., 16, 954–969, https://doi.org/10.1039/c4em00081a, 2014.

Fischer, E., Jacob, D. J., Millet, D., Yantosca, R. M., and Mao, J.: The role of the ocean in the global atmospheric budget of acetone, Geophysical Research Letters, 39, https://doi.org/10.1029/2011GL050086, 2012.

Fuhrer, J., Val Martin, M., Mills, G., Heald, C. L., Harmens, H., Hayes, F., Sharps, K., Bender, J., and Ashmore, M. R.: Current and future ozone risks to global terrestrial biodiversity and ecosystem processes, Ecology and evolution, 6, 8785-8799, https://doi.org/10.1002/ece3.2568, 2016.

Gelencsér, A., Siszler, K., and Hlavay, J.: Toluene-Benzene Concentration Ratio as a Tool for Characterizing the Distance from Vehicular Emission Sources, Environ. Sci. Technol., 31, 2869–2872, https://doi.org/10.1021/es970004c, 1997.

Ghosh, B.: Impact of Changes in Oil and Gas Production Activities on Air Quality in Northeastern Oklahoma: Ambient Air Studies in 2015–2017, Environ. Sci. Technol., 52, 3285–3294, https://doi.org/10.1021/acs.est.7b05726, 2018.

Ghude, S. D., Jena, C., Chate, D., Beig, G., Pfister, G., Kumar, R., and Ramanathan, V.: Reductions in India's crop yield due to ozone, Geophysical Research Letters, 41, 5685-5691, https://doi.org/10.1002/2014GL060930, 2014.

Gilman, J. B., Lerner, B. M., Kuster, W. C., and de Gouw, J. A.: Source Signature of Volatile Organic Compounds from Oil and Natural Gas Operations in Northeastern Colorado, Environ. Sci. Technol., 47, 1297–1305, https://doi.org/10.1021/es304119a, 2013.

Gilman, J. B., Kuster, W. C., Goldan, P. D., Herndon, S. C., Zahniser, M. S., Tucker, S. C., Brewer, W. A., Lerner, B. M., Williams, E. J., Harley, R. A., Fehsenfeld, F. C., Warneke, C., and De Gouw, J. A.: Measurements of volatile organic compounds during the 2006 TexAQS/GoMACCS campaign: Industrial influences, regional characteristics, and diurnal dependencies of the OH reactivity, J. Geophys. Res.-Atmos., 114, 1–17, https://doi.org/10.1029/2008JD011525, 2009.

Gkatzelis, G. I., Coggon, M. M., McDonald, B. C., Peischl, J., Aikin, K. C., Gilman, J. B., Trainer, M., and Warneke, C.: Identifying Volatile Chemical Product Tracer Compounds in U.S. Cities, Environ. Sci. Technol., 55, 188–199, https://doi.org/10.1021/acs.est.0c05467, 2021.

Goetz, A. R., & Boschmann, E. E.: Metropolitan Denver: Growth and Change in the Mile High City, University of Pennsylvania Press (BOOK), ISBN: 978-0-8122-5045-9, 2018.

Goldberg, D. L., Anenberg, S. C., Kerr, G. H., Mohegh, A., Lu, Z., and Streets, D. G.: TROPOMI NO2 in the United States: A detailed look at the annual averages, weekly cycles, effects of temperature, and correlation with surface NO2 concentrations, Earth's future, 9, e2020EF001665, https://doi.org/10.1029/2020EF001665, 2021.

Grulke, N. and Heath, R.: Ozone effects on plants in natural ecosystems, Plant Biology, 22, 12-37, https://doi.org/10.1111/plb.12971, 2020.

Halliday, H. S., Thompson, A. M., Wisthaler, A., Blake, D. R., Hornbrook, R. S., Mikoviny, T., Müller, M., Eichler, P., Apel, E. C., and Hills, A. J.: Atmospheric benzene observations from oil and gas production in the Denver-Julesburg Basin in July and August 2014, J. Geophys. Res.-Atmos., 121, 11055–11074, https://doi.org/10.1002/2016JD025327, 2016.

Harriss, R., Alvarez, R. A., Lyon, D., Zavala-Araiza, D., Nelson, D., and Hamburg, S. P.: Using multi-scale measurements to improve methane emission estimates from oil and gas operations in the Barnett Shale region, Texas, https://doi.org/10.1021/acs.est.5b02305, 2015.

Hecobian, A., Clements, A. L., Shonkwiler, K. B., Zhou, Y., MacDonald, L. P., Hilliard, N., Wells, B. L., Bibeau, B., Ham, J. M., Pierce, J. R., and Collett, J. L.: Air Toxics and Other Volatile Organic Compound Emissions from Unconventional Oil and Gas Development, Environ. Sci. Tech. Let., 6, 720–726, https://doi.org/10.1021/acs.estlett.9b00591, 2019.

Helmig, D.: Air quality impacts from oil and natural gas development in Colorado, Elementa: Science of the Anthropocene, 8, https://doi.org/10.1525/elementa.398, 2020.

Helmig, D., Thompson, C., Evans, J., Boylan, P., Hueber, J., and Park, J.-H.: Highly elevated atmospheric levels of volatile organic compounds in the Uintah Basin, Utah, Environ. Sci. Technol., 48, 4707–4715, https://doi.org/10.1021/es405046r, 2014.

Hildenbrand, Z. L., Mach, P. M., McBride, E. M., Dorreyatim, M. N., Taylor, J. T., Carlton Jr, D. D., Meik, J. M., Fontenot, B. E., Wright, K. C., and Schug, K. A.: Point source attribution of ambient contamination events near unconventional oil and gas development, Sci. Total Environ., 573, 382–388, https://doi.org/10.1016/j. scitotenv.2016.08.118, 2016.

Hobbs, P. V., Sinha, P., Yokelson, R. J., Christian, T. J., Blake, D. R., Gao, S., Kirchstetter, T. W., Novakov, T., and Pilewskie, P.: Evolution of gases and particles from a savanna fire in South Africa, J. Geophys. Res., 108, 8485, https://doi.org/10.1029/2002JD002352, 2003.

Holder, C., Hader, J., Avanasi, R., Hong, T., Carr, E., Mendez, B., Wignall, J., Glen, G., Guelden, B., and Wei, Y.: Evaluating potential human health risks from modeled inhalation exposures to volatile organic compounds emitted from oil and gas operations, J. Air Waste Manag. Assoc., 69 (12), 1503–1524. https://doi.org/10.1080/10962247.2019.1680459, 2019.

Jarosławski, J., Pawlak, I., Guzikowski, J., Pietruczuk, A.: Impact of shale gas exploration and exploitation activities on the quality of ambient air - the case study of Wysin, Poland. Atmosphere 13 (8), 1228, https://doi.org/10.3390/atmos13081228, 2022.

Jobson, B. T., Berkowitz, C. M., Kuster, W. C., Goldan, P. D., Williams, E. J., Fesenfeld, F. C., Apel, E. C., Karl, T., Lonneman, W. A., and Riemer, D.: Hydrocarbon source signatures in Houston, Texas: Influence of the petrochemical industry, J. Geophys. Res.-Atmos., 109, D24305, https://doi.org/10.1029/2004jd004887, 2004.

Karl, T., Apel, E., Hodzic, A., Riemer, D. D., Blake, D. R., and Wiedinmyer, C.: Emissions of volatile organic compounds inferred from airborne flux measurements over a megacity, Atmos. Chem. Phys., 9, 271–285, https://doi.org/10.5194/acp-9- 271-2009, 2009.

Kim, S.-Y., Kim, E., and Kim, W. J.: Health effects of ozone on respiratory diseases, Tuberculosis and Respiratory Diseases, 83, S6, https://doi.org/10.4046/trd.2020.0154, 2020.

Ku, I.-T., Zhou, Y., Hecobian, A., Benedict, K., Buck, B., Lachenmayer, E., Terry, B., Frazier, M., Zhang, J., and Pan, D.: Air quality impacts from the development of unconventional oil and gas well pads: Air toxics and other volatile organic compounds, Atmospheric Environment, 120187, https://doi.org/10.1016/j.atmosenv.2023.120187, 2024.

Lachenmayer, E.: Impacts of Oil and Natural Gas Development and Other Sources on Volatile Organic Compound Concentrations in Broomfield, Colorado. M.S. thesis, Colorado State University, Fort Collins, Colorado, USA, 124 pp., 2022.

Leuchner, M. and Rappenglück, B.: VOC source–receptor relationships in Houston during TexAQS-II, Atmos. Environ., 44, 4056– 4067, https://doi.org/10.1016/j.atmosenv.2009.02.029, 2010

Lin, M., Horowitz, L. W., Payton, R., Fiore, A. M., and Tonnesen, G.: US surface ozone trends and extremes from 1980 to 2014: quantifying the roles of rising Asian emissions, domestic controls, wildfires, and climate, Atmospheric Chemistry and Physics, 17, 2943-2970, https://doi.org/10.5194/acp-17-2943-2017, 2017.

Lin, M., Fiore, A. M., Cooper, O. R., Horowitz, L. W., Langford, A. O., Levy, H., Johnson, B. J., Naik, V., Oltmans, S. J., and Senff, C. J.: Springtime high surface ozone events over the western United States: Quantifying the role of stratospheric intrusions, Journal of Geophysical Research: Atmospheres, 117, https://doi.org/10.1029/2012JD018151, 2012.

Lindaas, J., Farmer, D. K., Pollack, I. B., Abeleira, A., Flocke, F., and Fischer, E. V.: Acyl peroxy nitrates link oil and natural gas emissions to high ozone abundances in the Colorado Front Range during summer 2015, J. Geophys. Res.-Atmos., 124, 2336-2350, https://doi.org/10.1029/2018JD028825, 2019.

Lou, S., Holland, F., Rohrer, F., Lu, K., Bohn, B., Brauers, T., Chang, C., Fuchs, H., Häseler, R., and Kita, K.: Atmospheric OH reactivities in the Pearl River Delta–China in summer 2006: measurement and model results, Atmospheric Chemistry and Physics, 10, 11243-11260, https://doi.org/10.5194/acp-10-11243-2010, 2010.

Lui, K., Ho, S. S. H., Louie, P. K., Chan, C., Lee, S., Hu, D., Chan, P., Lee, J. C. W., and Ho, K.: Seasonal behavior of carbonyls and source characterization of formaldehyde (HCHO) in ambient air, Atmospheric environment, 152, 51-60, https://doi.org/10.1016/j.atmosenv.2016.12.004, 2017.

Lyon, D. R., Zavala-Araiza, D., Alvarez, R. A., Harriss, R., Palacios, V., Lan, X., Talbot, R., Lavoie, T., Shepson, P., and Yacovitch, T. I.: Constructing a spatially resolved methane emission inventory for the Barnett Shale region, Environmental science & technology, 49, 8147-8157, https://doi.org/10.1021/es506359c, 2015.

Lyu, C., Capps, S. L., Kurashima, K., Henze, D. K., Pierce, G., Hakami, A., Zhao, S., Resler, J., Carmichael, G. R., and Sandu, A.: Evaluating oil and gas contributions to ambient nonmethane hydrocarbon mixing ratios and ozone-related metrics in the Colorado Front Range, Atmospheric Environment, 246, 118113, https://doi.org/10.1016/j.atmosenv.2020.118113, 2021.

Macey, G. P., Breech, R., Chernaik, M., Cox, C., Larson, D., Thomas, D., and Carpenter, D. O.: Air concentrations of volatile compounds near oil and gas production: a community-based exploratory study, Environ. Health, 13, 82, https://doi.org/10.1186/1476-069X13-82, 2014.

Marrero, J. E., Townsend-Small, A., Lyon, D. R., Tsai, T. R., Meinardi, S., and Blake, D. R.: Estimating emissions of toxic hydrocarbons from natural gas production sites in the Barnett Shale region of Northern Texas, Environmental science & technology, 50, 10756-10764, https://doi.org/10.1021/acs.est.6b02827, 2016.

Martins, L. D. and Andrade, M. d. F.: Ozone formation potentials of volatile organic compounds and ozone sensitivity to their emission in the megacity of São Paulo, Brazil, Water, Air, and Soil Pollution, 195, 201-213, https://doi.org/10.1007/s11270-008-9740-x, 2008.

McDuffie, E. E., Edwards, P. M., Gilman, J. B., Lerner, B. M., Dube, W. P., Trainer, M., Wolfe, D. E., Angevine, W. M., deGouw, J., Williams, E. J., Tevlin, A. G., Murphy, J. G., Fischer, E. V., McKeen, S., Ryerson, T. B., Peischl, J., Holloway, J. S., Aikin, K., Langford, A. O., Senff, C. J., Alvarez, R. J., Hall, S. R., Ullmann, K., Lantz, K. O., and Brown, S. S.: Influence of oil and gas emissions on summertime ozone in the Colorado Northern Front Range, J. Geophys. Res.-Atmos., 121, 8712–8729, https://doi.org/10.1002/2016jd025265, 2016.

McKenzie, L. M., Allshouse, W. B., Burke, T., Blair, B. D., and Adgate, J. L.: Population size, growth, and environmental justice near oil and gas wells in Colorado, Environ. Sci. Technol., 50, 21, 11471-11480, https://doi.org/10.1021/acs.est.6b04391, 2016.

McKenzie, L. M., Blair, B., Hughes, J., Allshouse, W. B., Blake, N. J., Helmig, D., Milmoe, P., Halliday, H., Blake, D. R., and Adgate, J. L.: Ambient nonmethane hydrocarbon levels along Colorado's Northern Front Range: Acute and chronic health risks, Environ. Sci. Technol., 52, 4514-4525, https://doi.org/10.1021/acs.est.7b05983, 2018.

McMullin, T. S., Bamber, A. M., Bon, D., Vigil, D. I., and Van Dyke, M.: Exposures and health risks from volatile organic compounds in communities located near oil and gas exploration and production activities in Colorado (USA), Int. J. Environ. Res. Publ. Health, 15 (7), 1500, https://doi.org/10.3390/ijerph15071500, 2018.

Mead, G. J., Waxman, E. M., Bon, D., Herman, D. I., Baumann, E., Giorgetta, F. R., Friedlein, J. T., Ycas, G., Newbury, N. R., and Coddington, I.: Open-path dual-comb spectroscopy of methane and VOC emissions from an unconventional oil well development in Northern Colorado, Frontiers in Chemistry, 11, 1202255, https://doi.org/10.3389/fchem.2023.1202255, 2023.

Milford, J. B.: Out in front? State and federal regulation of air pollution emissions from oil and gas production activities in the western United States, Natural Resources Journal, 55, 1-46, http://www.jstor.org/stable/24889749, 2014.

Millet, D. B., Guenther, A., Siegel, D. A., Nelson, N. B., Singh, H. B., de Gouw, J. A., Warneke, C., Williams, J., Eerdekens, G., and Sinha, V.: Global atmospheric budget of acetaldehyde: 3-D model analysis and constraints from in-situ and satellite observations, Atmospheric Chemistry and Physics, 10, 3405-3425, https://doi.org/10.5194/acp-10-3405-2010, 2010.

Myhre, G., D. Shindell, F.-M. Bréon, W. Collins, J. Fuglestvedt, J. Huang, D. Koch, J.-F. Lamarque, D. Lee, B. Mendoza, T. Nakajima, A. Robock, G. Stephens, T. Takemura and H. Zhang : Intergovernmental Panel on Climate Change (IPCC). Anthropogenic and Natural Radiative Forcing. In: Climate Change 2013 – The Physical Science Basis: Working Group I Contribution to the Fifth Assessment Report of the Intergovernmental Panel on Climate Change. Cambridge: Cambridge University Press; 2014:659-740, https://doi.org/10.1017/CBO9781107415324.018, 2013

Na, K., Kim, Y. P., Moon, I., and Moon, K.-C.: Chemical composition of major VOC emission sources in the Seoul atmosphere, Chemosphere, 55, 585–594, https://doi.org/10.1016/j.chemosphere.2004.01.010, 2004.

Naimie, L. E., Sullivan, A. P., Benedict, K., Prenni, A. J., Sive, B., Schichtel, B. A., Fischer, E. V., Pollack, I., and Collett, J.: PM2. 5 in Carlsbad Caverns National Park: Composition, sources, and visibility impacts, Journal of the Air & Waste Management Association, 72, 1201-1218, https://doi.org/10.1080/10962247.2022.2081634, 2022.

O'Dell, K., Hornbrook, R. S., Permar, W., Levin, E. J. T., Garofalo, L. A., Apel, E. C., Blake, N. J., Jarnot, A., Pothier, M. A., Farmer, D. K., Hu, L., Campos, T., Ford, B., Pierce, J. R., and Fischer, E. V: Hazardous Air Pollutants in Fresh and Aged Western US Wildfire Smoke and Implications for Long-Term Exposure, Environ. Sci. Technol., 54, 11838–11847, https://doi.org/10.1021/acs.est.0c04497, 2020.

Orak, N. H., Reeder, M., and Pekney, N. J.: Identifying and quantifying source contributions of air quality contaminants during unconventional shale gas extraction, Atmos. Chem. Phys., 21, 4729-4739, https://doi.org/10.5194/acp-21-4729-2021, 2021.

Pang, Y., Fuentes, M., and Rieger, P.: Trends in selected ambient volatile organic compound (VOC) concentrations and a comparison to mobile source emission trends in California's South Coast Air Basin, Atmos. Environ., 122, 686-695, https://doi.org/10.1016/j.atmosenv.2015.10.016, 2015.

Parrish, D., Ryerson, T., Mellqvist, J., Johansson, J., Fried, A., Richter, D., Walega, J., Washenfelder, R. d., De Gouw, J., and Peischl, J.: Primary and secondary sources of formaldehyde in urban atmospheres: Houston Texas region, Atmospheric Chemistry and Physics, 12, 3273-3288, https://doi.org/10.5194/acp-12-3273-2012, 2012.

Peischl, J., Ryerson, T., Aikin, K., De Gouw, J., Gilman, J., Holloway, J., Lerner, B., Nadkarni, R., Neuman, J., and Nowak, J.: Quantifying atmospheric methane emissions from the Haynesville, Fayetteville, and northeastern Marcellus shale gas production regions, Journal of Geophysical Research: Atmospheres, 120, 2119-2139, https://doi.org/10.1002/2014JD022697, 2015.

Peischl, J., Ryerson, T., Brioude, J., Aikin, K., Andrews, A., Atlas, E., Blake, D., Daube, B., De Gouw, J., and Dlugokencky, E.: Quantifying sources of methane using light alkanes in the Los Angeles basin, California, Journal of Geophysical Research: Atmospheres, 118, 4974-4990, https://doi.org/10.1002/jgrd.50413, 2013.

Peng, Q., Palm, B. B., Fredrickson, C. D., Lee, B. H., Hall, S. R., Ullmann, K., Campos, T., Weinheimer, A. J., Apel, E. C., and Flocke, F.: Observations and Modeling of NOx Photochemistry and Fate in Fresh Wildfire Plumes, ACS Earth Space Chem., 5, 2652–2667, https://doi.org/10.1021/acsearthspacechem.1c00086, 2021.

Permar, W., Wang, Q., Selimovic, V., Wielgasz, C., Yokelson, R. J., Hornbrook, R. S., Hills, A. J., Apel, E. C., Ku, I.-T., Zhou, Y., Sive, B. C., Sullivan, A. P., Collett Jr., J. L., Campos, T. L., Palm, B. B., Peng, Q., Thornton, J. A., Garofalo, L. A., Farmer, D. K., Kreidenweis, S. M., Levin, E. J. T., DeMott, P. J., Flocke, F., Fischer, E. V., and Hu, L.: Emissions of trace organic gases from western U.S. wildfires based on WE-CAN aircraft measurements, J. Geophys. Res., 126, e2020JD033838, https://doi.org/10.1029/2020JD033838, 2021.

Pétron, G., Frost, G., Miller, B. R., Hirsch, A. I., Montzka, S. A., Karion, A., Trainer, M., Sweeney, C., Andrews, A. E., Miller, L., Kofler, J., Bar-Ilan, A., Dlugokencky, E. J., Patrick, L., Moore Jr., C. T., Ryerson, T. B., Siso, C., Kolodzey, W., Lang, P. M., Conway, T., Novelli, P., Masarie, K., Hall, B., Guenther, D., Kitzis, D., Miller, J., Welsh, D., Wolfe, D., Neff, W., and Tans, P.: Hydrocarbon emissions characterization in the Colorado Front Range: A pilot study, J. Geophys. Res.-Atmos., 117, D04304, https://doi.org/10.1029/2011JD016360, 2012.

Pétron, G., Karion, A., Sweeney, C., Miller, B. R., Montzka, S. A., Frost, G. J., Trainer, M., Tans, P., Andrews, A., Kofler, J., Helmig, D., Guenther, D., Dlugokencky, E., Lang, P., Newberger, T., Wolter, S., Hall, B., Novelli, P., Brewer, A., Conley, S., Hardesty, M., Banta, R., White, A., Noone, D., Wolfe, D., and Schnell, R.: A new look at methane and nonmethane hydrocarbon emissions from oil and natural gas operations in the Colorado Denver-Julesburg Basin, J. Geophys. Res.-Atmos., 119, 6836–6852, https://doi.org/10.1002/2013JD021272, 2014.

Pierce, T., Geron, C., Bender, L., Dennis, R., Tonnesen, G., and Guenther, A.: Influence of increased isoprene emissions on regional ozone modeling, Journal of Geophysical Research: Atmospheres, 103, 25611-25629, https://doi.org/10.1029/98JD01804, 1998.

Pollack, I. B., Helmig, D., O'Dell, K., and Fischer, E. V.: Seasonality and source apportionment of nonmethane volatile organic compounds at Boulder Reservoir, Colorado, between 2017 and 2019, J. Geophys. Res.-Atmos., 126, e2020JD034234, https://doi.org/10.1029/2020JD034234, 2021.

Prenni, A. J., Day, D. E., Evanoski-Cole, A. R., Sive, B. C., Hecobian, A., Zhou, Y., Gebhart, K. A., Hand, J. L., Sullivan, A. P., Li, Y., Schurman, M. I., Desyaterik, Y., Malm, W. C., Collett Jr., J. L., and Schichtel, B. A.: Oil and gas impacts on air quality in federal lands in the Bakken region: an overview of the Bakken Air Quality Study and first results, Atmos. Chem. Phys., 16, 1401–1416, https://doi.org/10.5194/acp-16-1401-2016, 2016.

Prenni, A. J., Benedict, K. B., Day, D. E., Sive, B. C., Zhou, Y., Naimie, L., Gebhart, K. A., Dombek, T., De Boskey, M., and Hyslop, N. P.: Wintertime haze and ozone at Dinosaur National Monument, Journal of the Air & Waste Management Association, 72, 951-968, https://doi.org/10.1080/10962247.2022.2048922, 2022.

Rappenglück, B., Ackermann, L., Alvarez, S., Golovko, J., Buhr, M., Field, R., Soltis, J., Montague, D. C., Hauze, B., and Adamson, S.: Strong wintertime ozone events in the Upper Green River basin, Wyoming, Atmospheric Chemistry and Physics, 14, 4909-4934, https://doi.org/10.5194/acp-14-4909-2014, 2014.

Ren, X., Brune, W. H., Mao, J., Mitchell, M. J., Lesher, R. L., Simpas, J. B., Metcalf, A. R., Schwab, J. J., Cai, C., and Li, Y.: Behavior of OH and HO2 in the winter atmosphere in New York City, Atmospheric Environment, 40, 252-263, https://doi.org/10.1016/j.atmosenv.2005.11.073, 2006.

Riddick, S. N. and Mauzerall, D. L.: Likely substantial underestimation of reported methane emissions from United Kingdom upstream oil and gas activities, Energy & Environmental Science, 16, 295-304, 2023.

Roest, G. S. and Schade, G. W.: Air quality measurements in the western Eagle Ford Shale, Elem Sci Anth, 8, 18, https://doi.org/10.1525/elementa.414, 2020.

Rogers, T., Grimsrud, E., Herndon, S., Jayne, J., Kolb, C. E., Allwine, E., Westberg, H., Lamb, B., Zavala, M., and Molina, L.: On-road measurements of volatile organic compounds in the Mexico City metropolitan area using proton transfer reaction mass spectrometry, Int. J. Mass Spectrom., 252, 26–37, https://doi.org/10.1016/j.ijms.2006.01.027, 2006.

Russo, R. S., Zhou, Y., White, M. L., Mao, H., Talbot, R., and Sive, B. C.: Multi-year (2004–2008) record of nonmethane hydrocarbons and halocarbons in New England: seasonal variations and regional sources, Atmos. Chem. Phys., 10, 4909–4929, https://doi.org/10.5194/acp-10-4909-2010, 2010.

Rutter, A. P., Griffin, R. J., Cevik, B. K., Shakya, K. M., Gong, L., Kim, S., Flynn, J. H., and Lefer, B. L.: Sources of air pollution in a region of oil and gas exploration downwind of a large city, Atmos. Environ., 120, 89–99, https://doi.org/10.1016/j.atmosenv.2015.08.073, 2015.

Ryerson, T. B., Trainer, M., Angevine, W. M., Brock, C. A., Dissly, R. W., Fehsenfeld, F. C., Frost, G. J., Goldan, P. D., Holloway, J. S., Hübler, G., Jakoubek, R. O., Kuster, W. C., Neuman, J. A., Nicks, D. K., Jr., Parrish, D. D., Roberts, J. M., Sueper, D. T., Atlas, E. L., Donnelly, S. G., Flocke, F., Fried, A., Potter, W. T., Schauffler, S., Stroud, V., Weinheimer, A. J., Wert, B. P., Wiedinmyer, C., Alvarez, R. J., Banta, R. M., Darby, L. S., and Senff, C. J.: Effect of petrochemical industrial emissions of reactive alkenes and NOx on tropospheric ozone formation in Houston, Texas, J. Geophys. Res., 108, 4249, https://doi.org/10.1029/2002JD003070, 2003.

Schade, G. W. and Roest, G.: Analysis of non-methane hydrocarbon data from a monitoring station affected by oil and gas development in the Eagle Ford shale, Texas, Elementa, 4, 000096, https://doi.org/ 10.12952/journal.elementa.000096, 2016.

Schade, G. W. and Roest, G.: Source apportionment of non-methane hydrocarbons, NOx and H2S data from a central monitoring station in the Eagle Ford shale, Texas, Elem Sci Anth, 6, 35, https://doi.org/10.1525/elementa.289, 2018.

Schlink, U., Herbarth, O., Richter, M., Dorling, S., Nunnari, G., Cawley, G., and Pelikan, E.: Statistical models to assess the health effects and to forecast ground-level ozone, Environmental Modelling & Software, 21, 547-558, https://doi.org/10.1016/j.envsoft.2004.12.002, 2006.

Schnell, R. C., Oltmans, S. J., Neely, R. R., Endres, M. S., Molenar, J. V., and White, A. B.: Rapid photochemical production of ozone at high concentrations in a rural site during winter, Nature Geoscience, 2, 120-122, https://doi.org/10.1038/ngeo415, 2009.

Schwietzke, S., Griffin, W. M., Matthews, H. S., and Bruhwiler, L. M.: Natural gas fugitive emissions rates constrained by global atmospheric methane and ethane, Environmental science & technology, 48, 7714-7722, https://doi.org/10.1021/es501204c, 2014.

Seco, R., Penuelas, J., and Filella, I.: Short-chain oxygenated VOCs: Emission and uptake by plants and atmospheric sources, sinks, and concentrations, Atmospheric Environment, 41, 2477-2499, https://doi.org/10.1016/j.atmosenv.2006.11.029, 2007.

Shaw, J. T., Rickard, A. R., Newland, M. J., and Dillon, T. J.: Rate coefficients for reactions of OH with aromatic and aliphatic volatile organic compounds determined by the multivariate relative rate technique, Atmospheric Chemistry and Physics, 20, 9725-9736, https://doi.org/10.5194/acp-20-9725-2020, 2020.

Shirley, T., Brune, W., Ren, X., Mao, J., Lesher, R., Cardenas, B., Volkamer, R., Molina, L., Molina, M. J., and Lamb, B.: Atmospheric oxidation in the Mexico city metropolitan area (MCMA) during April 2003, Atmospheric Chemistry and Physics, 6, 2753-2765, https://doi.org/10.5194/acp-6-2753-2006, 2006.

Sillman, S.: Tropospheric ozone and photochemical smog, Treatise on geochemistry, 9, 612, https://doi.org/10.1016/B0-08-043751-6/09053-8, 2003.

Simon, H., Reff, A., Wells, B., Xing, J., and Frank, N.: Ozone trends across the United States over a period of decreasing NOx and VOC emissions, Environmental science & technology, 49, 186-195, https://doi.org/10.1021/es504514z, 2015.

Simpson, I. J., Blake, N. J., Barletta, B., Diskin, G. S., Fuelberg, H. E., Gorham, K., Huey, L. G., Meinardi, S., Rowland, F. S., Vay, S. A., Weinheimer, A. J., Yang, M., and Blake, D. R.: Characterization of trace gases measured over Alberta oil sands mining operations: 76 speciated C2–C10 volatile organic compounds (VOCs), CO2, CH4, CO, NO, NO2, NOy , O3 and SO2, Atmos. Chem. Phys., 10, 11931–11954, https://doi.org/10.5194/acp-10-11931-2010, 2010.

Singh, H. B., O'hara, D., Herlth, D., Sachse, W., Blake, D., Bradshaw, J., Kanakidou, M., and Crutzen, P.: Acetone in the atmosphere: Distribution, sources, and sinks, Journal of Geophysical Research: Atmospheres, 99, 1805-1819, https://doi.org/10.1021/es504514z, 1994.

Sive, B. C., Zhou, Y., Troop, D., Wang, Y., Little, W. C., Wingenter, O. W., Russo, R. S., Varner, R. K., and Talbot, R.: Development of a Cryogen-Free Concentration System for Measurements of Volatile Organic Compounds, Anal. Chem., 77, 6989– 6998, https://doi.org/10.1021/ac0506231, 2005.

Smith, M. L., Kort, E. A., Karion, A., Sweeney, C., Herndon, S. C., and Yacovitch, T. I.: Airborne ethane observations in the Barnett Shale: Quantification of ethane flux and attribution of methane emissions, Environmental science & technology, 49, 8158-8166, https://doi.org/10.1021/acs.est.5b00219, 2015.

Sommariva, R., De Gouw, J., Trainer, M., Atlas, E., Goldan, P., Kuster, W., Warneke, C., and Fehsenfeld, F.: Emissions and photochemistry of oxygenated VOCs in urban plumes in the Northeastern United States, Atmospheric chemistry and physics, 11, 7081-7096, https://doi.org/10.5194/acp-11-7081-2011, 2011.

Sørensen, M., Kaiser, E., Hurley, M., Wallington, T., and Nielsen, O.: Kinetics of the reaction of OH radicals with acetylene in 25–8000 Torr of air at 296 K, International journal of chemical kinetics, 35, 191-197, https://doi.org/10.1002/kin.10119, 2003.

Sprengnether, M. M., Demerjian, K. L., Dransfield, T. J., Clarke, J. S., Anderson, J. G., and Donahue, N. M.: Rate Constants of nine C6− C9 Alkanes with OH from 230 to 379 K: Chemical Tracers for [OH], The Journal of Physical Chemistry A, 113, 5030-5038, https://doi.org/10.1021/jp810412m, 2009.

Sujith, B. and Sehgal, M.: Characteristics of the ozone pollution and its health effects in India, International Journal of Medicine and Public Health, 7, http://www.ijmedph.org/v7/i1, 2017.

Sullivan, J. T., McGee, T. J., Langford, A. O., Alvarez, R. J., Senff, C. J., Reddy, P. J., Thompson, A. M., Twigg, L. W., Sumnicht, G. K., Lee, P., Weinheimer, A., Knote, C., Long, R. W., and Hoff, R. M.: Quantifying the contribution of thermally driven recirculation to a high-ozone event along the Colorado Front Range using lidar, J. Geophys. Res.-Atmos., 121, 1,377–310390, https://doi.org/10.1002/2016JD025229, 2016.

Swarthout, R. F., Russo, R. S., Zhou, Y., Hart, A. H., and Sive, B. C.: Volatile organic compound distributions during the NACHTT campaign at the Boulder Atmospheric Observatory: Influence of urban and natural gas sources, J. Geophys. Res.-Atmos., 118, 10614–10637, https://doi.org/10.1002/jgrd.50722, 2013.

Thompson, C. R., Hueber, J., and Helmig, D.: Influence of oil and gas emissions on ambient atmospheric non-methane hydrocarbons in residential areas of Northeastern Colorado, Elem. Sci. Anth., 3, 35, https://doi.org/10.12952/journal.elementa.000035, 2014.

Townsend-Small, A., Marrero, J. E., Lyon, D. R., Simpson, I. J., Meinardi, S., and Blake, D. R.: Integrating source apportionment tracers into a bottom-up inventory of methane emissions in the Barnett Shale hydraulic fracturing region, Environmental science & technology, 49, 8175-8182, https://doi.org/10.1021/acs.est.5b00057, 2015.

U.S. EPA (2023). Inventory of U.S. Greenhouse Gas Emissions and Sinks: 1990-2021. U.S. Environmental Protection Agency, EPA 430-R-23-002. https://www.epa.gov/ghgemissions/inventory-us-greenhouse-gas-emissions-and-sinks-1990-2021, last access: 19 December 2023.

U.S. EPA: Initial List of Hazardous Air Pollutants with Modifications: https://www.epa.gov/haps/initial-list-hazardous-air-pollutants-modifications, last access: 17 May 2023.

U.S. EPA: The Process of Unconventional Natural Gas Production: https://www.epa.gov/uog/process-unconventional-natural-gas-production, last access: 17 May 2023.

Vallero, D. A.: Chapter 8 - Air pollution biogeochemistry.Air pollution biogeochemistry, Air Pollution Calculations, Elsevier, https://doi.org/10.1016/B978-0-12-814934-8.00008-9, 2019.

Van Dingenen, R., Dentener, F. J., Raes, F., Krol, M. C., Emberson, L., and Cofala, J.: The global impact of ozone on agricultural crop yields under current and future air quality legislation, Atmospheric Environment, 43, 604-618, https://doi.org/10.1016/j.atmosenv.2008.10.033, 2009.

Velasco, E., Lamb, B., Westberg, H., Allwine, E., Sosa, G., ArriagaColina, J. L., Jobson, B. T., Alexander, M. L., Prazeller, P., Knighton, W. B., Rogers, T. M., Grutter, M., Herndon, S. C., Kolb, C. E., Zavala, M., de Foy, B., Volkamer, R., Molina, L. T., and Molina, M. J.: Distribution, magnitudes, reactivities, ratios and diurnal patterns of volatile organic compounds in the Valley of Mexico during the MCMA 2002 & 2003 field campaigns, Atmos. Chem. Phys., 7, 329–353, https://doi.org/10.5194/acp-7- 329-2007, 2007.

Wang, P., Chen, Y., Hu, J., Zhang, H., and Ying, Q.: Attribution of tropospheric ozone to NO x and VOC emissions: considering ozone formation in the transition regime, Environmental science & technology, 53, 1404-1412, https://doi.org/10.1021/acs.est.8b05981, 2018.

Warneke, C., McKeen, S.A., de Gouw, J.A., Goldan, P.D., Kuster, W.C., Holloway, J.S., Williams, E.J., Lerner, B.M., Parrish, D.D., Trainer, M., Fehsenfeld, F.C., Kato, S., Atlas, E.L., Baker, A., Blake, D.R., 2007. Determination of urban volatile organic compound emission ratios and comparison with an emissions database. J. Geophys. Res. Atmos. 112 https://doi.org/10.1029/2006jd007930, 2007.

Warneke, C., Geiger, F., Edwards, P. M., Dube, W., Pétron, G., Kofler, J., Zahn, A., Brown, S. S., Graus, M., Gilman, J. B., Lerner, B. M., Peischl, J., Ryerson, T. B., de Gouw, J. A., and Roberts, J. M.: Volatile organic compound emissions from the oil and natural gas industry in the Uintah Basin, Utah: oil and gas well pad emissions compared to ambient air composition, Atmos. Chem. Phys., 14, 10977–10988, https://doi.org/10.5194/acp-14- 10977-2014, 2014.

Weisner, M. L., Allshouse, W. B., Erjavac, B. W., Valdez, A. P., Vahling, J. L., and McKenzie, L. M.: Health Symptoms and Proximity to Active Multi-Well Unconventional Oil and Gas Development Sites in the City and County of Broomfield, Colorado, *Int. J. Environ. Res. Public Health*, 20 (3), 2634, https://doi.org/10.3390/ijerph20032634, 2023.

Wells, D.: Consequences of the evolution of oil and gas control and production technology in the Denver ozone nonattainment area, Colorado Department of Public Health and Environment, Air Pollution Control Division. August, 2017.

Wert, B., Trainer, M., Fried, A., Ryerson, T., Henry, B., Potter, W., Angevine, W., Atlas, E., Donnelly, S., and Fehsenfeld, F.: Signatures of terminal alkene oxidation in airborne formaldehyde measurements during TexAQS 2000, Journal of Geophysical Research: Atmospheres, 108, https://doi.org/10.1029/2002JD002502, 2003.

Whalley, L. K., Stone, D., Bandy, B., Dunmore, R., Hamilton, J. F., Hopkins, J., Lee, J. D., Lewis, A. C., and Heard, D. E.: Atmospheric OH reactivity in central London: observations, model predictions and estimates of in situ ozone production, Atmospheric Chemistry and Physics, 16, 2109-2122, https://doi.org/10.5194/acp-16-2109-2016, 2016.

White, M. L., Russo, R. S., Zhou, Y., Ambrose, J. L., Haase, K., Frinak, E. K., Varner, R. K., Wingenter, O. W., Mao, H., Talbot, R., and Sive, B. C.: Are biogenic emissions a significant source of summertime atmospheric toluene in the rural Northeastern United States?, Atmos. Chem. Phys., 9, 81–92, https://doi.org/10.5194/acp-9-81-2009, 2009.

Wilbur, S. B., Keith, S., Faroon, O., and Wohlers, D.: Toxicological profile for benzene, https://stacks.cdc.gov/view/cdc/6992, 2007.

Wilde, S. E., Dominutti, P. A., Allen, G., Andrews, S. J., Bateson, P., Bauguitte, S. J.-B., Burton, R. R., Colfescu, I., France, J., Hopkins, J. R., Huang, L., Jones, A. E., Lachlan-Cope, T., Lee, J. D., Lewis, A. C., Mobbs, S. D., Weiss, A., Young, S., and Purvis, R. M.: Speciation of VOC emissions related to offshore North Sea oil and gas production, Atmos. Chem. Phys., 21, 3741–3762, https://doi.org/10.5194/acp-21-3741-2021, 2021.

Wilson, E. W., Hamilton, W. A., Kennington, H. R., Evans, B., Scott, N. W., and DeMore, W. B.: Measurement and estimation of rate constants for the reactions of hydroxyl radical with several alkanes and cycloalkanes, The Journal of Physical Chemistry A, 110, 3593-3604, https://doi.org/10.1021/jp055841c, 2006.

Yokelson, R. J., Bertschi, I. T., Christian, T. J., Hobbs, P. V., Ward, D. E., and Hao, W. M.: Trace gas measurements in nascent, aged, and cloud-processed smoke from African savanna fires by airborne Fourier transform infrared spectroscopy (AFTIR), J. Geophys. Res., 108, 8478, https://doi.org/10.1029/2002JD002322, 2003.

Yokelson, R. J., Karl, T., Artaxo, P., Blake, D. R., Christian, T. J., Griffith, D. W. T., Guenther, A., and Hao, W. M.: The Tropical Forest and Fire Emissions Experiment: overview and airborne fire emission factor measurements, Atmos. Chem. Phys., 35 7, 5175–5196, https://doi.org/10.5194/acp-7-5175-2007, 2007.

Yokelson, R. J., Crounse, J. D., DeCarlo, P. F., Karl, T., Urbanski, S., Atlas, E., Campos, T., Shinozuka, Y., Kapustin, V., Clarke, A. D., Weinheimer, A., Knapp, D. J., Montzka, D. D., Holloway, J., Weibring, P., Flocke, F., Zheng, W., Toohey, D., Wennberg, P. O., Wiedinmyer, C., Mauldin, L., Fried, A., Richter, D., Walega, J., Jimenez, J. L., Adachi, K., Buseck, P. R., Hall, S. R., and Shetter, R.: Emissions from biomass burning in the Yucatan, Atmos. Chem. Phys., 9, 5785–5812, https://doi.org/10.5194/acp-9-5785- 2009, 2009.

Yoshino, A., Nakashima, Y., Miyazaki, K., Kato, S., Suthawaree, J., Shimo, N., Matsunaga, S., Chatani, S., Apel, E., and Greenberg, J.: Air quality diagnosis from comprehensive observations of total OH reactivity and reactive trace species in urban central Tokyo, Atmospheric Environment, 49, 51-59, https://doi.org/10.1016/j.atmosenv.2011.12.029, 2012.

Zavala, M., Herndon, S. C., Slott, R. S., Dunlea, E. J., Marr, L. C., Shorter, J. H., Zahniser, M., Knighton, W. B., Rogers, T. M., Kolb, C. E., Molina, L. T., and Molina, M. J.: Characterization of on-road vehicle emissions in the Mexico City Metropolitan Area using a mobile laboratory in chase and fleet average measurement modes during the MCMA-2003 field campaign, Atmos. Chem. Phys., 6, 5129–5142, https://doi.org/10.5194/acp-6-5129- 2006, 2006.

Zheng, H., Kong, S., Xing, X., Mao, Y., Hu, T., Ding, Y., Li, G., Liu, D., Li, S., and Qi, S.: Monitoring of volatile organic compounds (VOCs) from an oil and gas station in northwest China for 1 year, Atmos. Chem. Phys., 18, 4567–4595, https://doi.org/10.5194/acp-18-4567-2018, 2018.

Zhou, Y., Varner, R. K., Russo, R. S., Wingenter, O. W., Haase, K. B., Talbot, R., and Sive, B. C.: Coastal water source of shortlived halocarbons in New England, J. Geophys. Res.-Atmos., 110, D21302, https://doi.org/10.1029/2004jd005603, 2005.

Appendix A

Additional Information for Air Quality Impacts from the Development of Unconventional Oil and Gas Well Pads: Air Toxics and other Volatile Organic Compounds

Table A.1: Broomfield sampling site information including site name, location, type, distance to closest pad, and numbers of weekly (from October 2018 to July 2021) and triggered (from February 2020 to December 20222) canisters collected at each location.

Sampling Site	Site Location (degrees)	Site Type	Distance to Closest Pad (m)	Number of Weekly Canisters	Number of Triggered Canisters
Commons	39.93416, -105.04866	Background	5030 (Livingston)	146	0
Anthem 01	38.98161, -105.04122	Neighborhood Impact	330 (Livingston)	146	3
Anthem 02	39.99983, -105.03976	Neighborhood Impact	2400 (Livingston)	16	0
Broadlands	39.95617, -105.03728	Neighborhood Impact	2370 (Livingston)	21	0
Adams 01	39.97410, -105.00175	Neighborhood Impact	950 (Interchange A)	50	0
Prospect Ridge 01	39.99361, -105.01821	Neighborhood Impact	1210 (Northwest A)	31	0
Soaring Eagle	39.98363, -105.03624	Neighborhood Impact	570 (Livingston)	0	1
Thunder Vista 01	39.98830, -105.03224	Neighborhood Impact	1200 (Livingston)	50	0
Wildgrass 01	39.97242, -105.04853	Neighborhood Impact	1050 (Livingston)	96	0
Wilcox 01	39.96167, -105.02510	Neighborhood Impact	2140 (Livingston)	40	0
Interchange 01	39.98008, -104.99034	O&G	150 (Interchange A)	141	2
Interchange 02	39.97744, -104.99058	O&G	120 (Interchange A)	64	2
Interchange 03	39.97959, -104.99453	O&G	150 (Interchange A)	91	2
Livingston 01	39.97889, -105.04239	O&G	260 (Livingston)	117	2

Table A.1: Broomfield sampling site information including site name, location, type, distance to closest pad, and numbers of weekly (from October 2018 to July 2021) and triggered (from February 2020 to December 20222) canisters collected at each location (continued).

Sampling Site	Site location	Site Description	Distance to Closest Pad (m)	Number of Weekly Canisters	Number of Triggered Canisters
Livingston 02	39.97883, -105.03789	O&G	110 (Livingston)	133	12
NWPKWY 01	39.98253, -105.01462	O&G	150 (Northwest A)	37	0
NWPKWY 02	39.98361, -105.01121	O&G	130 (Northwest A)	36	26
NWPKWY 03	39.98342, -105.00679	O&G	155 (Northwest B)	40	1
United 01	39.98579, -105.00286	O&G	230 (United)	26	9
United 02	39.98563, -104.99780	O&G	200 (United)	43	27
United 03	39.98563, -104.99780	O&G	205 (United)	0	4
			Total Canisters	1324	91

Table A.2: Sampling period information.

Period	Dates (yyyy-mm-dd)	Number of Weekly Canisters
None (Prior to the start of pad construction)	2018-10-04 to 2018-12-31	51
Pre-Production	2019-07-05 to 2020-03-31	436
Production	2020-09-24 to 2021-07-31	316

Table A.3: Pre-production activity timelines for the first 2 of 6 wellpads developed in Broomfield.

	Interchange B (12 wells)		**Livingston (18 wells)**	
	Dates (yyyy-mm-dd)	# Days	Dates (yyyy-mm-dd)	# Days
Drilling	2019-04-20 to 2019-06-28	69	2019-07-05 to 2019-11-14	132
Hydraulic Fracturing	2019-07-15 to 2019-08-17 (10 wells); 2019-11-18 to 2019-11-29 (2 wells)	33; 11	2019-12-02 to 2020-02-13	73
Coiled Tubing/Millout	2019-08-20 to 2019-08-30 (10 wells); 2019-12-03 to 2019-12-10 (2 wells)	10; 7	2022-02-20 to 2020-03-27	36
Production Tubing Installation	2019-08-30 to 2019-09-05 (10 wells); 2019-12-20 to 2019-12-22 (2 wells)	6; 2	2020-03-16 to 2020-04-01	16
Flowback	2019-10-02 to 2020-01-08 (10 wells); 2019-12-26 to 2020-03-31 (2 wells)	98; 96	2020-04-15 to 2020-09-23	161

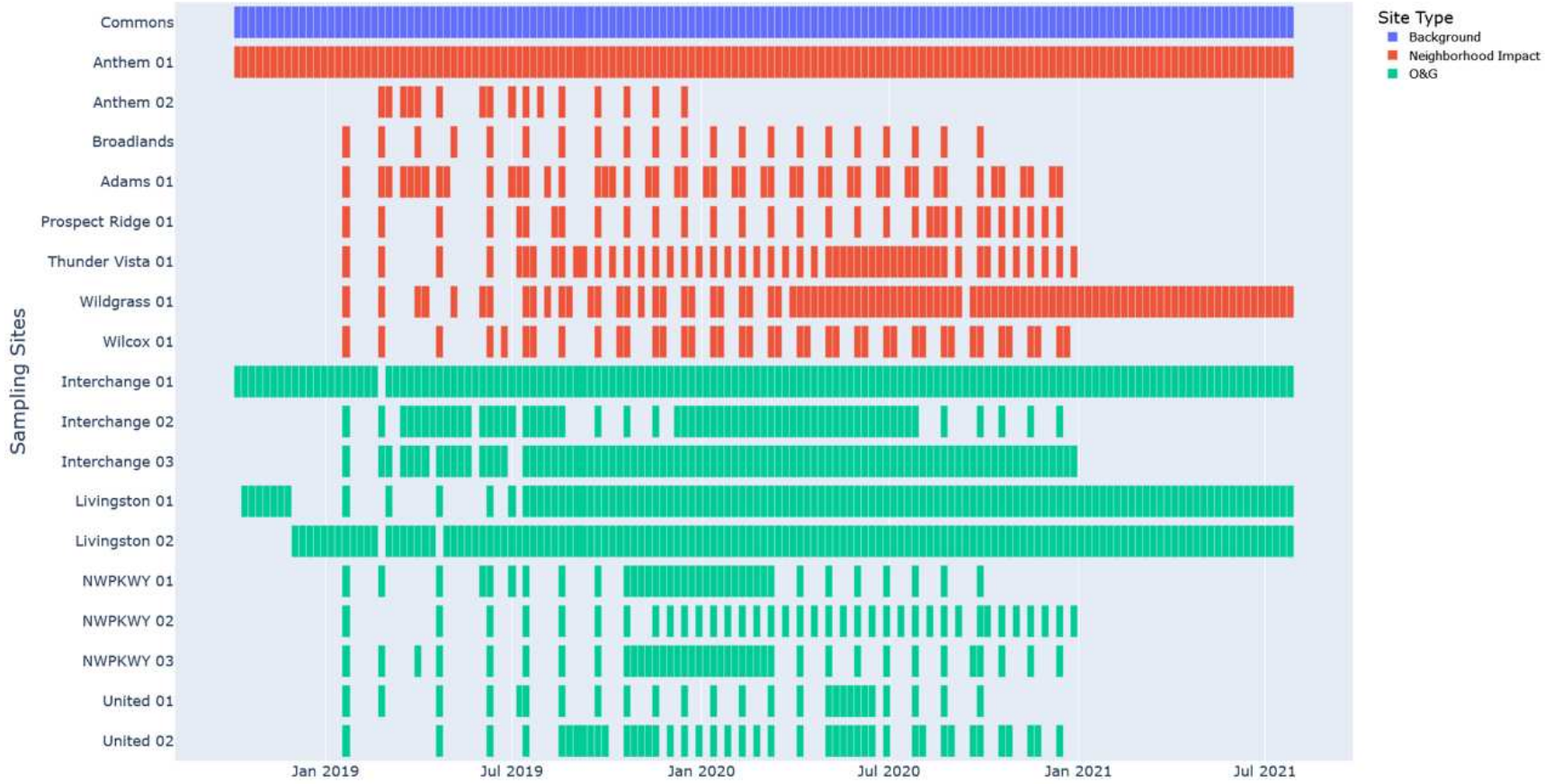

Figure A.1: The weekly canister deployment schedule from October 2018 through July 2021.

Table A.4: Detection limits of methane and different compounds measured by the 5-channel GC.

Compounds	Precision (1 RSD, %)	Standard Accuracy (%)	LOD	LOD unit
Methane	3.69	± 1	0.0500	ppmv
Ethane	2.83	± 5	0.2082	ppbv
Propane	2.31	± 5	0.0419	ppbv
i-Butane	2.38	± 5	0.0147	ppbv
n-Butane	2.59	± 5	0.0216	ppbv
i-Pentane	2.52	± 5	0.0167	ppbv
n-Pentane	2.48	± 5	0.0054	ppbv
n-Hexane	2.91	± 5	0.0222	ppbv
n-Heptane	3.24	± 5	0.0173	ppbv
n-Octane	2.90	± 5	0.0121	ppbv
n-Nonane	3.70	± 5	0.0221	ppbv
n-Decane	4.12	± 5	0.0262	ppbv
Cyclopentane	2.45	± 5	0.0098	ppbv
Cyclohexane	3.39	± 5	0.0380	ppbv
Methylcyclohexane	3.19	± 5	0.0414	ppbv
2,3,4-Trimethylpentane	3.06	± 5	0.0211	ppbv
2,2,4-Trimethylpentane	3.29	± 5	0.0238	ppbv
2,3-Dimethylpentane	3.35	± 5	0.0320	ppbv
2,4-Dimethylcyclopentane	2.44	± 5	0.0241	ppbv
2-Methylhexane	3.87	± 5	0.0100	ppbv
3-Methylhexane	3.64	± 5	0.0189	ppbv
2-Methylheptane	3.19	± 5	0.0284	ppbv
3-Methylheptane	3.48	± 5	0.0091	ppbv
Ethene	4.73	± 5	0.0228	ppbv
Propene	2.75	± 5	0.0170	ppbv
trans-2-Butene	3.54	± 5	0.0056	ppbv
1-Butene	3.32	± 5	0.0159	ppbv
cis-2-Butene	2.83	± 5	0.0115	ppbv

Table A.4: Detection limits of methane and different compounds measured by the 5-channel GC (continued).

Compounds	Precision (1 RSD, %)	Standard Accuracy (%)	LOD	LOD unit
trans-2-Pentene	3.80	± 5	0.0079	ppbv
1-Pentene	6.39	± 5	0.0361	ppbv
cis-2-Pentene	3.73	± 5	0.0139	ppbv
Benzene	3.38	± 5	0.0160	ppbv
Toluene	3.21	± 5	0.0177	ppbv
Ethylbenzene	3.42	± 5	0.0085	ppbv
m- and p-Xylene	3.51	± 5	0.0207	ppbv
o-Xylene	3.08	± 5	0.0230	ppbv
Styrene	9.58	± 5	0.0153	ppbv
i-Propylbenzene	13.40	± 5	0.0184	ppbv
n-Propylbenzene	17.69	± 5	0.0247	ppbv
3-Ethyltoluene	7.45	± 5	0.0068	ppbv
4-Ethyltoluene	7.06	± 5	0.0306	ppbv
2-Ethyltoluene	5.55	± 5	0.0184	ppbv
1,3,5-Trimethylbenzene	4.59	± 5	0.0101	ppbv
1,2,4-Trimethylbenzene	5.89	± 5	0.0096	ppbv
1,2,3-Trimethylbenzene	8.18	± 5	0.1550	ppbv
1,3-Diethylbenzene	6.99	± 5	0.0226	ppbv
1,4-Diethylbenzene	5.79	± 5	0.0134	ppbv
Ethyne	2.59	± 5	0.0194	ppbv
Isoprene	2.78	± 5	0.0030	ppbv
C_2Cl_4	19.12	± 5	0.0898	pptv
C_2HCl_3	14.16	± 5	1.0000	pptv

Table A.5: Rate constants of the individual neutral compounds with H_3O^+ ions.

m/e	Compounds	Formula	k (10^{-9} cm^3 s^{-1})
33	Methanol	CH_4O	2.22
42	Acetonitrile	C_2H_3N	3.99
45	Acetaldehyde	C_2H_4O	3.12
47	Ethanol	C_2H_6O	2.18
59	Acetone	C_3H_6O	3.32
63	DMS	C_2H_6S	2
69	Isoprene	C_5H_8	1.96
71	Methacrolein	C_4H_6O	3.2
71	MVK	C_4H_6O	3.39
73	MEK	C_4H_8O	3.28
79	Benzene	C_6H_6	1.93
93	Toluene	C_7H_8	2.08
101	cis-3-Hexenol	$C_6H_{12}O$	3.25
101	Hexanal	$C_6H_{12}O$	3.35
107	Xylene	C_8H_{10}	2.26
121	Ethylbenzene	C_9H_{12}	2.4
129	Naphthalene	$C_{10}H_8$	2.71
137	Camphene	$C_{10}H_{16}$	2.37

Table A.6: Descriptive statistics of methane and 50 VOCs for weekly canister samples collected from 4 October 2018 to 29 July 2021 in Broomfield.

Compounds	Max. (ppbv)	Min. (ppbv)	Mean (ppbv)	Median (ppbv)	Standard Deviation (ppbv)
Methane (ppmv)	2.795	1.736	2.000	1.984	0.097
Ethane	61.550	3.306	12.192	9.481	7.512
C_3-C_7 n-Alkanes					
Propane	34.081	1.303	6.067	4.677	4.035
i-Butane	6.318	0.228	1.076	0.833	0.722
n-Butane	17.121	0.613	2.844	2.176	1.935
i-Pentane	6.729	0.263	0.949	0.800	0.559
n-Pentane	7.611	0.248	0.930	0.741	0.644
n-Hexane	4.701	0.076	0.389	0.287	0.334
n-Heptane	2.559	0.024	0.150	0.099	0.177
C_8-C_{10} n-Alkanes					
n-Octane	1.735	0.014	0.098	0.055	0.145
n-Nonane	2.040	0.011	0.078	0.034	0.176
n-Decane	3.481	0.013	0.096	0.028	0.286
Cyclic Alkanes					
Cyclopentane	0.617	0.017	0.075	0.059	0.052
Cyclohexane	2.026	0.019	0.127	0.088	0.144
Methylcyclohexane	3.864	0.021	0.158	0.083	0.237
Branched Alkanes					
2,3,4-Trimethylpentane	0.216	0.011	0.012	0.011	0.009
2,2,4-Trimethylpentane	0.475	0.012	0.055	0.046	0.040
2,3-Dimethylpentane	1.140	0.016	0.073	0.056	0.073
2,4-Dimethylpentane	0.240	0.012	0.021	0.012	0.017
2-Methylhexane	0.328	0.005	0.039	0.033	0.026
3-Methylhexane	1.298	0.009	0.082	0.053	0.093
2-Methylheptane	0.965	0.014	0.040	0.014	0.063
3-Methylheptane	0.519	0.005	0.029	0.018	0.042

Table A.6: Descriptive statistics of methane and 50 VOCs for weekly canister samples collected from 4 October 2018 to 29 July 2021 in Broomfield (continued).

Compounds	Max. (ppbv)	Min. (ppbv)	Mean (ppbv)	Median (ppbv)	Standard Deviation (ppbv)
Alkenes					
Ethene	5.602	0.214	0.899	0.725	0.561
Propene	0.692	0.028	0.150	0.133	0.072
trans-2-Butene	0.284	0.003	0.012	0.010	0.014
1-Butene	0.442	0.008	0.026	0.024	0.020
cis-2-Butene	0.238	0.006	0.010	0.006	0.012
trans-2-Pentene	0.103	0.004	0.005	0.004	0.004
1-Pentene	0.069	0.018	0.018	0.018	0.003
cis-2-Pentene	0.330	0.007	0.007	0.007	0.009
BTEX					
Benzene	0.798	0.030	0.172	0.158	0.080
Toluene	7.788	0.009	0.302	0.254	0.290
Ethylbenzene	0.247	0.004	0.034	0.029	0.022
m- and p-Xylene	1.165	0.010	0.130	0.107	0.095
o-Xylene	0.332	0.011	0.042	0.036	0.033
Aromatics Other than BTEX					
Styrene	0.062	0.008	0.008	0.008	0.003
i-Propylbenzene	0.163	0.009	0.012	0.009	0.012
n-Propylbenzene	0.068	0.012	0.013	0.012	0.004
3-Ethyltoluene	0.372	0.003	0.019	0.014	0.025
4-Ethyltoluene	0.148	0.015	0.016	0.015	0.007
2-Ethyltoluene	0.057	0.009	0.010	0.009	0.004

Table A.6: Descriptive statistics of methane and 50 VOCs for weekly canister samples collected from 4 October 2018 to 29 July 2021 in Broomfield (continued).

Compounds	Max. (ppbv)	Min. (ppbv)	Mean (ppbv)	Median (ppbv)	Standard Deviation (ppbv)
1,3,5-Trimethylbenzene	0.699	0.005	0.010	0.005	0.039
1,2,4-Trimethylbenzene	2.737	0.005	0.038	0.022	0.118
1,2,3-Trimethylbenzene	0.252	0.078	0.078	0.078	0.010
1,3-Diethylbenzene	0.087	0.011	0.011	0.011	0.002
1,4-Diethylbenzene	0.061	0.007	0.007	0.007	0.002
Halogenated Hydrocarbon					
C_2Cl_4	0.129	0.0004	0.005	0.003	0.007
C_2HCl_3	0.220	0.001	0.015	0.012	0.019
Ethyne	18.027	0.104	0.815	0.603	0.960
Isoprene	0.659	0.002	0.033	0.007	0.058
TVOC-49*	99.165	4.665	16.276	12.935	10.071

* TVOC-49 mixing ratios were calculated by summing up all compounds in Table A.6 except for methane and ethane.

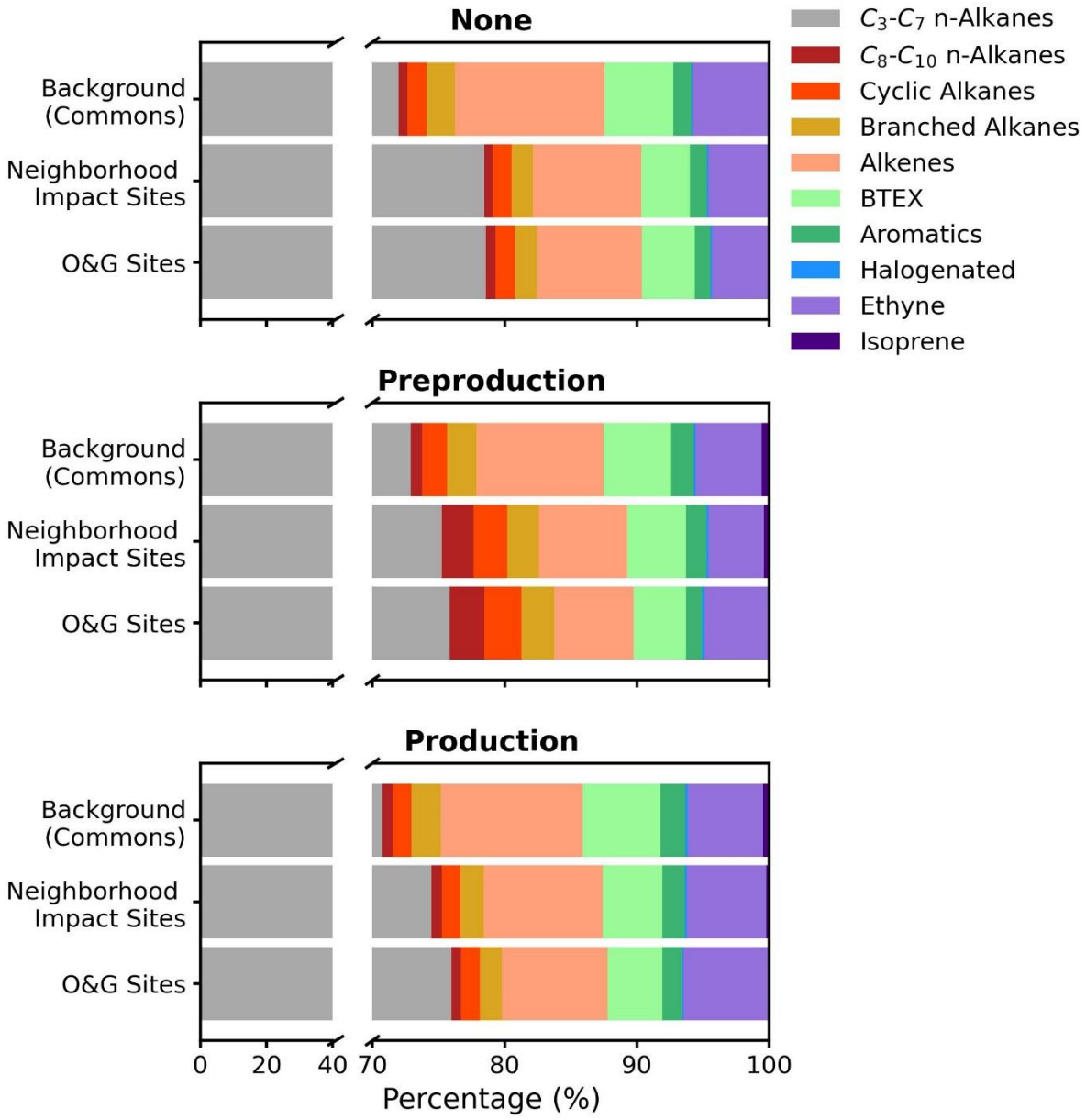

Figure A.2: Comparison of the average weekly integrated VOC compositions during different operation phases for the three site categories.

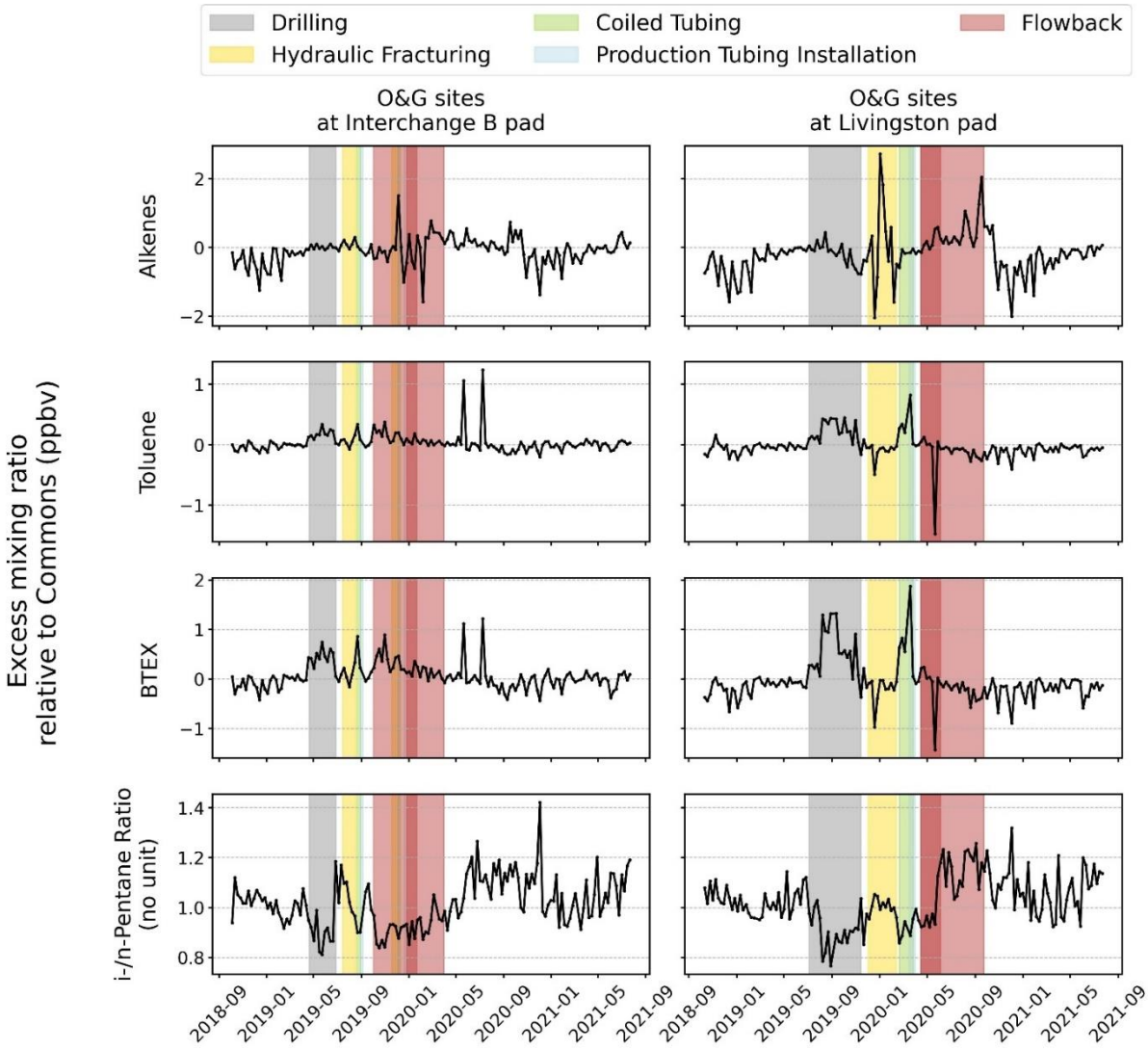

Figure A.3: Time series of alkenes, toluene, and BTEX excess mixing ratios (ppbv) and i/n-pentane ratio averaged across the Interchange and Livingston well pad sites relative to values at the Commons (background) site. Overlaid colors indicate different O&G pre-production activities.

A.1 Additional Discussion for VOC Ratios

Benzene and toluene are often co-emitted from the same sources, including biogenic emission, fuel evaporation, vehicle exhaust and O&G activities, but with different emission rates (Hildenbrand et al., 2016; Karl et al., 2009; Pang et al., 2015; Rutter et al., 2015; Simpson et al., 2010; Warneke et al., 2014; White et al., 2009). Due to different OH reaction rates (Atkinson and Arey, 2003), changes in toluene/benzene ratios have been used to determine photochemical ages of ambient air (Gelencsér et al., 1997). Close to emission sources, their ratio can provide insight into source types. Emission ratios of toluene to benzene have been reported as approximately 0.6 for biomass burning emissions (Andreae and Merlet, 2001; Yokelson et al., 2007); ~1 for O&G production emissions (Halliday et al., 2016; Helmig et al., 2014; Swarthout et al., 2013; Wilde et al., 2021); ranging from 1.6 to 3.1 for on-road emissions with a typical fuel combustion (light-duty, gasoline fuel vehicles) signature of 2.5 (Chin and Batterman, 2012; Jobson et al., 2004; Rogers et al., 2006; Zavala et al., 2006); and much larger (> 3) for industrial, diesel-fuel vehicles, urban and fuel evaporation emissions (Chin and Batterman, 2012; Choi and Ehrman, 2004; Karl et al., 2009; Velasco et al., 2007; Wilde et al., 2021). Toluene/benzene ratios in Broomfield mostly fall in a range from 1.4 to 1.8, spanning the range of values previously defined by observations in Denver (mean value of 2.47), at Boulder Reservoir (1.87) and at the BAO Tower in Erie (0.57 to 1.09). Similar mean values of the toluene/benzene ratio (1.6, 1.7, and 1.5) were obtained prior to pad development, during pre-production, and in the production phase in Broomfield, all reflecting a mixed influence from O&G and on-road emissions.

Examining ratios of benzene to O&G and traffic emission tracers propane and ethyne (Figure A.5), a number of interesting relationships are observed. Benzene shows moderate to strong correlations with propane at all three site types (O&G, neighborhood impact, and

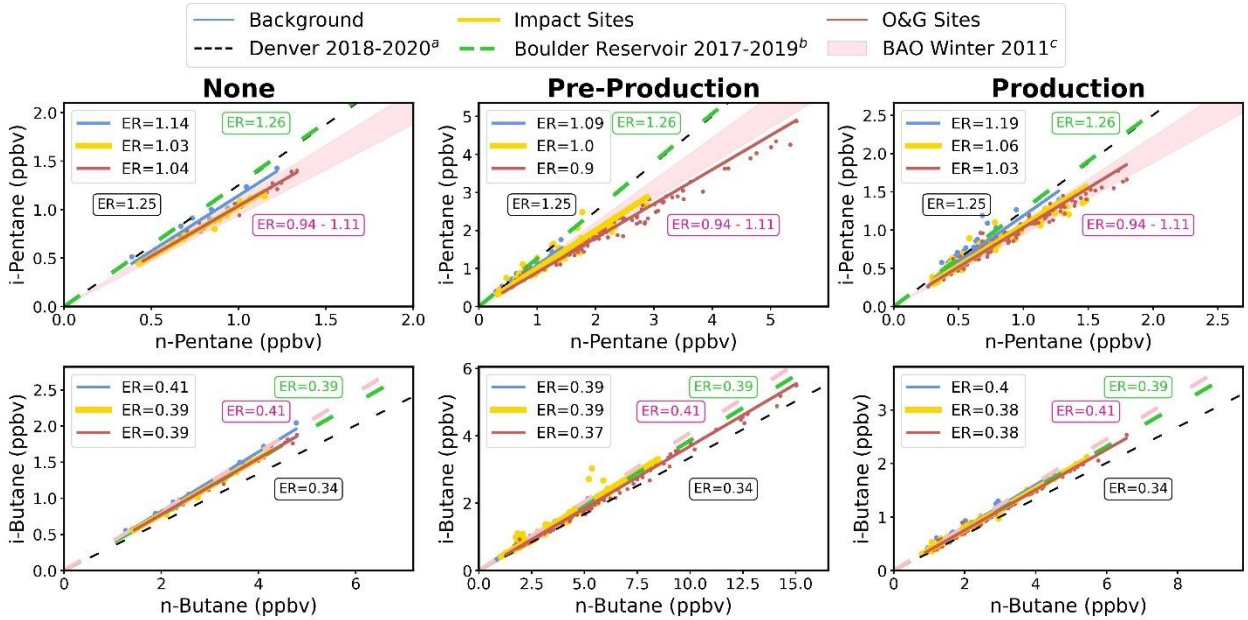

Figure A.4: Scatter plots and the results of correlation analysis for various hydrocarbons including pentane isomers (top) and butane isomers (bottom) for the three site categories of prior to the pre-production (None, left), during the pre-production (center), and after the pre-production (production, right). Data from the Denver-CAMP site (black dashed line, observed by CDPHE from October 2018 to 2020, data available at CDPHE website)[a], the Boulder Reservoir site from 2017 to 2019 (green dashed line) (Pollack et al., 2021][b], and the BAO Tower during winter 2021 (pink dashed line and rectangular) (Swarthout et al., 2013)[c] are also shown. Emission ratios (ER) are slopes determined by the linear fits.

background) prior to wellpad development and during the pre-production phase, suggesting O&G is likely an important contributor to Broomfield benzene concentrations. Both benzene and propane concentrations are substantially higher in some O&G and neighborhood impact site samples than at the background site during pre-production operations, while more similar concentration ranges across site types are seen prior to pad development. A more complex relationship between benzene and propane is observed during the production period, with a set of points that fall along a steeper benzene/propane ratio. Prior to pad development, benzene showed moderate to strong correlation with ethyne across all three site types, indicative of the expected contributions of vehicle traffic and other combustion sources to regional benzene emissions. A strong correlation is maintained at the background site during pre-production activities while correlation at the O&G and neighborhood impact sites decreases sharply during this period.

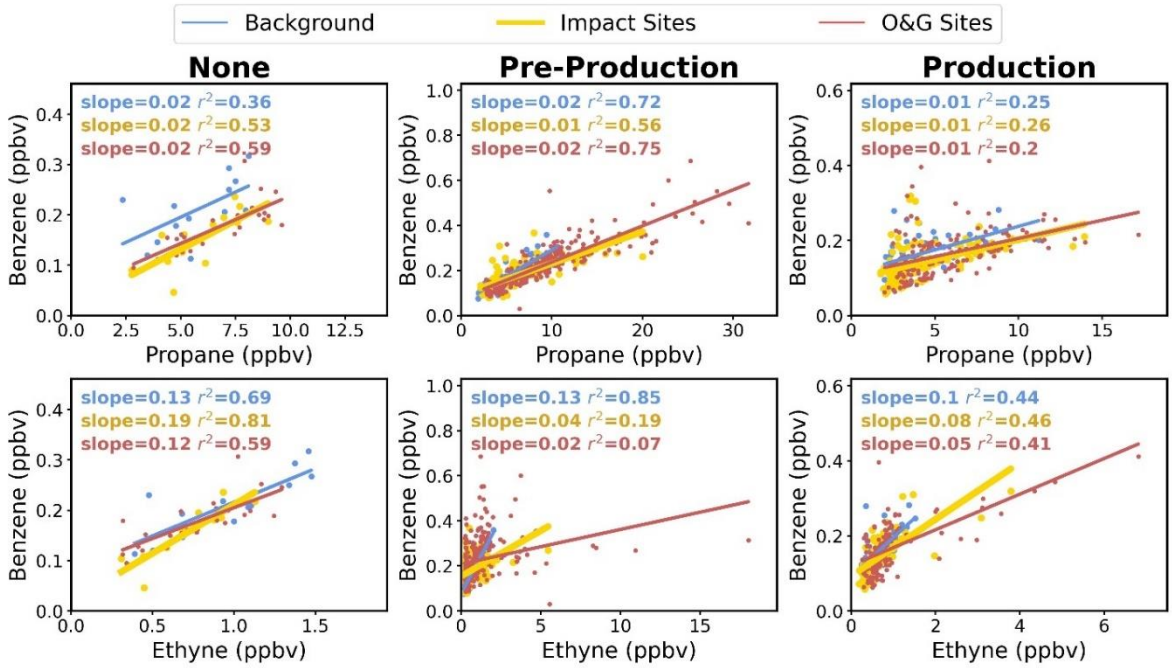

Figure A.5: Scatter plots and the results of correlation analysis for benzene with O&G (propane) and urban/traffic (ethyne) tracers for the three site categories prior to pre-production (None, left), during pre-production (center), and after wells move to production (right).

Benzene correlations with ethyne strengthen again at the O&G and neighborhood impact sites during the production phase. During both the pre-production and production phases, there are several weeks where ethyne concentrations at the O&G and neighborhood impact sites increase well above levels seen at the Commons background site, despite the closer proximity of the Commons site to busy roads and the Denver metro area. As we will explore below, these increased ethyne levels reflect a previously unidentified well pad source that emitted plumes rich in ethyne and benzene during two well-defined periods.

Although n-hexane has been designated as a hazardous air pollutant (HAP) by U.S. EPA since the 1990s (U.S. EPA, 2022), hexane emissions have historically received less attention than benzene and toluene. Previous studies reported elevated n-hexane levels near well pads and around on-site equipment (Helmig et al., 2014; Macey et al., 2014). In the current study, the average n-hexane concentrations during pre-production operations were 2 times higher than prior to well pad

development or during production. Concentrations of n-hexane were more strongly correlated with propane than with ethyne at all three site types throughout the study (mean r^2 is 0.75 with propane vs. 0.34 with ethyne), but especially at O&G and neighborhood impact sites during pre-production activities (mean r^2 was 0.66 for n-hexane with propane, but less than 0.01 with ethyne). Strong correlations between n-hexane and propane were also previously reported at the Boulder Reservoir (Pollack et al., 2021). These findings highlight important contributions of O&G activities to n-hexane emissions in the region. Moderate correlations of n-hexane with ethyne were observed across all three Broomfield site types prior to pad development and at the Commons background site throughout the study, suggesting urban/traffic sources may also be an important hexane source. Moderate correlations of n-hexane with both O&G and combustion tracers were found in the Southern UK reflecting mixed influence from marine traffic (shipping) and O&G emissions (Wilde et al., 2021).

Varying degrees of correlation were seen between concentrations of other VOC classes and concentrations of ethyne and propane during the Broomfield study (Table B.2). In general, all C_2 to C_7 light alkanes and some C_5 to C_7 cyclic alkanes showed strong correlations ($0.51 < r^2 < 0.99$, $p < 0.05$) with propane across all site categories throughout the entire sampling period. Branched alkanes also exhibited relatively high correlations with propane ($0.54 < r^2 < 0.59$, $p < 0.05$) with little correlation to ethyne at the O&G and neighborhood impact sites during the pre-production period. Moderate correlations of these compounds with ethyne ($0.35 < r^2 < 0.79$, $p < 0.05$) were observed at the background site throughout the entire sampling period and at the neighborhood impact and the O&G sites prior to well pad development, suggesting a regional influence from combustion sources. Many alkenes, especially ethene and propene, were well correlated with ethyne at the background site throughout the entire sampling period and at the neighborhood

impact and O&G sites prior to pad development. Not surprisingly, isoprene showed little correlation with either propane or ethyne due to its biogenic origin.

This simple look at species ratios provides useful insight into the importance of various local and regional activities as VOC sources. Lachenmayer (2022) use positive matrix factorization (PMF) to examine this dataset and quantify Broomfield VOC source contributions in greater detail.

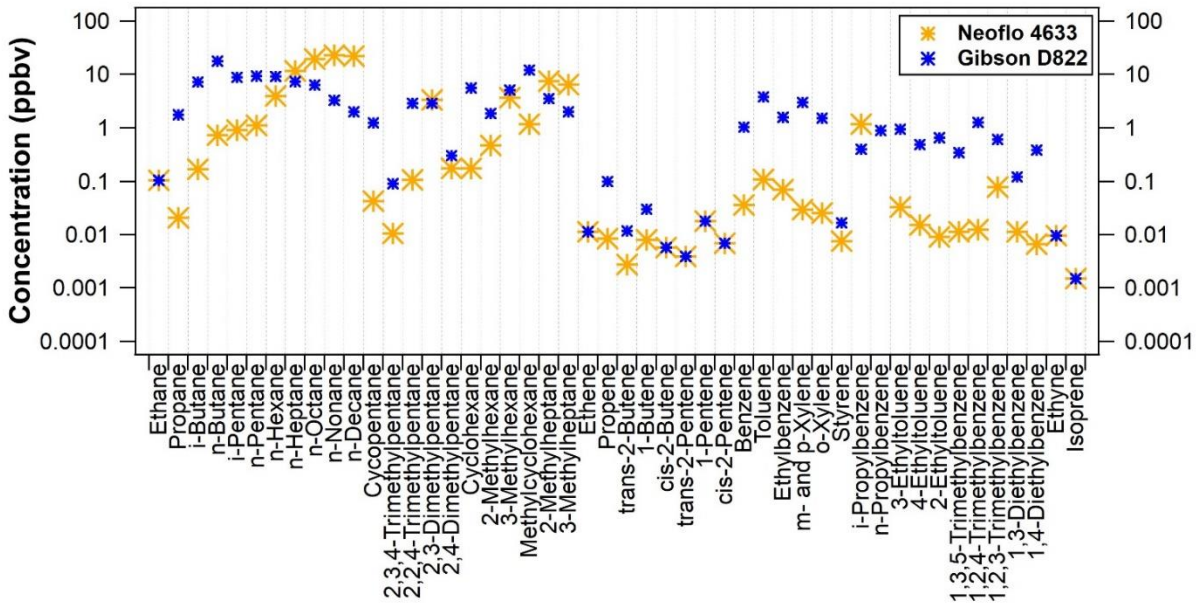

Figure A.6: Comparisons of VOC compositions for Neoflo 4633 and Gibson D822 drilling mud from the headspace analyses.

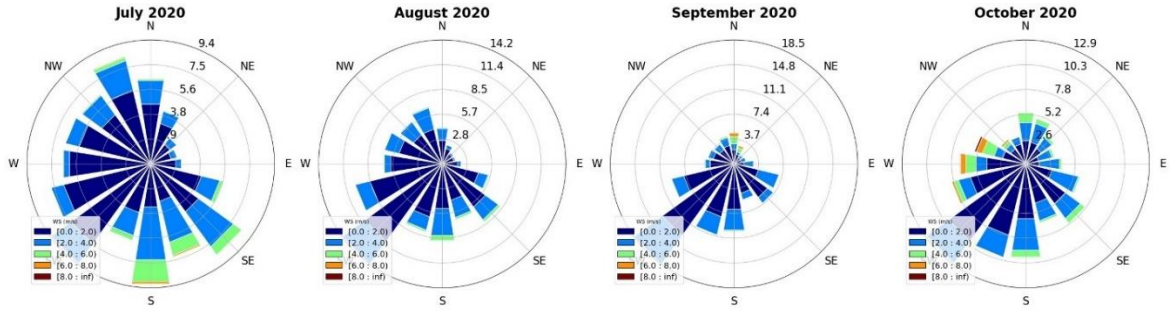

Figure A.7: Wind roses depicting overnight (22:00 to 4:00 local time) wind patterns at the Soaring Eagle Park monitoring site from July to October 2020.

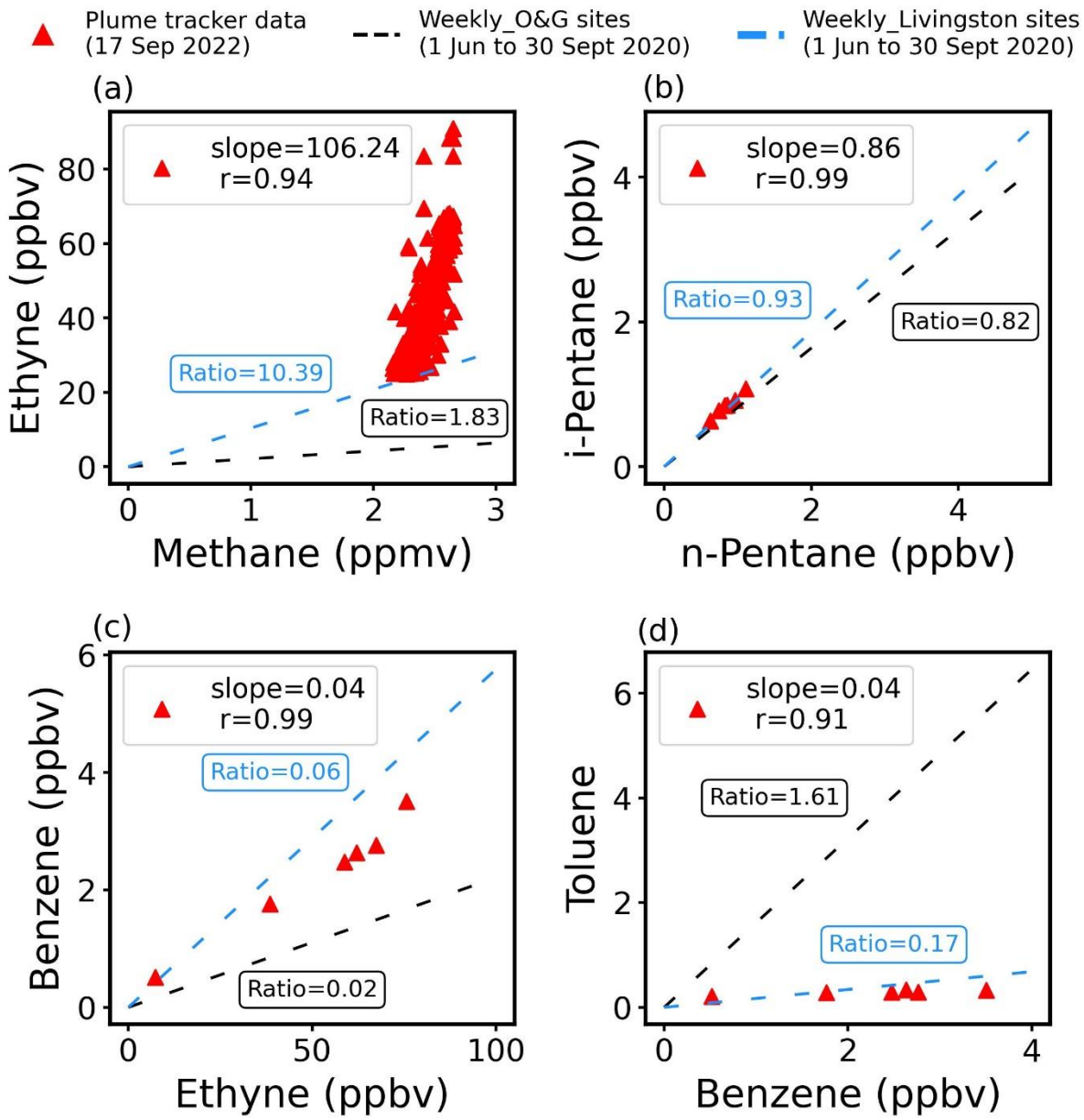

Figure A.8: Correlation of (a) continuously measured ethyne versus methane mixing ratios in the high ethyne plume (for ethyne mixing ratios > 25 ppbv) during the plume tracker drive on 17 September 2020. Correlations of (b) i-pentane versus n-pentane, (c) benzene versus ethyne, and (d) benzene versus toluene from canister samples that were collected in the high ethyne plumes (canisters 1-4 and 6-7, Figure 2.7 (b)). The black dashed lines show the linear regression lines for all weekly canister samples collected around O&G sites. The dashed blue lines show the regression lines for weekly canister samples collected at Livingston near-pad sites during the high ethyne period (1 June 2020 to 30 September 2020).

Table A.7: Statistics grouped by well development operations in the triggered canisters collected across the Broomfield air monitoring network. Weekly canister data collected at the Commons (background) site from February 2020 to December 2022 are shown here for reference. Methane is in unit of ppmv, while other VOC species are in units of ppbv.

Species	Mean	Min	Max
Commons (N = 151)			
Benzene	0.16	0.04	0.38
TVOC	10.60	3.90	24.97
Drilling (N = 45)			
Methane	3.78	1.97	16.87
Ethane	493.42	9.76	2907.64
Propane	293.80	4.24	1532.27
Benzene	6.22	0.40	21.26
Toluene	14.15	0.71	41.32
C_8-C_{10} n-Alkanes	64.51	0.16	210.67
Cyclic Alkanes	45.37	0.39	152.27
Branched Alkanes	31.97	0.70	101.88
BTEX	38.02	1.76	111.40
TVOC-49	873.60	36.58	3454.72
Hydraulic Fracturing (N = 1)			
Methane	16.71		
Ethane	3605.19		
Propane	1709.64		
Benzene	18.90		
Toluene	24.55		
C_8-C_{10} n-Alkanes	29.77		
Cyclic Alkanes	139.50		
Branched Alkanes	79.77		
BTEX	59.34		
TVOC-49	4003.02		
Coil Tubing (N = 9)			
Methane	25.78	2.46	95.18
Ethane	5197.01	65.86	23176.14
Propane	2670.11	46.93	15003.84
Benzene	13.69	0.67	25.66
Toluene	19.38	1.31	33.49
C_8-C_{10} n-Alkanes	25.98	1.77	64.98
Cyclic Alkanes	108.59	5.04	187.46
Branched Alkanes	64.86	3.70	115.00
BTEX	47.70	2.96	83.41
TVOC-49	5038.95	138.57	23596.11

Table A.7: Statistics grouped by well development operations in the triggered canisters collected across the Broomfield air monitoring network. Weekly canister data collected at the Commons (background) site from February 2020 to December 2022 are shown here for reference. Methane is in unit of ppmv, while other VOC species are in units of ppbv (continued).

Species	Mean	Min	Max
Coil Tubing and production tubing installation (N = 5)			
Methane	5.32	2.27	10.08
Ethane	837.11	62.30	1797.63
Propane	430.44	41.63	807.71
Benzene	9.43	0.79	20.44
Toluene	19.79	1.60	36.25
C_8-C_{10} n-Alkanes	26.81	2.75	47.87
Cyclic Alkanes	83.15	6.84	169.00
Branched Alkanes	61.58	4.83	128.80
BTEX	46.63	4.54	84.39
TVOC-49	1242.32	125.85	2098.51
Flowback (N = 23)			
Methane	38.80	1.86	301.03
Ethane	8466.06	265.30	79593.05
Propane	6004.46	180.40	57187.84
Benzene	99.09	3.54	818.90
Toluene	120.46	0.28	871.85
C_8-C_{10} n-Alkanes	140.27	5.75	920.90
Cyclic Alkanes	624.79	22.18	4975.70
Branched Alkanes	380.33	15.37	2652.71
BTEX	300.14	12.39	2089.22
TVOC-49	15330.27	564.68	141616.65
Production (N = 8)			
Methane	3.48	1.91	10.75
Ethane	1581.04	8.31	8435.96
Propane	2104.52	11.33	10700.50
Benzene	12.66	0.52	30.85
Toluene	12.27	0.64	30.47
C_8-C_{10} n-Alkanes	9.72	0.64	26.15
Cyclic Alkanes	86.52	3.31	233.87
Branched Alkanes	43.64	1.78	114.37
BTEX	31.61	1.56	76.87
TVOC-49	4505.65	55.45	17951.29

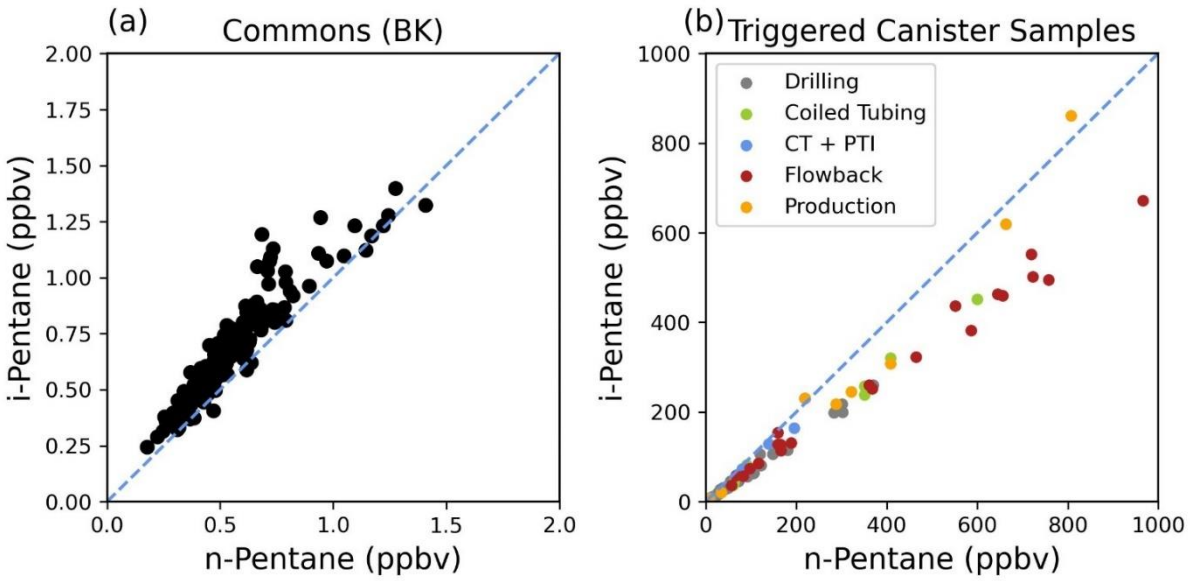

Figure A.9: Scatter plots of i-pentane versus n-pentane for (a) weekly canisters collected at the Commons background site, and (b) triggered canister samples collected during different well pad operations from February 2020 to December 2022. A 1:1 line in blue is included as a reference.

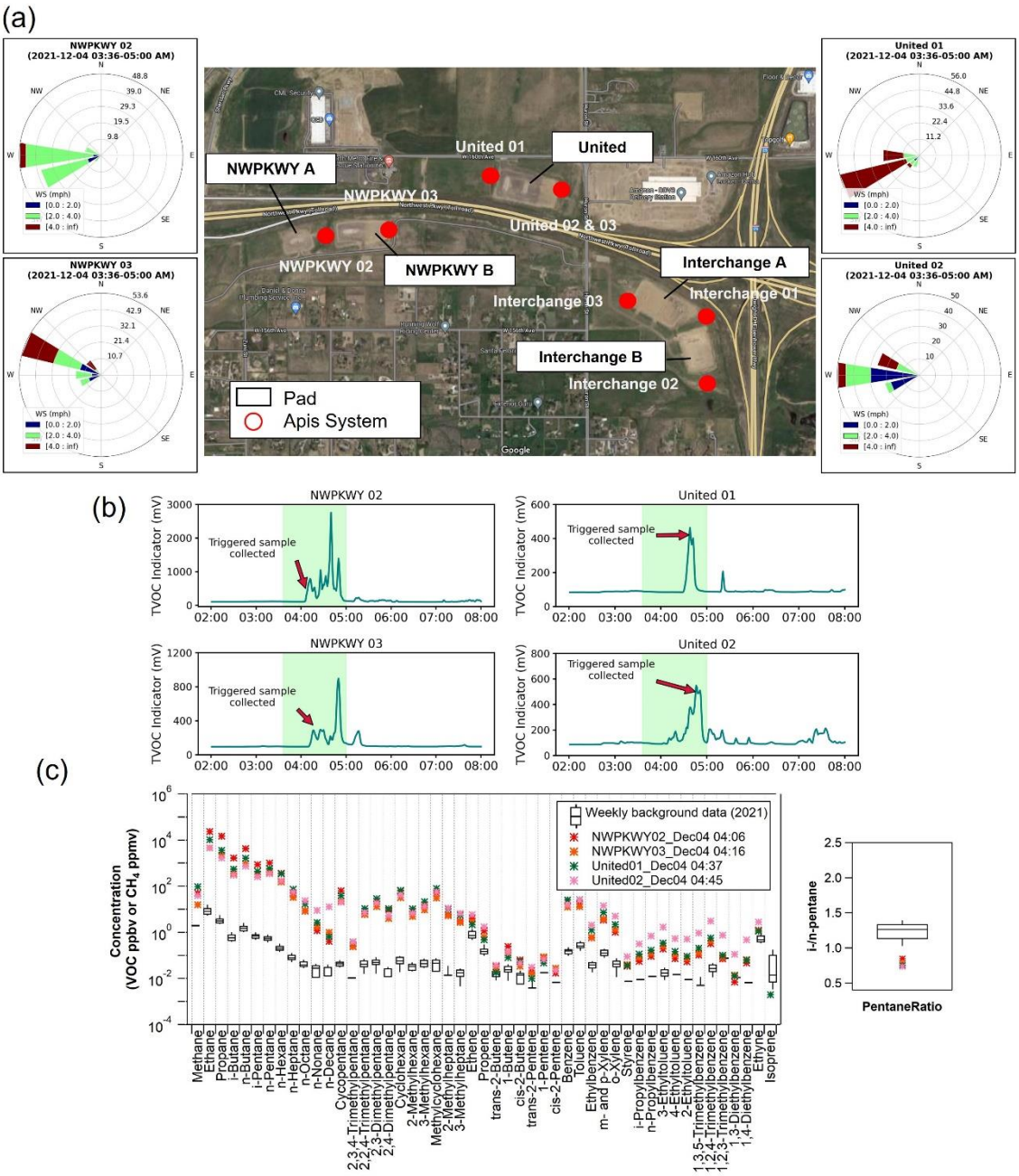

Figure A.10: (a) Wind information from 4 December 2021 at 03:36 to 5:00 LT (base map from Google map), and (b) Apis-PID response time series for that morning at the NWPKWY and United sites. The green-shaded areas in (b) represent time intervals of the wind data, the red arrows indicate the time when the triggered canister samples were collected. (c) Comparisons of VOC and i/n-pentane ratios for the triggered canister samples along with the distributions of weekly values measured at the Commons background site in 2021. The box and whisker plots show the 25th and 75th percentiles as the box, the 50th percentile as the line in the box, and the 10th and 90th percentiles as whiskers.

Appendix B

Additional Information for Contributions to atmospheric OH reactivity during oil and gas well development

Table B.1: Descriptive statistics of O3 precursors from adjacent monitoring sites or weekly canister samples collected from 4 October 2018 to 23 December 2022 in Broomfield.

Compounds	Max. (ppbv)	Min. (ppbv)	Mean (ppbv)	Median (ppbv)	Standard Deviation (ppbv)	LOD (ppbv)	$k_{OH, VOC}$ (X 10^{-12} cm^3 $molecule^{-1}$ s^{-1})	Average OHRs (s^{-1})
CO[a]	541.59	138.50	248.38	235.28	77.06	-	0.24[d]	1.49
NO_2[b]	31.51	4.53	13.21	11.35	6.26	-	9.2[d]	3.03
Methane	2795.0	1723.0	2005.2	1989.0	96.7	0.1	0.01[d]	0.3
Ethane	64.79	3.00	11.33	8.95	7.20	0.21	0.25[d]	0.07
C_3-C_7 n-alkanes								
Propane	39.24	1.13	5.58	4.34	3.81	0.04	1.11[d]	0.15
i-Butane	6.66	0.23	0.97	0.75	0.67	0.02	2.1[d]	0.05
n-Butane	20.07	0.49	2.56	1.98	1.84	0.02	2.4[d]	0.15
i-Pentane	6.92	0.21	0.88	0.74	0.54	0.02	3.7[d]	0.08
n-Pentane	9.44	0.18	0.86	0.68	0.65	0.01	3.9[d]	0.08
n-Hexane	4.82	0.06	0.36	0.26	0.35	0.02	5.2[e]	0.05
n-Heptane	2.72	0.01	0.15	0.09	0.19	0.02	6.76[e]	0.02
C_8-C_{10} n-alkanes								
n-Octane	1.74	0.01	0.09	0.05	0.14	0.01	8.11[e]	0.02
n-Nonane	2.04	0.01	0.07	0.03	0.16	0.02	9.7[e]	0.02
n-Decane	3.48	0.01	0.10	0.03	0.28	0.03	11[e]	0.03
Cyclic Alkanes								
Cyclopentane	0.74	0.01	0.07	0.05	0.05	0.01	4.85[e]	0.01
Cyclohexane	0.22	0.01	0.01	0.01	0.01	0.02	6.6[e]	< 0.005
Methylcyclohexane	0.48	0.01	0.05	0.04	0.04	0.02	3.34[e]	< 0.005
Branched Alkanes								
2,3,4-Trimethylpentane	0.22	0.01	0.01	0.01	0.01	0.02	6.6[e]	< 0.005
2,2,4-Trimethylpentane	0.48	0.01	0.05	0.04	0.04	0.02	3.34[e]	< 0.005

Table B.1: Descriptive statistics of O3 precursors from adjacent monitoring sites or weekly canister samples collected from 4 October 2018 to 23 December 2022 in Broomfield (continued).

Compounds	Max. (ppbv)	Min. (ppbv)	Mean (ppbv)	Median (ppbv)	Standard Deviation (ppbv)	LOD (ppbv)	$k_{OH, VOC}$ (X 10^{-12} cm^3 $molecule^{-1}$ s^{-1})	Average OHRs (s^{-1})
Branched Alkanes								
2,3-Dimethylpentane	1.14	0.02	0.07	0.05	0.07	0.03	6.47[f]	0.01
2,4-Dimethylpentane	0.24	0.01	0.02	0.01	0.02	0.02	4.77[e]	< 0.005
2-Methylhexane	0.33	0.01	0.04	0.03	0.03	0.01	6.72[g]	0.01
3-Methylhexane	1.30	0.01	0.07	0.05	0.09	0.02	6.54[g]	0.01
2-Methylheptane	0.97	0.01	0.04	0.01	0.06	0.03	9[h]	0.01
3-Methylheptane	0.52	0.01	0.03	0.02	0.04	0.01	9[h]	0.01
Alkenes								
Ethene	5.6	0.20	0.85	0.66	0.52	0.02	7.9[e]	0.17
Propene	0.69	0.02	0.15	0.13	0.07	0.02	25[e]	0.09
trans-2-Butene	0.28	< 0.005	0.01	0.01	0.01	0.01	70[e]	0.02
1-Butene	0.44	0.01	0.03	0.02	0.02	0.02	32[e]	0.02
cis-2-Butene	0.24	0.01	0.01	0.01	0.01	0.01	55[e]	0.01
trans-2-Pentene	0.10	< 0.005	0.01	< 0.005	< 0.005	0.01	67[e]	0.01
1-Pentene	0.07	0.02	0.02	0.02	< 0.005	0.04	31.4[e]	0.01
cis-2-Pentene	0.33	0.01	0.01	0.01	0.01	0.01	65[e]	0.01
BTEX								
Benzene	0.80	0.03	0.17	0.15	0.08	0.02	1.22[e]	0.01
Toluene	7.79	0.01	0.29	0.25	0.26	0.02	5.63[e]	0.04
Ethylbenzene	0.25	< 0.005	0.03	0.03	0.02	0.01	7[e]	0.01
m- and p-Xylene	1.17	0.01	0.13	0.10	0.10	0.02	18.7[e]	0.06
o-Xylene	0.46	0.01	0.04	0.03	0.04	0.02	13.6[e]	0.01
Aromatics (Other than BTEX)								
Styrene	0.06	0.01	0.01	0.01	< 0.005	0.02	58[e]	0.01
i-Propylbenzene	0.16	0.01	0.01	0.01	0.01	0.02	6.3[e]	0.02
n-Propylbenzene	0.07	0.01	0.01	0.01	< 0.005	0.03	5.8[e]	< 0.005
3-Ethyltoluene	0.37	< 0.005	0.02	0.01	0.02	0.01	18.6[e]	0.01
4-Ethyltoluene	0.15	0.02	0.02	0.02	0.01	0.03	11.8[e]	0.01
2-Ethyltoluene	0.06	0.01	0.01	0.01	< 0.005	0.02	11.9[e]	< 0.005

Table B.1: Descriptive statistics of O3 precursors from adjacent monitoring sites or weekly canister samples collected from 4 October 2018 to 23 December 2022 in Broomfield (continued).

Compounds	Max. (ppbv)	Min. (ppbv)	Mean (ppbv)	Median (ppbv)	Standard Deviation (ppbv)	LOD (ppbv)	$k_{OH, VOC}$ (X 10^{-12} cm^3 $molecule^{-1}$ s^{-1})	Average OHRs (s^{-1})
Aromatics (Other than BTEX)								
1,3,5-Trimethylbenzene	0.67	0.01	0.01	0.01	0.03	0.01	56.7[e]	0.01
1,2,4-Trimethylbenzene	2.74	0.01	0.04	0.02	0.10	0.01	32.5[e]	0.03
1,2,3-Trimethylbenzene	0.25	0.08	0.08	0.08	0.01	0.16	32.7[e]	0.06
1,3-Diethylbenzene	0.09	0.01	0.01	0.01	< 0.005	0.02	22[i]	0.01
1,4-Diethylbenzene	0.06	0.01	0.01	0.01	< 0.005	0.01	16[i]	< 0.005
Halogenated Hydrocarbon								
C_2HCl_3	0.22	< 0.005	0.01	0.01	0.02	0.001	2.2[d]	< 0.005
C_2Cl_4	0.16	< 0.005	0.01	0.01	0.01	<0.005	0.17[d]	< 0.005
OVOCs								
Acetone	28.72	0.17	2.35	1.94	1.60	0.33	0.18[d]	0.01
Acetaldehyde	23.50	0.42	2.32	1.85	1.92	0.83	15[d]	0.83
Formaldehyde[c]	4.63	2.18	3.16	3.05	0.70	0.02	8.5[d]	0.65
Ethyne	18.03	0.10	0.71	0.52	0.81	0.02	0.849[j]	0.02
Isoprene	0.66	< 0.005	0.03	0.01	0.06	<0.005	99[d]	0.08

[a]CO was measured at the Greeley – Weld County Tower and the Welby sites by CDPHE. [b]NO_2 was measured at the Platteville Atmospheric Observatory and the Welby sites by CDPHE. [C]Formaldehyde was from 3-h (6 to 9 AM) whole air samples collected at downtown Denver and at the Platteville site by CDPHE. Reference for $k_{OH, VOC}$: [d]Burkholder et al. (2020), [e]Atkinson and Arey (2003), [f]Wilson et al. (2006), [g]Sprengnether et al. (2009), [h]Abeleira et al. (2017), [i]Shaw et al. (2020), [j]Sørensen et al. (2003).

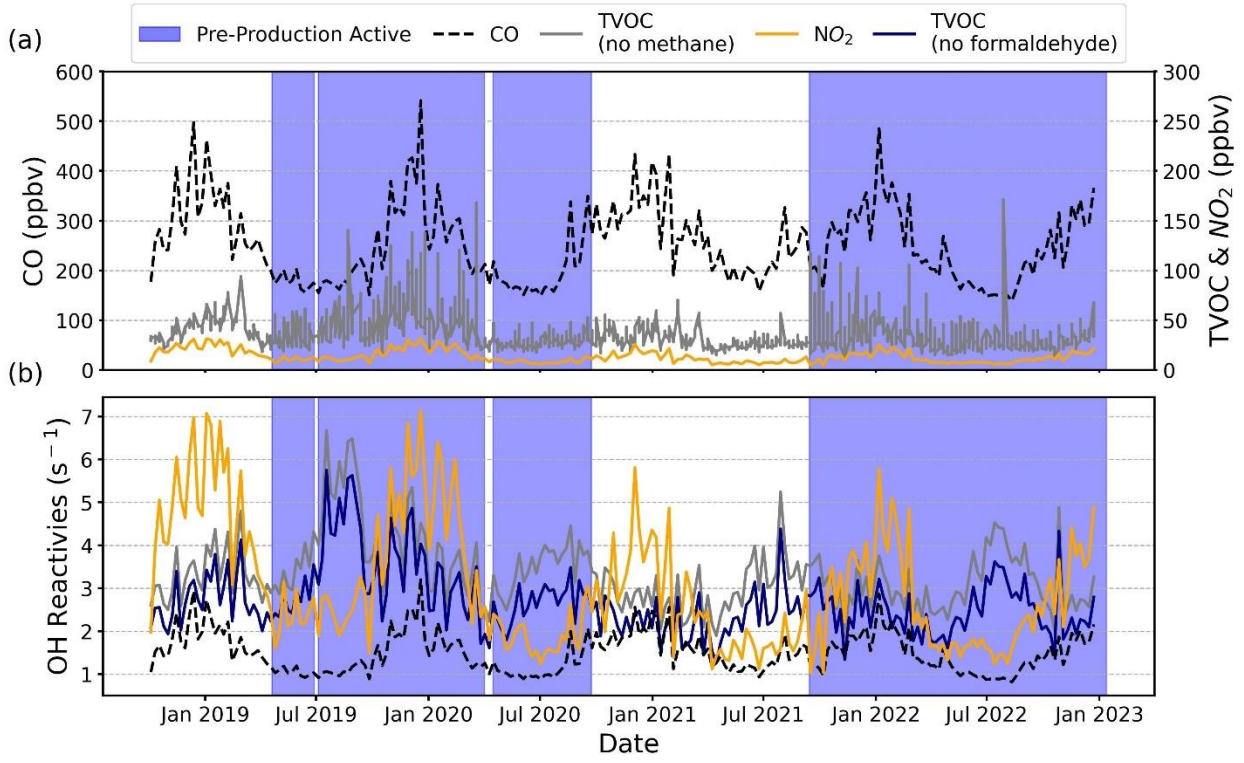

Figure B.1: Time series of (a) CO, TVOC (excluding methane), and NO_2 mixing ratios, and (b) the calculated OH reactivities for these precursors from the weekly integrated canister samples from October 2018 to December 2022. Observations started before O&G development and continued during pre-production activities (purple shading) and production.

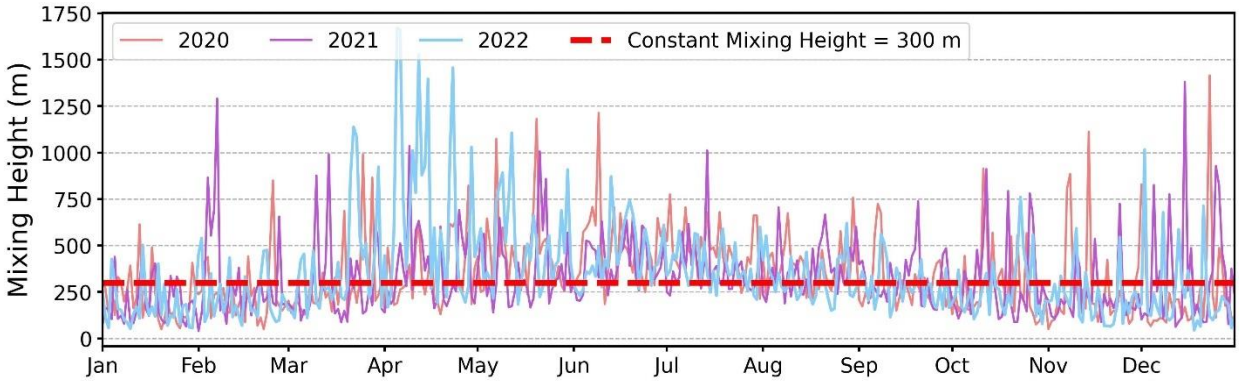

Figure B.2: Three years of mixing height data estimated from the Weather Research and Forecasting Model (WRF) in the Broomfield area. The chosen constant mixing height, 300 m, is marked in a red dashed line.

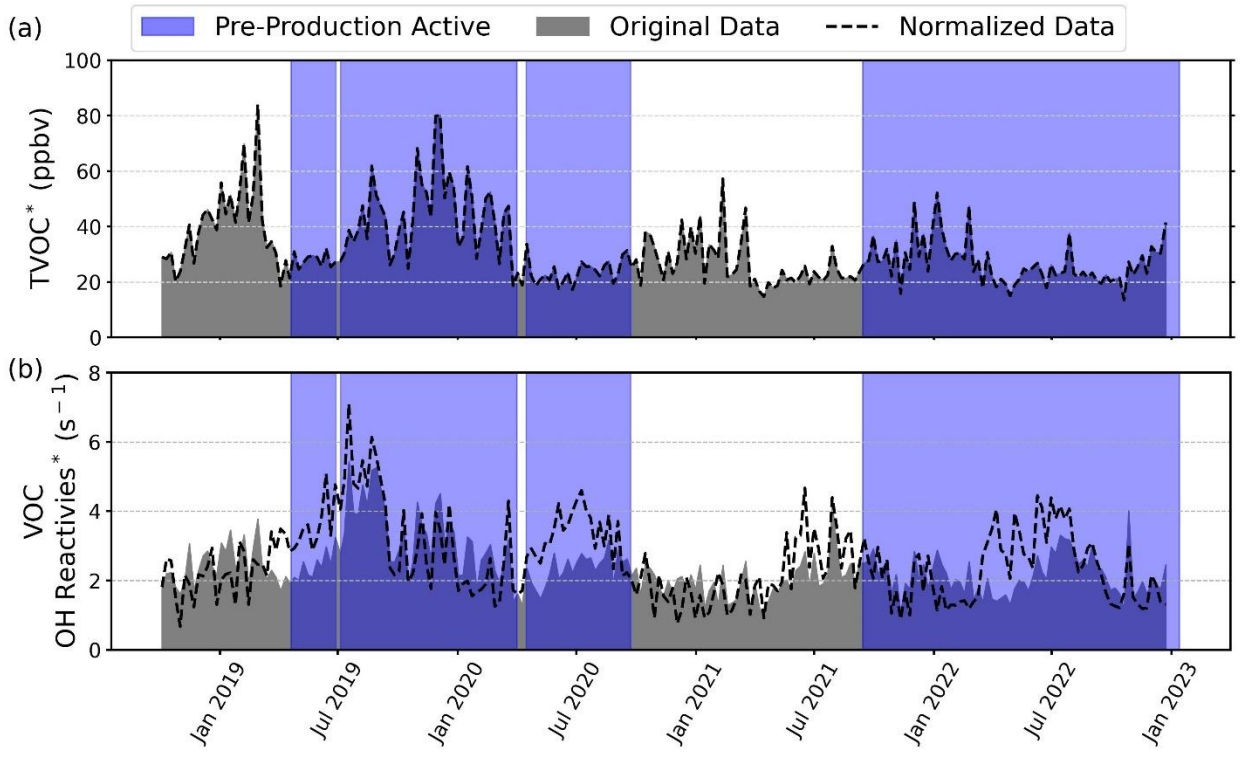

Figure B.3: Time series of weekly average of (a) TVOC and (b) calculated VOC OHRs (grey shade) overlapped with the normalized (a) TVOC and (b) VOC OHRs, which are shown in the black dashed line. *Methane and formaldehyde were not included in the TVOC and the calculated VOC OHRs shown here.

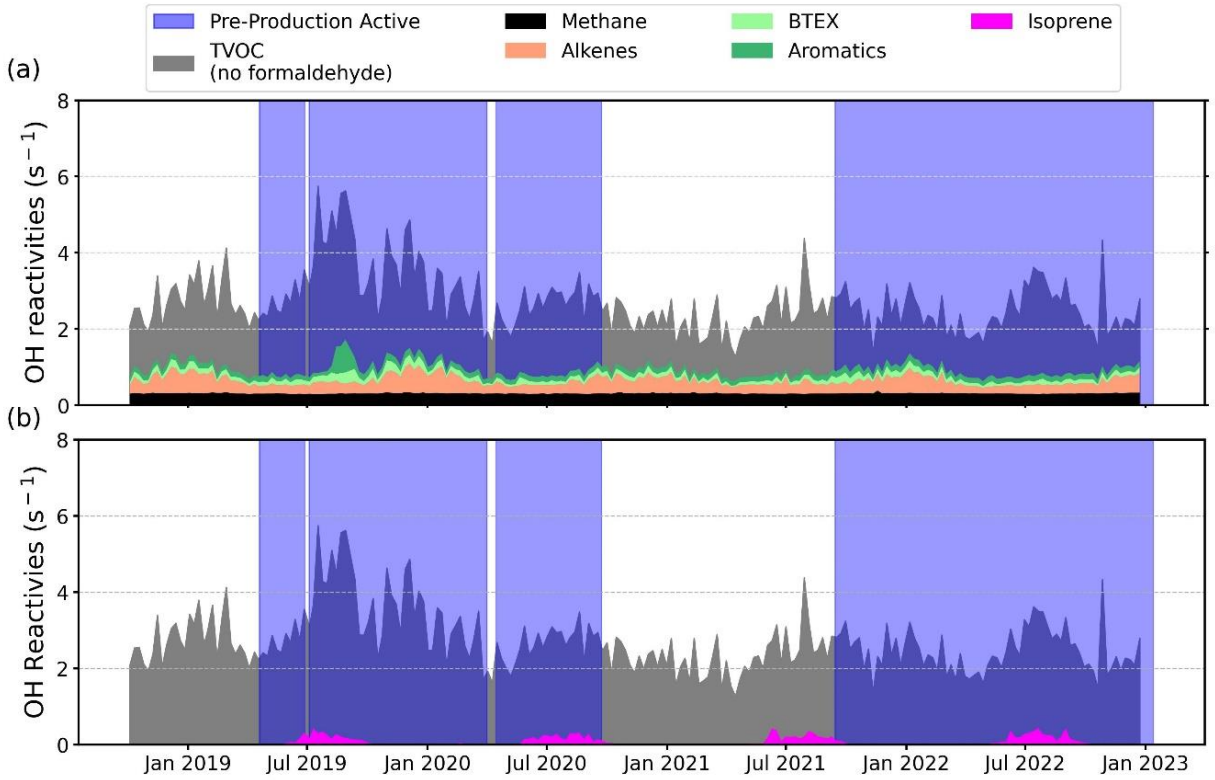

Figure B.4: Time series of the weekly average OHRs for (a) methane, alkenes, BTEX, and aromatics, and (b) isoprene overlapped with total OHRs calculated from the weekly integrated canister samples collected from October 2018 to December 2022. The purple shading represents the pre-production activities periods.

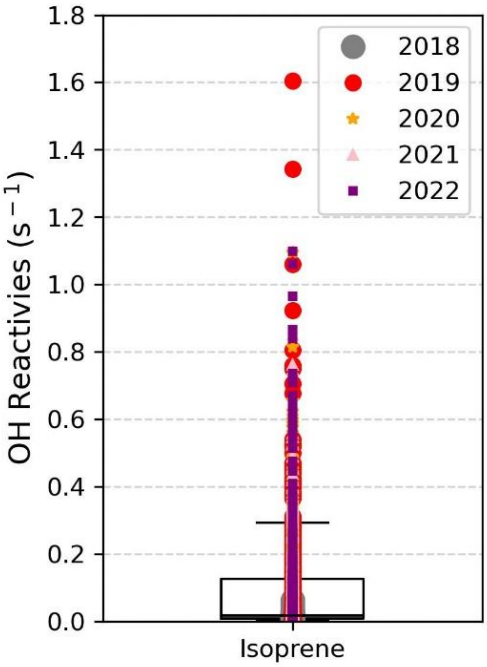

Figure B.5: Statistics of weekly average isoprene OHRs from October 2018 to December 2022. The boxes show the 25th to 75th percentiles of the data, the line represents the 50th percentile, and the 10th and 90th percentiles are represented as whiskers. The calculated isoprene OHRs across Broomfield sampling sites are marked in different colors for samples collected in different years.

Table B.2: The result of Multivariate regression analysis (MRA) fits of the ozone precursors for each season.

	Winter				Spring				Summer				Fall			
	$ER_{Propane}$	$r^2\_{Propane}$	ER_{Ethyne}	r^2_{Ethyne}	$ER_{Propane}$	$r^2\_{Propane}$	ER_{Ethyne}	r^2_{Ethyne}	$ER_{Propane}$	$r^2\_{Propane}$	ER_{Ethyne}	r^2_{Ethyne}	$ER_{Propane}$	$r^2\_{Propane}$	ER_{Ethyne}	r^2_{Ethyne}
Methane	30.106	0.893	88.262	0.808	29.874	0.893	333.606	0.808	38.074	0.893	260.302	0.808	44.397	0.893	93.284	0.808
Ethane	1.864	0.990	0.618	0.795	1.551	0.990	3.522	0.795	1.550	0.990	0.488	0.795	1.816	0.990	0.543	0.795
Propane	1	1	-	0.786	1	1	-	0.786	1	1	-	0.786	1	1	-	0.786
i-Butane	0.159	0.991	0.107	0.812	0.167	0.991	-0.033	0.812	0.164	0.991	-0.081	0.812	0.173	0.991	-0.020	0.812
n-Butane	0.428	0.992	0.298	0.814	0.474	0.992	-0.094	0.814	0.472	0.992	-0.140	0.814	0.477	0.992	-0.060	0.814
i-Pentane	0.105	0.974	0.163	0.835	0.131	0.974	0.049	0.835	0.173	0.974	0.150	0.835	0.143	0.974	0.048	0.835
n-Pentane	0.113	0.975	0.154	0.828	0.160	0.975	-0.130	0.828	0.194	0.975	-0.047	0.828	0.159	0.975	-0.034	0.828
n-Hexane	0.040	0.929	0.115	0.840	0.073	0.929	-0.090	0.840	0.094	0.929	-0.097	0.840	0.076	0.929	-0.049	0.840
n-Heptane	0.012	0.828	0.069	0.810	0.032	0.828	-0.029	0.810	0.048	0.828	-0.058	0.810	0.037	0.828	-0.036	0.810
n-Octane	0.006	0.760	0.043	0.763	0.021	0.760	-0.039	0.763	0.039	0.760	-0.072	0.763	0.027	0.760	-0.040	0.763
n-Nonane	0.001	0.554	0.044	0.671	0.010	0.554	-0.001	0.671	0.040	0.554	-0.101	0.671	0.026	0.554	-0.051	0.671
n-Decane	-0.0001	0.372	0.071	0.482	0.019	0.372	-0.018	0.482	0.057	0.372	-0.156	0.482	0.049	0.372	-0.094	0.482
Cyclopentane	0.008	0.953	0.023	0.858	0.013	0.953	0.005	0.858	0.017	0.953	0.007	0.858	0.014	0.953	-0.002	0.858
2,3,4-Trimethylpentane	0.0005	0.736	0.008	0.795	0.026	0.736	-0.149	0.795	0.010	0.736	-0.010	0.795	0.004	0.736	-0.013	0.795
2,2,4-Trimethylpentane	0.004	0.844	0.025	0.837	0.008	0.844	0.001	0.837	0.010	0.844	0.014	0.837	0.009	0.844	0.003	0.837
2,3-Dimethylpentane	0.005	0.859	0.034	0.851	0.012	0.859	0.006	0.851	0.018	0.859	-0.017	0.851	0.015	0.859	-0.008	0.851
2,4-Dimethylpentane	0.001	0.810	0.010	0.806	0.004	0.810	0.005	0.806	0.007	0.810	0.002	0.806	0.004	0.810	0.001	0.806
Cyclohexane	0.009	0.857	0.059	0.844	0.026	0.857	-0.031	0.844	0.043	0.857	-0.082	0.844	0.028	0.857	-0.027	0.844
2-Methylhexane	0.003	0.881	0.017	0.860	0.004	0.881	0.021	0.860	0.007	0.881	0.012	0.860	0.007	0.881	0.004	0.860
3-Methylhexane	0.004	0.800	0.054	0.864	0.011	0.800	0.007	0.864	0.019	0.800	-0.017	0.864	0.018	0.800	-0.015	0.864
Methylcyclohexane	0.009	0.730	0.084	0.756	0.038	0.730	-0.084	0.756	0.058	0.730	-0.140	0.756	0.042	0.730	-0.071	0.756
2-Methylheptane	0.002	0.669	0.024	0.721	0.017	0.669	-0.040	0.721	0.018	0.669	-0.020	0.721	0.014	0.669	-0.033	0.721
3-Methylheptane	0.002	0.769	0.014	0.790	0.005	0.769	-0.001	0.790	0.011	0.769	-0.014	0.790	0.008	0.769	-0.010	0.790
Ethene	0.071	0.875	0.563	0.886	0.031	0.875	0.666	0.886	0.035	0.875	0.705	0.886	0.083	0.875	0.540	0.886
Propene	0.011	0.838	0.081	0.844	0.008	0.838	0.103	0.844	0.016	0.838	0.119	0.844	0.018	0.838	0.057	0.844

Table B.2: The result of Multivariate regression analysis (MRA) fits of the ozone precursors for each season (continued).

	Winter				Spring				Summer				Fall			
	$ER_{Propane}$	$r^2\_Propand$	ER_{Ethyne}	r^2_Ethyne	$ER_{Propane}$	$r^2\_Propand$	ER_{Ethyne}	r^2_Ethyne	$ER_{Propane}$	$r^2\_Propand$	ER_{Ethyne}	r^2_Ethyne	$ER_{Propane}$	$r^2\_Propand$	ER_{Ethyne}	r^2_Ethyne
trans-2-Butene	0.0005	0.760	0.009	0.842	0.0005	0.760	0.014	0.842	0.002	0.760	0.008	0.842	0.002	0.760	0.002	0.842
1-Butene	0.001	0.830	0.010	0.833	0.0008	0.830	0.026	0.833	0.005	0.830	0.018	0.833	0.003	0.830	0.007	0.833
cis-2-Butene	0.001	0.710	0.008	0.769	0.002	0.710	0.011	0.769	0.002	0.710	0.023	0.769	0.001	0.710	0.005	0.769
trans-2-Pentene	0.001	0.595	0.002	0.536	0.008	0.595	-0.036	0.536	0.002	0.595	0.007	0.536	0.0004	0.595	0.004	0.536
cis-2-Pentene	0.002	0.788	-0.001	0.635	-0.002	0.788	0.051	0.635	0.016	0.788	-0.020	0.635	0.002	0.788	-0.002	0.635
Benzene	0.014	0.921	0.070	0.885	0.014	0.921	0.114	0.885	0.023	0.921	0.153	0.885	0.019	0.921	0.088	0.885
Toluene	0.022	0.849	0.123	0.826	0.017	0.849	0.349	0.826	0.069	0.849	0.204	0.826	0.050	0.849	0.067	0.826
Ethylbenzene	0.002	0.810	0.017	0.817	0.003	0.810	0.022	0.817	0.007	0.810	0.016	0.817	0.006	0.810	0.005	0.817
m- and p-Xylene	0.009	0.815	0.054	0.796	0.014	0.815	0.071	0.796	0.033	0.815	0.038	0.796	0.025	0.815	0.015	0.796
o-Xylene	0.003	0.782	0.017	0.774	0.005	0.782	0.023	0.774	0.009	0.782	0.008	0.774	0.008	0.782	0.003	0.774
Styrene	0.002	0.827	-0.001	0.801	0.001	0.827	0.038	0.801	-	0.827	-	0.801	0.004	0.827	-0.032	0.801
i-Propylbenzene	0.001	0.759	0.008	0.777	0.007	0.759	-0.006	0.777	0.005	0.759	0.013	0.777	0.010	0.759	-0.090	0.777
n-Propylbenzene	0.003	0.947	-0.003	0.796	-0.0002	0.947	0.086	0.796	0.001	0.947	0.066	0.796	0.005	0.947	0.006	0.796
3-Ethyltoluene	0.001	0.757	0.006	0.738	0.003	0.757	-0.004	0.738	0.009	0.757	-0.011	0.738	0.002	0.757	0.004	0.738
2-Ethyltoluene	0.002	0.834	-0.002	0.697	0.003	0.834	0.055	0.697	0.002	0.834	0.075	0.697	0.002	0.834	0.007	0.697
1,3,5-Trimethylbenzene	0.001	0.668	0.001	0.577	0.007	0.668	-0.004	0.577	0.013	0.668	-0.040	0.577	0.002	0.668	0.000	0.577
1,2,4-Trimethylbenzene	0.002	0.758	0.009	0.734	0.005	0.758	-0.003	0.734	0.026	0.758	-0.051	0.734	0.004	0.758	0.007	0.734
1,4-Diethylbenzene	0.001	0.861	0.001	0.766	-0.0001	0.861	0.041	0.766	0.003	0.861	0.009	0.766	-0.001	0.861	0.033	0.766
Ethyne	-	0.786	1	1	<0.0001	0.786	1	1	-	0.786	1	1	-	0.786	1	1
Isoprene	0.001	0.380	0.001	0.330	0.001	0.380	0.011	0.330	0.016	0.380	0.119	0.330	0.001	0.380	0.014	0.330
C2HCl3	-0.0001	0.607	0.015	0.793	0.002	0.607	0.002	0.793	0.002	0.607	0.005	0.793	0.002	0.607	0.003	0.793
C2Cl4	0.001	0.473	0.002	0.421	0.0002	0.473	0.015	0.421	0.002	0.473	0.006	0.421	0.001	0.473	0.001	0.421
Acetone	0.094	0.893	0.339	0.825	0.207	0.893	2.013	0.825	0.719	0.893	4.221	0.825	0.178	0.893	1.040	0.825
Acetaldehyde	0.094	0.847	0.183	0.738	0.129	0.847	2.345	0.738	0.716	0.847	3.011	0.738	0.152	0.847	0.910	0.738
Formaldehyde	0.059	0.659	-0.130	0.406	0.045	0.659	1.428	0.406	0.322	0.659	2.407	0.406	0.021	0.659	0.739	0.406

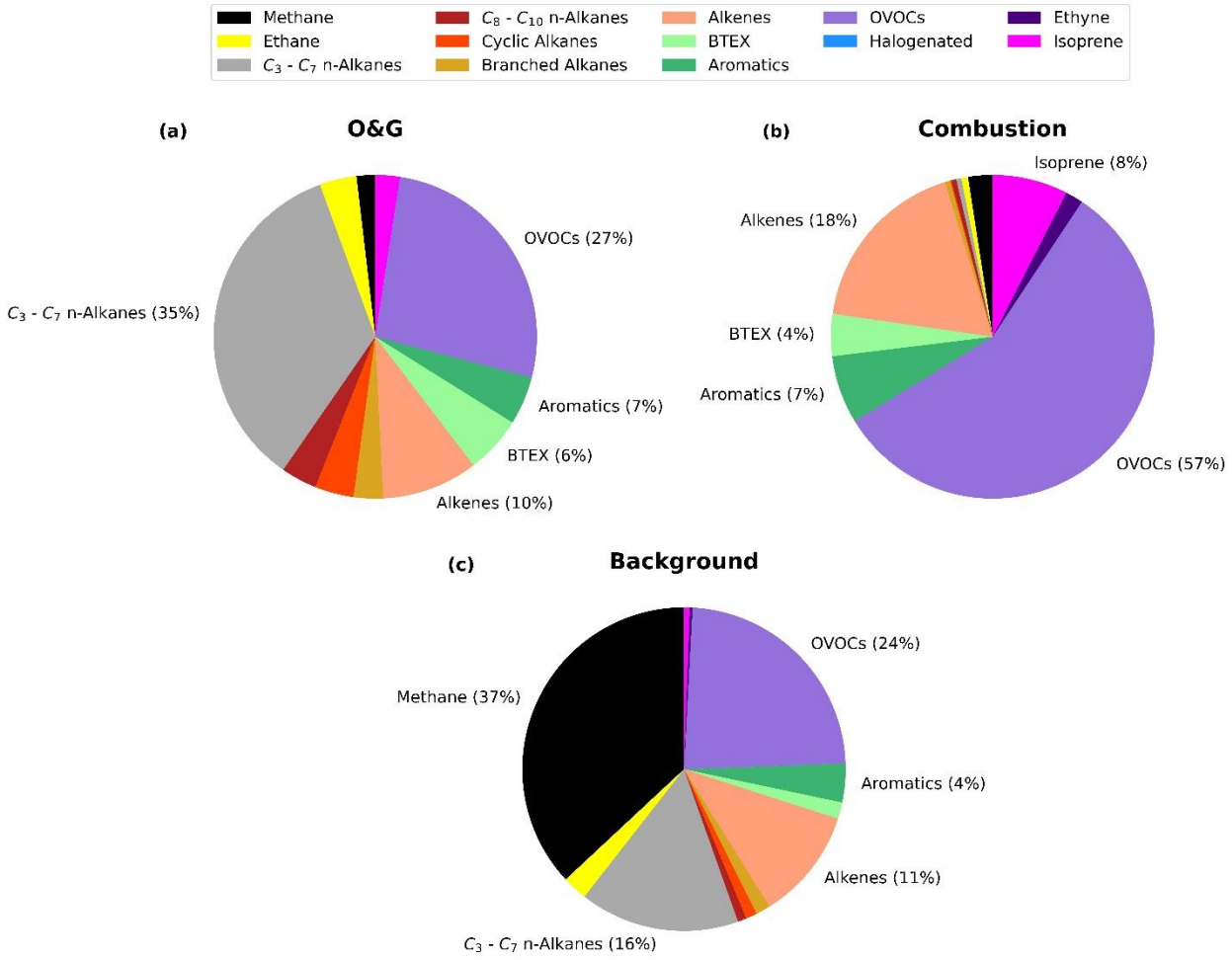

Figure B.6: The VOC source signatures for (a) O&G, (b) combustion, and (c) background factors from the Multivariate Regression Analysis.

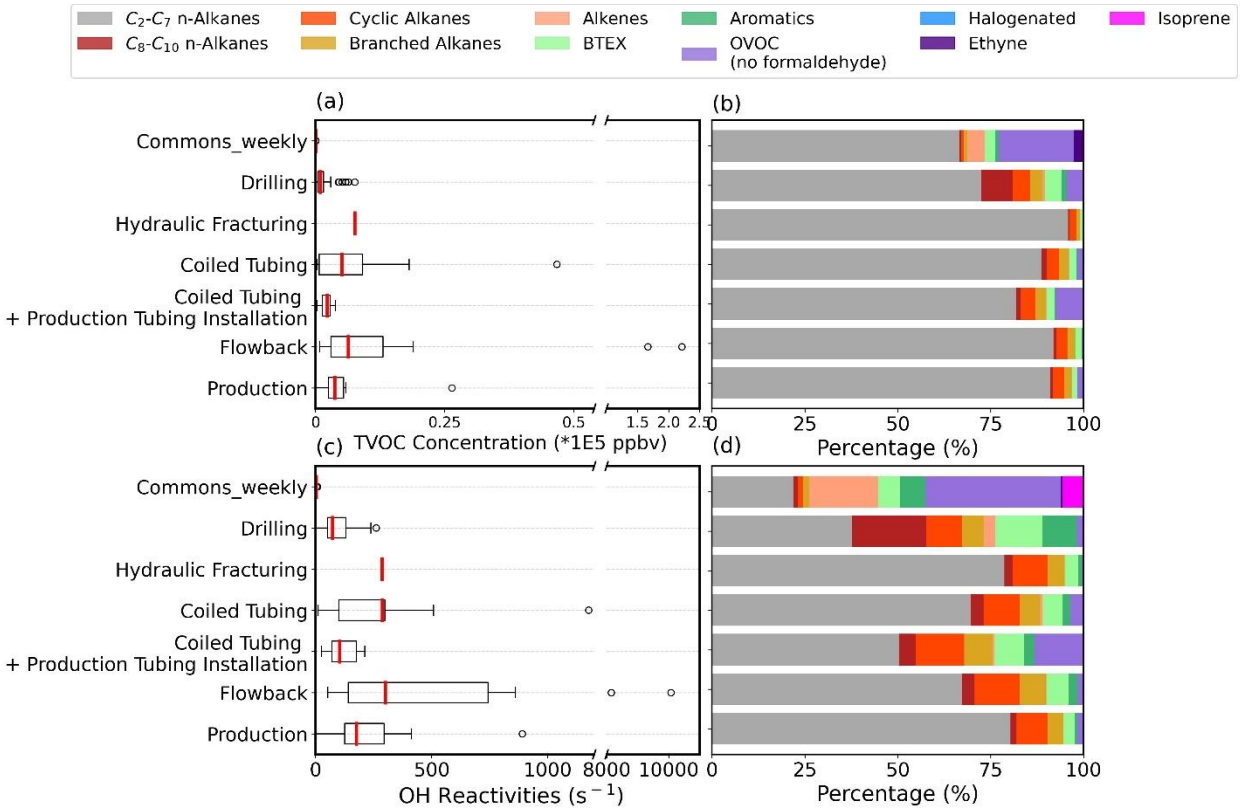

Figure B.7: Box and whisker plots (90th, 75th, 50th, 25th, 10th percentiles) of (a) TVOC mixing ratio (ppbv) and (c) OHRs (s^{-1}) and (b and d) the corresponding VOC signature throughout different O&G operations from February 2020 to December 2022. Weekly canister data collected at the Commons (background) site from February 2020 to December 2022 are shown here for comparison. *Methane was not included in these figures.

Appendix C

Additional Information for Characterizing potential surrogates for VOC emissions from unconventional oil and gas development

Table C.1: Detection limits of methane and different compounds measured by the 5-channel GC.

Compounds	Precision (1 RSD, %)	Standard Accuracy (%)	LOD	LOD unit
Methane	3.69	± 1	0.0500	ppmv
Ethane	2.83	± 5	0.2082	ppbv
Propane	2.31	± 5	0.0419	ppbv
i-Butane	2.38	± 5	0.0147	ppbv
n-Butane	2.59	± 5	0.0216	ppbv
i-Pentane	2.52	± 5	0.0167	ppbv
n-Pentane	2.48	± 5	0.0054	ppbv
n-Hexane	2.91	± 5	0.0222	ppbv
n-Heptane	3.24	± 5	0.0173	ppbv
n-Octane	2.90	± 5	0.0121	ppbv
n-Nonane	3.70	± 5	0.0221	ppbv
n-Decane	4.12	± 5	0.0262	ppbv
Cyclopentane	2.45	± 5	0.0098	ppbv
Cyclohexane	3.39	± 5	0.0380	ppbv
Methylcyclohexane	3.19	± 5	0.0414	ppbv
2,3,4-Trimethylpentane	3.06	± 5	0.0211	ppbv
2,2,4-Trimethylpentane	3.29	± 5	0.0238	ppbv
2,3-Dimethylpentane	3.35	± 5	0.0320	ppbv
2,4-Dimethylcyclopentane	2.44	± 5	0.0241	ppbv
2-Methylhexane	3.87	± 5	0.0100	ppbv
3-Methylhexane	3.64	± 5	0.0189	ppbv
2-Methylheptane	3.19	± 5	0.0284	ppbv
3-Methylheptane	3.48	± 5	0.0091	ppbv

Table C.1: Detection limits of methane and different compounds measured by the 5-channel GC (continued).

Compounds	Precision (1 RSD, %)	Standard Accuracy (%)	LOD	LOD unit
Ethene	4.73	± 5	0.0228	ppbv
Propene	2.75	± 5	0.0170	ppbv
trans-2-Butene	3.54	± 5	0.0056	ppbv
1-Butene	3.32	± 5	0.0159	ppbv
cis-2-Butene	2.83	± 5	0.0115	ppbv
trans-2-Pentene	3.80	± 5	0.0079	ppbv
1-Pentene	6.39	± 5	0.0361	ppbv
cis-2-Pentene	3.73	± 5	0.0139	ppbv
Benzene	3.38	± 5	0.0160	ppbv
Toluene	3.21	± 5	0.0177	ppbv
Ethylbenzene	3.42	± 5	0.0085	ppbv
m- and p-Xylene	3.51	± 5	0.0207	ppbv
o-Xylene	3.08	± 5	0.0230	ppbv
Styrene	9.58	± 5	0.0153	ppbv
i-Propylbenzene	13.40	± 5	0.0184	ppbv
n-Propylbenzene	17.69	± 5	0.0247	ppbv
3-Ethyltoluene	7.45	± 5	0.0068	ppbv
4-Ethyltoluene	7.06	± 5	0.0306	ppbv
2-Ethyltoluene	5.55	± 5	0.0184	ppbv
1,3,5-Trimethylbenzene	4.59	± 5	0.0101	ppbv
1,2,4-Trimethylbenzene	5.89	± 5	0.0096	ppbv
1,2,3-Trimethylbenzene	8.18	± 5	0.1550	ppbv
1,3-Diethylbenzene	6.99	± 5	0.0226	ppbv
1,4-Diethylbenzene	5.79	± 5	0.0134	ppbv
Ethyne	2.59	± 5	0.0194	ppbv
Isoprene	2.78	± 5	0.0030	ppbv